⟨S|P|S⟩
swiss physical society

Nr. 62
Oktober 2020

SPG MITTEILUNGEN
COMMUNICATIONS DE LA SSP

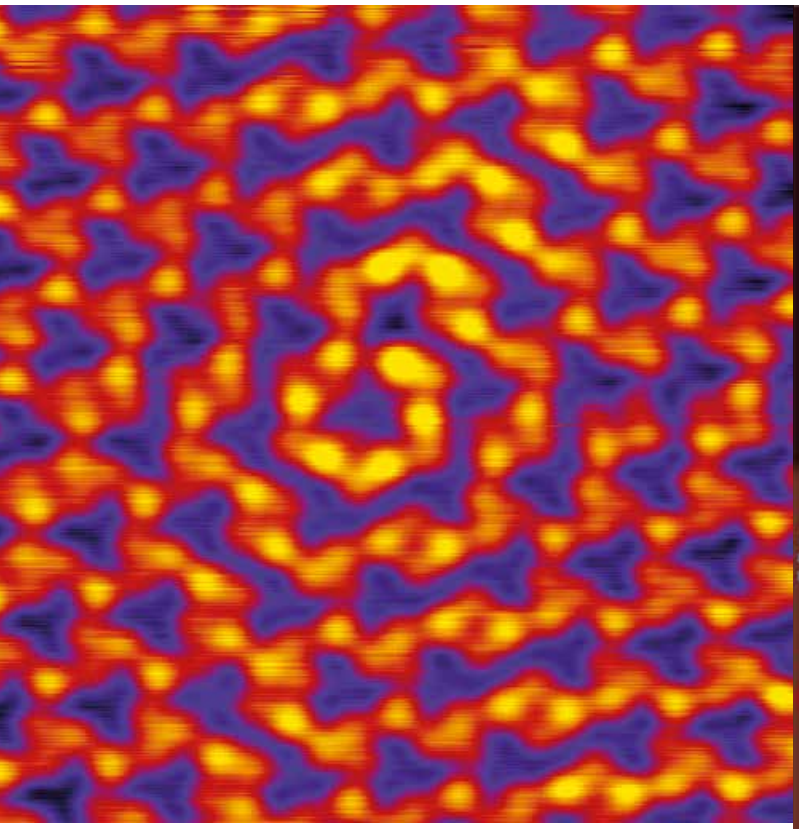

Silicon atoms on a silver surface form a two-dimensional arrangement, called silicene. In this picture a vortex structure is discovered. More on atomic buckling on p. 15.

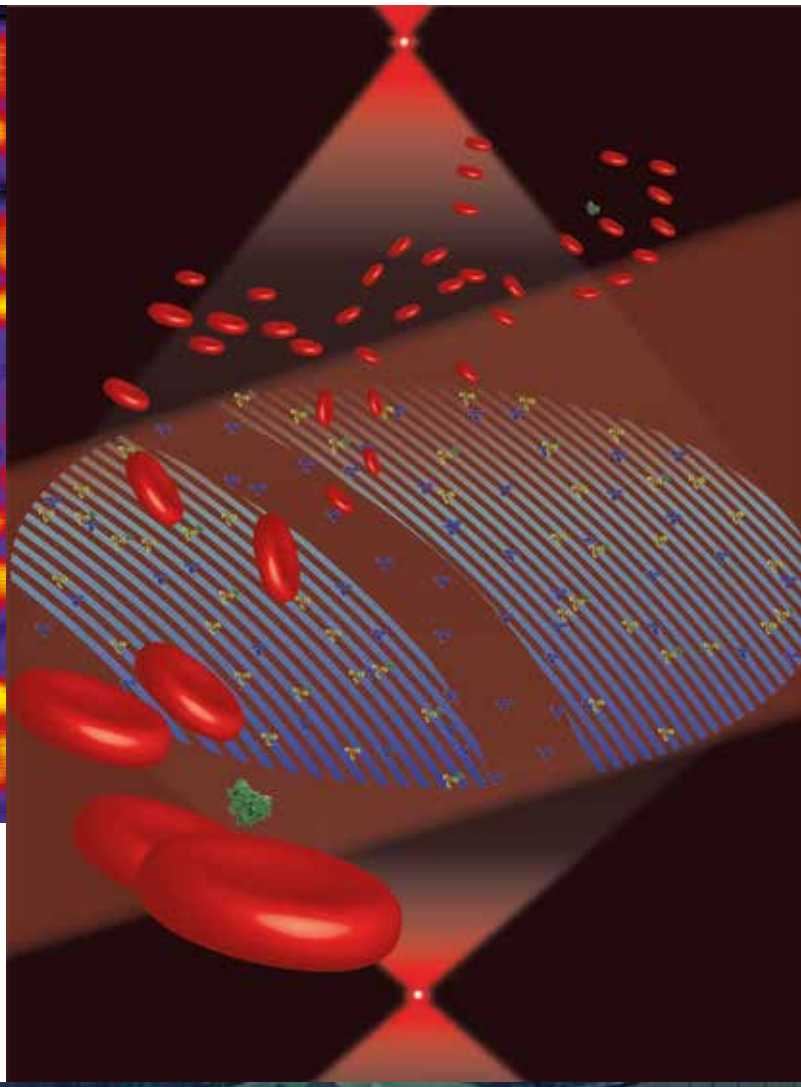

Mology is a biooptical method for analytical purposes. The coherent mologic signal picks out specific biomolecular interactions in complex samples. Read the article on p. 20.

The Gordon Conference on Superconductivity in 1995 in Les Diablerets with Phil Anderson, pionieer in modern condensed matter physics, who passed away on 29 March 2020. Read on p. 27 some personal remarks from his Swiss colleagues.

Inhalt - Contenu - Contents

Impressum:

Die SPG Mitteilungen erscheinen ca. 2-4 mal jährlich und werden an alle Mitglieder abgegeben.

Abonnement für Nichtmitglieder:
CHF 20.- pro Jahrgang (Inland; Ausland auf Anfrage), incl. Lieferung der Hefte sofort nach Erscheinen frei Haus. Bestellungen bzw. Kündigungen jeweils zum Jahresende senden Sie bitte formlos an folgende Adresse:

Verlag und Redaktion:
Schweizerische Physikalische Gesellschaft, Klingelbergstr. 82, CH-4056 Basel, sps@unibas.ch, www.sps.ch

Redaktionelle Beiträge und Inserate sind willkommen, bitte wenden Sie sich an die obige Adresse.
Namentlich gekennzeichnete Beiträge geben grundsätzlich die Meinungen der betreffenden Autoren wieder. Die SPG übernimmt hierfür keine Verantwortung.

Druck:
Werner Druck & Medien AG, Leimgrubenweg 9, 4053 Basel

Editorial

Kohärente Netze für schwache Signale

Bernhard Braunecker

"Cyberphysische Systeme", ursprünglich als Weiterführung des Konzepts Industrie 4.0 eingeführt, beschreiben mittlerweile all die Prozesse, bei denen physische Realitäten (Objekte, Maschinen, Abläufe, etc.) digital modelliert werden und mit diesen virtuellen "Zwillingen" in Echtzeit interagieren. Das erfasst nahezu alle Bereiche einer modernen Gesellschaft wie das Gesundheitswesen, Landwirtschaft, Industrie und Produktion, Transport, Energie, Finanzen, Aus- und Weiterbildung, etc. Es ist zu erwarten, dass laufend neue Lösungen, neue Geschäftsmodelle und Dienste entstehen werden.

Grundlage für die erfolgreiche Realisierung sind jedoch flächendeckende, breitbandige und robuste Internet-Infrastrukturen, und dazu gehören auch mobile Geräte und moderne Kommunikationsnetze wie 5G und die noch in Entwicklung sich befindende 6G Technologie. Die zunehmende Verknüpfungsdichte könnte jedoch zu einer höheren Antennendichte und zu stärkeren Emissionswerten elektromagnetischer Strahlung führen, die die Gesundheit oder zumindest das Wohlbefinden von Personen belasten würden. Im Artikel "How dangerous is the non-ionizing radiation used in mobile communication?" von HR Völkle auf Seite 33 wird zwar gezeigt, dass eine kritische thermische Belastung des Menschen beim Einhalten der amtlichen Grenzwerte nicht gegeben ist, und dass auch Prozesse subtilerer Art wie der Einfluss auf biologische Strukturen wie Zellen mit grosser Wahrscheinlichkeit auszuschliessen sind. Dennoch sind die Bedenken mancher Kreise in der Bevölkerung gegen den Ausbau leistungsstarker Netze ernst zu nehmen, und es ist ratsam, durch Aufzeigen der Faktenlage präventiv einer unnötigen Verhärtung emotionaler und politischer Positionen entgegenzuwirken.

Das erfordert jedoch ein besseres Verständnis der biophysikalischen Wechselwirkungen zwischen elektromagnetischer Strahlung und dem menschlichen Organismus, um notwendige Verhaltensregeln und Schutzmassnahmen abzuleiten und dafür die Bevölkerung zu gewinnen. Zudem ist zu erwarten, dass bei der Auslegung des zukünftigen 6G Standards alle physikalischen und technischen Möglichkeiten in Betracht gezogen werden, um die angestrebten höheren Datenraten nicht allein durch eine Erhöhung der Signalamplituden, sondern mehr durch geschickte Modulation der biologisch harmlosen Signalphasen zu erreichen. Wie erfolgreich Phasentechnologien sein können, illustriert der Datentransfer zwischen Satelliten mittels Laserlicht. Wegen der mitunter sehr grossen Entfernungen von bis zu 70000 km, aber auch wegen immer kleiner werdender Sende- und Empfangsaperturen treffen die Datensignale mit sehr geringer Intensität am Empfangssatellit ein. Um dennoch für eine vorgegebene Fehlerrate ein genügend gutes Signal zu Rausch Verhältnis zu erhalten, überlagert man die Signale phasengerecht mit einem lokalen (Laser-) Oszillator, so dass das Interferenzsignal über dem Systemrauschen liegt und somit Datenraten von etwa 10 Gbps zulässt. Zusätzlich wird jeder Satellit als Relaisstation benutzt und weiter sind alle Datenformate so mit redundanten Bits versehen, dass Bitfehler erkannt und automatisch korrigiert werden können [1]. All diese Phasentechnologien sind auch auf terrestrische Kommunikationsnetze anwendbar. Es ist zu erwarten, dass jedes Smartphone in Zukunft die erforderliche Signalsensitivität, Rechenleistung und Speicherkapazität aufweisen wird, um die zunehmend komplexer werdenden Algorithmen in Echtzeit auszuführen. Gelingt es, diese Trends der Bevölkerung in nachvollziehbarer Weise zu vermitteln, dann sollten die Bedenken hinsichtlich einer zunehmenden Strahlenbelastung deutlich geringer werden.

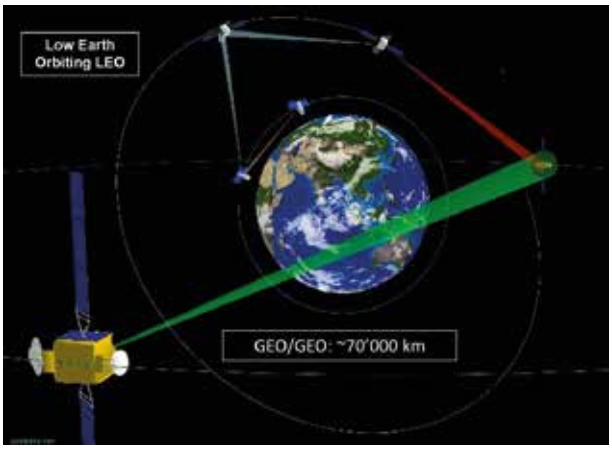

Quelle: ESA

Ein weiterer Artikel in dieser Ausgabe ist ebenfalls gedacht, durch sachliche und unaufgeregte Information Vorbehalte und Ängste in der Öffentlichkeit zu einem Reizthema abzubauen. Unsere Autoren W. Kröger und A. Stankovski (Seite 8) berichten über Fortschritte bei den Kernreaktoren, die vermutlich nicht jedermann geläufig sind. Gerade im Hinblick auf die CO_2 und Klimaproblematik, die momentan wegen der Corona-Pandemie nicht im Fokus der Medien steht, aber dennoch nichts an Brisanz verloren hat, findet weltweit ein Umdenken statt. Die Schweiz und weitere Länder haben entschieden, künftig auf Kernenergie zu verzichten, während andere Länder in neue Konzepte investieren, bei denen Sicherheit, Effizienz und Vermeidung, sowie Abbau bestehender langlebiger Isotope im Vordergrund stehen.

Beim Bürgi Symposium 2020 in Lichtensteig (Seite 40), das leider dieses Jahr der Pandemie zum Opfer fiel, aber 2021 stattfinden soll, wurde von jüngeren Kantonspolitikern angeregt, die Themen Kernenergie und Klimaproblematik öffentlich anzusprechen. Sie beobachten, dass die Bevölkerung und vor allem junge Leute stärker denn je an Varianten ihrer Zukunftsgestaltung interessiert sind. Es obliegt uns Physikern, Tatsachen anschaulich und wertefrei zu übermitteln.

1 *https://www.sps.ch/artikel/physiker-in-der-industrie/optical-space-communication-information-transfer-from-point-to-point-reinhard-h-czichy-synopta-gmbh-st-gallen-2/*

Rückblick auf die Generalversammlung 2020
Rétrospective de l'Assemblée Générale 2020

Wie in der letzten Ausgabe der *SPG Mitteilungen* berichtet, musste die diesjährige Jahrestagung leider abgesagt werden. Die Generalversammlung sowie die Preisverleihung fanden am 1. Juli virtuell in Form zweier Videokonferenzen statt.

Da diese Form der Durchführung einer Generalversammlung doch sehr ungewohnt war, waren im Zuge der Vorbereitungen Sorgen aufgekommen, ob überhaupt eine genügende Zahl von Mitgliedern teilnehmen würde, um repräsentative Ergebnisse bei den Wahlen und Abstimmungen zu erhalten.

Erfreulicherweise war die Zahl der Mitglieder jedoch ähnlicher gross wie bei einer realen Versammlung, und auch das virtuelle Abstimmungsprozedere verlief problemlos.

Die Preisverleihung konnte genauso reibungslos durchgeführt werden. Auch wenn den Gewinnern (vorgestellt in der letzten Ausgabe) nicht die Zeit für einen ausführlichen Vortrag zugestanden werden konnte, konnten sie doch jeweils in rund 5 Minuten die wesentlichen Ergebnisse ihrer Arbeiten präsentieren.

Trotz der überwiegend positiven Erfahrungen mit der digitalen Variante zeigte sich doch sehr deutlich, wie wichtig der persönliche Kontakt an einer Tagung ist, um nicht nur Fakten zu vermitteln, sondern auch, um Diskussionen bei einer Tasse Kaffee unter vier Augen führen zu können.

Im Rahmen der Ankündigung der Generalversammlung haben wir in der letzten Ausgabe Ralph Eichler vorgestellt, welcher dem Vorstand als neues Ehrenmitglied vorgeschlagen worden war. Nach Redaktionsschluß wurde ein weiterer Vorschlag für Kathrin Altwegg-von Burg eingereicht, welcher glücklicherweise für die Generalversammlung noch berücksichtigt werden konnte. Wir reichen den Nominierungstext hier nach.

Weiterhin präsentieren wir anschliessend die neu gewählten Vorstandsmitglieder. Das Protokoll der Generalversammlung wird wie gewohnt zusammen mit den übrigen Mitglieder-Informationen in den *SPG Mitteilungen* Nr. 64 publiziert.

Wir gratulieren den neu ernannten Ehrenmitgliedern sowie den neu gewählten Vorstandsmitgliedern und wünschen diesen viel Freude und Erfolg in ihren jeweiligen Ämtern.

Comme annoncé dans le dernier numéro des *Communications de la SSP*, la conférence annuelle de cette année a malheureusement dû être annulée. L'Assemblée Générale et la cérémonie de remise des prix ont pu avoir lieu virtuellement le 1er juillet sous la forme de deux vidéoconférences.

Avec cette forme de tenue d'assemblée générale plutôt inhabituelle, des inquiétudes avaient fait jour au cours des préparatifs quant à savoir si le nombre de membres participants serait suffisant pour obtenir des élections et votes représentatifs.

Bien heureusement, le nombre de membres était proche de celui d'une réunion habituelle, et la procédure de vote virtuelle s'est déroulée sans problème.

La cérémonie de remise des prix a tout aussi bien fonctionné ; même si les lauréats (présentés dans le dernier numéro) n'ont pas eu le temps de faire une présentation détaillée, ils ont pu présenter les principaux résultats de leur travail en 5 minutes environ chacun.

Malgré l'expérience positive de cette version numérique, il apparaît bien évidemment que le contact personnel est important lors d'une conférence, non seulement pour transmettre des faits, mais aussi pour pouvoir discuter en privé informellement autour d'une tasse de café.

Dans le cadre de l'annonce de l'Assemblée Générale, nous avions présenté Ralph Eichler dans le dernier numéro, qui avait été proposé au comité comme nouveau membre d'honneur. Après la date limite de rédaction, une proposition similaire pour Kathrin Altwegg-von Burg a été soumise, qui a heureusement encore pu être prise en compte pour être présentée à l'Assemblée Générale. Nous soumettons le texte de la nomination ci-dessous.

En outre, nous présenterons les membres du comité nouvellement élus. Comme d'habitude, le procès-verbal de l'Assemblée Générale sera publié avec les autres informations pour les membres dans le n° 64 des *Communications de la SSP*.

Nous félicitons les nouveaux membres d'honneur fraichement nommés ainsi que les membres du comité nouvellement élus et leur souhaitons beaucoup de joie et de succès dans leurs fonctions respectives.

Neues Ehrenmitglied - Nouvelle membre d'honneur

Kathrin Altwegg-von Burg

After initial schooling in Balsthal and a classical Matura at the Gymnasium Solothurn, Kathrin studied experimental physics at the University of Basel. She completed her doctorate in 1980, based on a study of excitons in molecular crystals. Following two years as a post-doc at New York University, where she continued working in molecular physics, she returned to Switzerland. Through a then existing SPS job placement service she found a position in the Physics Institute of the University of Bern, where Johannes Geiss led a group preparing a space experiment for a fly-by of the nucleus of comet Halley in March 1986.

The space probe to be sent to Halley was called "Giotto" and carried a mass-spectrometer that was going to measure the abundance of elements in the comet's coma. It found, besides the light elements, atoms that occur in rocks and minerals, such as Na, Mg, Si, Fe and Ca.

Following the completion of the analysis of the Giotto observations, Hans Balsiger, with Kathrin Altwegg as Project Manager, started preparing a long-term project: design-

ing, constructing, testing and calibrating the "Rosina" instrument (the "Rosetta Orbiter Spectrometer for Ion and Neutral Analysis"). "Rosina" – mounted on ESA's Rosetta spacecraft – was launched in 2004 onto a ten-year journey through space, including several swing-by manoeuvres at planets, and reached the comet 67P/Churyumov-Gerasimenko (commonly known as "Chury") when the comet was ca. 30 light-minutes away from Earth. Prof. Altwegg then led the Rosina Science Team while the instrument with its mass-spectrometers and pressure gauges probed the tenuous neutral and ionized gas released by "Chury's" nucleus at distances ranging from 100 km to 30 km between August 2014 and September 2016, a time span that comprised the perihelion.

From the data collected in this time Prof. Altwegg's team found that the water evaporating from "Chury" has an isotopic composition that is different from that of water on Earth. There are even indications that the comet's ice is older than the Solar System – and this led to the conclusion that the water in the comet likely stems from the cold molecular cloud, out of which our Solar System later formed. Of interest are also the detections by "Rosina" of numerous organic molecules; these range from simple to rather complex, such as the amino acid Glycine. In discussions and publications with many international experts, the team came to the conclusion that the existence of organic compounds found in "Chury" may be considered as evidence that cometary impacts on Earth favoured the origin of life.

Beyond her intensive research activities, Prof. Altwegg took time to head University institutions, such as the "Center for Space and Habitability". She led the CSH as its first Director until early 2016 and thus stimulated and supported research in habitability – a still growing multi-disciplinary enterprise that emerged with the discovery of exo-planets. She also strongly encouraged the participation of small and medium size enterprises in technology developments for space missions like Rosetta, an activity made possible by ESA's PRODEX (PROgramme de Développement des EXpériences scientifiques). In this context the "Berner Handels- und Industrieverein" awarded Prof. Altwegg their 2015 Prize, acknowledging that efforts to convey the fascination of scientific knowledge to young people is her vocation, and that space missions like Rosetta do not only help the involved scientists, but also the local economy, where it stimulates advanced developments and facilitates the recruiting in the relevant professions.

Besides her scientific qualifications, Kathrin is a sought-after speaker for talks to a wide public. She regularly fascinates her audiences with the tale of the adventurous investigation of the far-away comet "Chury", which now appears to be a witness from a time that preceded even the formation of our Solar System!

The proposed laudatio reads as follows:

Für ihre grossen wissenschaftlichen Leistungen in der Physik des Sonnensystems, insbesondere der Kometenforschung, für ihren ausserordentlichen Einsatz in der Öffentlichkeitsarbeit und für ihr weitsichtiges Engagement in der Förderung von Verbindungen zu kleinen und mittleren Unternehmen, wird Kathrin Altwegg-von Burg zum Ehrenmitglied der Schweizerischen Physikalischen Gesellschaft ernannt.

Preisträger und neue Ehrenmitglieder während der virtuellen Preisverleihung - Lauréats et nouveaux membres d'honneur pendant la céremonie de remise des prix virtuelle: Oben - en haut: Kathrin Altwegg-von Burg, Hans Peter Beck (SPG Präsident), Michael Becker (SPG Preis). Mitte - au milieu: Philipp Werner (Charpak-Ritz Preis), Ralph Eichler, Frank Schindler (SPG Preis). Unten - en bas: Hiske Overweg, Katharina Schmeing (SPG Preise). Nicht abgebildet - pas montré: Shantanu Mishra (SPG Preis), Claudia Merlassino (CHIPP Preis).

Neue Vorstandsmitglieder - Nouveaux membres du comité

Prof. Dr. Johan Chang (Vice-president)

I am working in the field of experimental condensed matter physics and since 2015 I am professor at the University of Zürich. Originally from Denmark, I did my PhD (2005 - 2008) at the Paul Scherrer Institute under the supervision of Joël Mesot. My postdoc period gave me the opportunity to work with Prof. Louis Taillefer (Sherbrooke - Canada) and Prof. Henrik Rønnow (EPFL). My current group consists of about 12 people (postdocs, PhD students and technicians) working on physics of strongly correlated electrons and superconductivity.
My motivation for being a candidate for the vice-president and later the president position within the Swiss Physical Society is simple: I wish to contribute actively to the Swiss physics community. As vice-president, I will spend my first period learning the organizational tasks. Obviously, it is important to preserve and continue the traditions of the Swiss Physical Society. In term of new initiatives, I intend to work for more active outreach, which is ever more and more important to maintain a healthy with society at large.

Dr. Marisa Medarde (Section KOND)

Marisa Medarde obtained her PhD in Physics at the University of Barcelona. After a post-doc at the Paul Scherrer Institute (Switzerland) and two years at the Argonne National Laboratory (USA) she returned to Switzerland, where she is leader of the Physical Properties of Materials group at the Research with Neutrons and Muons Division of the Paul Scherrer Institute. Her research is focused on the study of complex transition metal oxides with highly correlated electrons using neutron and x-ray scattering techniques in combination with bulk transport and magnetic properties. Presently, her main scientific interests are multiferroic materials and complex oxides at the boundary between itinerant and localized behavior.

Prof. Dr. Guillermo Pedro Acuna
(Section Atomic Physics and Quantum Optics)

Since 2018 Guillermo Pedro Acuna is a Full Professor at the Physics department of the University of Fribourg where he leads the Photonic Nanosystems group. He has pioneered the use of the DNA origami technique for nanophotonics focusing on the fabrication of optical antennas for enhanced spectroscopies. Prof. Acuna obtained his Physics diploma at the Universidad de Buenos Aires (2005) and his PhD degree at the LMU München (2010) under the supervision of Prof. Roland Kersting. He has done a Post-Doc at Prof. Hermann Gaub's chair for Biophysics at the LMU München (2010). From 2011 till 2017 he was group leader at Prof. Philip Tinnefeld's chair at the Technical University of Braunschweig. In 2018, Prof. Acuna obtained a Full Professor (W3) position at the University of Rostock. His main interests are developing techniques to control and manipulate light-matter interactions at the nanoscale for a wide variety of applications in the fields of plasmonics, nanophotonics, single-molecule fluorescence, optical communication, super-resolution and bio-sensing.

Prof. Dr. Christof Aegerter
(Section Biophysics, Soft Matter and Medical Physics)

Christof Aegerter (born in Bern in 1972) is a professor of Physics at the University of Zürich (UZH), where he also studied after a high school internship with Walter Kündig on a project measuring the gravitational constant at intermediate distances. He has a long-standing interest in collective phenomena and disordered media, which started in 1998 with his Ph.D. in condensed matter physics at UZH with Hugo Keller, studying the melting of a lattice of magnetic flux lines inside superconductors, using neutrons and muons. This was mostly carried out at PSI as well as by using neutron and muon sources in France and the UK. Since then he has moved between different countries as well as fields, starting in California where he got involved in the physics of convection and fluid dynamics. From there he moved to the Netherlands to work on understanding how avalanches evolve in granular media, and how they connect with flux jumps in superconductors, finally arriving in Germany to study levitated foams and granular gases as well as light transport in turbid media. During the time in the Netherlands and Germany, he also started to get interested in the physical basis of biological development, which he studied mostly theoretically in the context of the fruit fly drosophila.
In 2008 he returned to Zürich, to lead a research programme in disordered and biological soft matter at the University of Zürich. Here, he started the experimental investigation of biological development and its connection to active materials, as well as applying the insights of light transport in turbid media he gained during his time in Germany to the imaging and microscopy in turbid media and the understanding of structural colours. Recently, he has started to extend his research concerning light transport into the optimization of materials for high absorption of light with an emphasis of harnessing solar energy. Just as important are the teaching and outreach aspects of his work, where he is trying to convey the fascination and fun of doing physics to students of biology and chemistry, to school children as well as for the public at large. In this context, he is a member of the

regional board of the Swiss academy of Sciences SCNAT and has recently shared the stage at Theater Rigiblick with stand-up comedian Hazel Brugger, showing that Physics can be fun and beautiful.

Dr. Christof Fattinger
(Section Biophysics, Soft Matter and Medical Physics)

An Austrian citizen born in 1954 in Brazil, Christof Fattinger moved with his family as a teenager from Wiesbaden (Germany) to the Basel region, where he graduated from the gymnasium in Münchenstein, Switzerland. He received the Swiss citizenship in 1979.
Christof Fattinger studied physics at ETH Zürich and received his Ph.D. degree in 1987. From 1987 to 1989, he worked as postdoc fellow at the IBM, T. J.Watson Research Center, NY, in the group of Daniel R. Grischkowsky. His work at IBM led to an optoelectronic technique for generating diffraction-limited beams of terahertz electromagnetic pulses. He co-authored the most frequently cited scientific article in the field of terahertz spectroscopy.
From 1989 - 2019 Christof Fattinger was working in pharmaceutical research at the Roche Innovation Center in Basel. In 2010, he was awarded the status of Distinguished Scientist, the highest accolade for a Roche researcher. His pioneering work at Roche is described for a non-technical audience in an essay entitled “Die Perlentaucher - Ingenieurskunst für neue Medikamente” by René Imhof und Sabine Päuser (The pearl divers - engineering art for new medications). The essay was published in the book edited by NZZ Libro “Ingenieure bauen die Schweiz” (Engineers build Switzerland).
His current research activities concentrate on molography, a new method for the investigation of biomolecular interactions. Molography uses a coherent arrangement of specific molecules on a sensor chip that enables the quantitative analysis of their interactions with molecules in complex biological samples.
Christof Fattinger is an Individual Member of the Swiss Academy of Engineering Sciences (SATW).

Dr. Gernot Scheerer
(Section Education and Promotion of Physics)

I am an experimental physicist in the domains of solid state and low-temperature physics and a science-outreach enthusiast, working at the Department of Quantum Mater Physics (DQMP) of the Geneva University. Soon, I will change for CERN, where I will be in charge of the educational program S’Cool Lab.
Before my scientific career, I studied Physics in the tri-national program SaarLorLux, which is proposed by the Universities of Luxemburg, Lorraine (FR) and Saarland (DE). Thanks to this program I studied in Luxemburg, France and Germany and obtained a French-German double diploma in 2010.

I did my PhD at the Laboratoire National des Champs Magnétiques Intenses (LNCMI) of Toulouse from 2010 to 2013. The theme was "heavy-fermion superconductors under extreme conditions”. I did experiments in the non-destructive pulsed field magnets of the LNCMI, which can go up to 80 T.
In 2013, I joined the DQMP, where I have since then collaborated with the teams of Prof. Didier Jaccard, Prof. Jean-Marc Triscone and Prof. Dirk van der Marel. I have been doing experimental work on the DQMP flagship themes: unconventional superconductors, strongly correlated electrons, low-dimensional electronic systems, and extreme conditions (milli-Kelvin temperatures, Giga-Pascal pressures).
Parallel to my research, I have guided practical physics exercises for bachelor students for several years, and since September 2018, I am part of the outreach program Physiscope of the University of Geneva.
Furthermore, I do many voluntary outreach activities, mostly about the themes: nature of science and superconductivity (e.g. at elementary schools, for the year of Superconductivity 2011, at the Toulouse Space center, at the Geneva science nights).

Dr. Margherita Boselli (Editorial team)

I am currently a post-doctoral researcher at the University of Geneva, where I completed my PhD in June 2019. I moved to Switzerland after my Bachelor and Master studies in Italy, at the University of Pavia, and in France, at the Laboratoire de Physique des Solides, University of Paris-Saclay.
Along with my scientific focus, which is on the electronic properties of complex oxide thin films, I am actively involved in physics outreach and I am part of the Physiscope group of the University of Geneva. Very soon I will step out of the laboratory to join the Education Team at CERN.
In Switzerland I found the perfect conditions to grow as a scientist and I believe that it is time to give something back. This is the reason why I am strongly motivated to get more involved in the Swiss Physical Society and contribute to the education and communication section. I am convinced that my scientific background, my curiosity and enthusiasm for physics will be assets for the continuous improvement of the Swiss Physical Society activities.

Progress in Physics (75)

Novel reactor concepts: Asset in a future de-carbonized energy mix?

Wolfgang Kröger, Andrej Stankovski, ETH Zürich, Chair of Entrepreneurial Risks

1. Background and motivation

By the end of 2018 [1] the global primary energy consumption totaled to 166,379 TWh, has doubled within the last 50 years and increased by 2.9 % compared to 2017. Almost 40 % are converted into electricity which corresponds to a 16 % share of the final energy demand. Scenario analyses predict a massive growth of primary energy, mainly driven by developing countries, to cope with the expected increase of world population and expand energy access and economic opportunities to billions of people. The electricity sector is expected to grow disproportionally, by a factor of 2.5 till 2050 [2], notably to penetrate non-traditional domains, i.e. e-mobility, digitalization, buildings.

This challenging trajectory is confronted by the requirement to deeply de-carbonize the energy system, currently relying at about 85 % on fossil fuels [1]. The electricity production, based at 64 % on coal, gas and oil, contributes almost 30 % to the global CO_2 emissions of 34 gigatons (increased by 2 % compared to 2017). Therefore, the electricity sector needs a new mix and roughly doubled share of low-carbon generation assets by 2050 to meet the "2 °C climate target", while other sustainability indicators like use of land and other resources, affordability, waste production, factorial and perceived risks must be kept in mind.

Most scenario-based projections (see also [3]) and strategies focus on expanded use of renewable energy sources. Besides hydro with a share of roughly 15 %, wind and solar contributed 9.3 % of the global power production (18.7 % in Europe) in 2018, with a 14.5 % annual growth, slightly below its historical average. However, there are growing concerns about whether (a) renewable generation will grow sufficiently fast, (b) variable energy sources alone will be sufficiently secure and (c) the required infrastructure including seasonal storage, upgraded grids and flexible backups can be provided.

Currently, nuclear power contributes 10.15 % to global electricity production – 23 % in Europe. The share increased from about 2 % in 1971 to 18 % in 1998, decreased afterwards but grew in 2018 by 2.4 %, the fastest growth since 2010, to which China contributed almost three quarters [1]. However, its prospects are dim in many parts of the world, with costs [4], lack of public acceptance and some unresolved issues including disposal of radioactive wastes as key problems [3]. Future shares of electricity production by nuclear energy are ambiguous, vary from zero [5] to a grow by 28 % till 2040 [2] – the latter corresponds to additional 510 GWe, and questions deployment readiness as well as industrial and regulatory capabilities.

2. Characteristics of nuclear energy and status of use

The use of nuclear power has proven to be a mature technology. In 2019 [6], there was a fleet of 450 reactor units with 398.9 GWe total net installed capacity in operation, distributed throughout 31 countries. The clear majority (80%) of all operating units are light water reactors (LWR), which use low enriched uranium (3-5% U-235). Experience accumulated to roughly 17000 reactor-years; the mean capacity factor was 80 %. There are 53 units under construction with 54.7 GWe in 20 countries, the majority of which in China (10). New builds in the Western world are rare and, like the European Pressurized Water Reactor (EPR) in Finland and France, confronted with tripled cost and construction time overruns, while projects in Asia tend to stay within basic conditions.

Uranium has incomparably high energy density: The energy density of a mix of natural (non-fissile) U-238 and Pu-239 used in breeder reactors is approximately 80.620 GJ/kg, meaning that, while undergoing full breeding and fission, one kg of uranium is the equivalent of burning 3500 tons of black coal [3]. Considering just the current proven uranium reserves in the low- and higher-cost range extraction the world can produce enough uranium for the next 125 years, with the current yearly consumption of uranium of roughly 63000 tons. When considering the inferred and reasonably assured resources, the total reserves and operating times are estimated to double [7]. Furthermore, moving to advanced nuclear options including breeder reactors, using thorium as fuel and application of new mining and extraction technologies could place nuclear as a practically unlimited resource.

Current nuclear technology has very low greenhouse gas emissions, comparable to hydro and wind, less than PV roof when considering the whole life cycle. By 2050, with the deployment of next generation reactors, the emissions are estimated to decrease further [8].

Nuclear power is not without its drawbacks, both in the physical process and current technologies. The decay of short-lived fission products is accountable for heat production after reactor nuclear shutdown while long-lived fission products together with actinides after neutron absorption

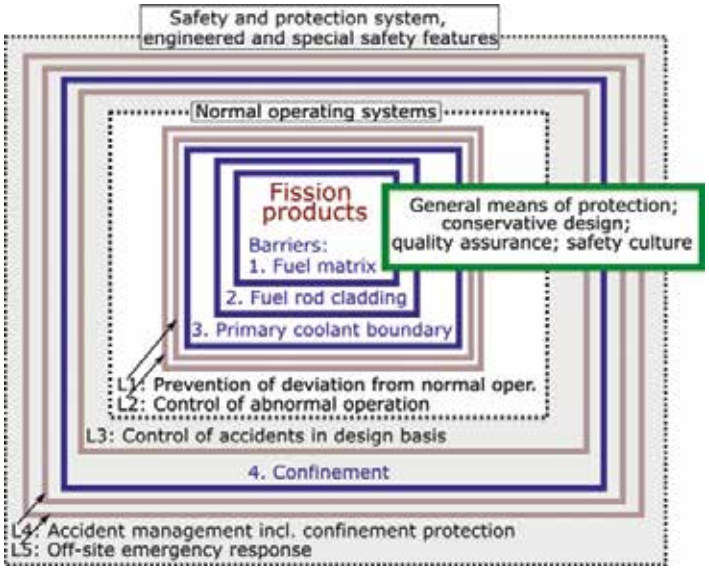

Fig. 1 Defense-in-depth: Four physical barriers (blue) and five levels of protection (brown), split into normal (white inner) and safety/ protection (grey outer) operation layers, adapted from (IAEA 1999).

call for ultra-long confinement times. This leads to major design challenges and implementation of safety functions as regards to fission product confinement, reactivity control and decay heat removal, under all conceivable circumstances as well as for management and long-term storage of nuclear waste. Current safety principles like defense-in-depth (Fig. 1) and proven technologies address these issues successfully.

However, certain aspects are still problematic, such as reliance on active safety systems, early operator actions, vulnerable structural metallic material, and little grace time (one to two hours) in case safety systems fail. Major safety improvements are demonstrated by decreasing core damage frequency (CDF) estimates – from 10^{-4} to 10^{-5} for operating LWR to as low as 10^{-6} for advanced and some retro-fitted plants, each per reactor-year [3][23]. The likelihood of large radioactive releases is roughly by one order of magnitude smaller, depending on the containment design. However, they cannot be excluded and provoke public fear.

The other issue of concern is radioactive waste burden. LWR follow one of three fuel cycle concepts, “once-through”, “partially closed” and “fully closed” [3]. In the once-through cycle, spent fuel (SF) is sent for extended interim storage and emplacement in deep geological repositories. On the other hand, SF can be reprocessed to extract fissile material such as uranium and plutonium before disposal (partially closed cycle). In the fully-closed fuel cycle, uranium, plutonium, and other minor actinides (long-lived radionuclides) are extracted and used as fuel in advanced fast reactors. The once-through cycle is the most favorable in terms of proliferation issues as no separation of fissile material, Pu in particular, takes place. In contrast closed fuel cycle concepts allow for better exploitation of fuel reserves, and bring down amounts of low-level nuclear waste.

All fuel cycle concepts require a safe and long-term disposal of radioactive wastes. However, due to inherent uncertainties, strong opposition and strict regulatory/safety requirements, the advancements are still slow, and there is no operating deep geological repository around the world, yet. Nevertheless, Finland is in the lead, granting license and starting construction at Olkiluoto site in 2015 with the disposal process expected to start by 2024.

There are major barriers to make future, potentially expanded, use of nuclear power acceptable to the public such as general safety concerns and risk aversion, in particular, including the (i) unequal treatment of extra-ordinarily low probabilities and high consequences of potential accidents and (ii) the perceived cancer dread of even low doses of radiation.

3. Challenges and means to overcome barriers

3.1 Key requirements

To overcome risk aversion-related barriers, we recommend a fundamental shift from reactor designs that depend on properly functioning (active) safety systems, requiring AC power and reliable actuation mechanisms, towards designs that incorporate passive and inherent safety features. Furthermore, nuclear plants should be less sensitive to adequate protection against natural events and malicious man-made physical or cyber-based attacks; they should warrant higher tolerability to human errors, lack of safety culture and socio-political instability within the operational environment. Fuel cycle concepts should allow more efficient use of resources and alleviate requirements to high-level waste disposal. The following key requirements, aiming at a deterministic exclusion of serious conditions and states, are put forward (see [3] for details):

1) *Reactivity control*, i.e. elimination of potential reactivity induced accidents, by
   a) weak/negative reactivity coefficients,
   b) small reactivity surplus at startup with fresh fuel.
2) *Assurance of heat removal* to ultimate heat sink and retention of fission products, by
   a) low power density and power size (to avoid exceeding critical temperature limits),
   b) resistant fuel cladding and structural material that will not melt or react chemically,
   c) sufficient heat storage capability and inherent/passive heat transfer mechanisms in case of loss of normal (forced) cooling.
3) *Securing structural integrity* to avoid loss of core cooling capability/confinement of radioactive inventory by
   a) low primary circuit pressure or rupture proof components (reactor pressure vessel),
   b) radiation resistant, chemically and physically robust core structures,
   c) underground siting for protection against extreme external impact, including weapons’ attack.
4) *Use of non-reactive, non-toxic materials/fluids* or avoid direct contact of reacting substances.
5) *Avoidance/incineration of long-lived radioisotopes*, by
   a) a switch to thorium with drastically smaller generation of long-lived minor actinides,
   b) waste burner core designs,
   c) striving for long-term stable, high burn-up SF as an open fuel cycle option.
6) *Enhanced intrinsic proliferation resistance* characteristics, basically by applying established principles, means and strategies by avoided use of highly enriched uranium (HEU) and off-line reprocessing of SF if there is no strategy to minimize the time during which weapons-grade material, notably plutonium, is in separated form and to avoid accumulating a stockpile.

3.2. Building blocks

To achieve these ambitious requirements, key design features for advanced nuclear reactors and related systems can be identified. They include neutron spectra and coolants, furthermore fuels, fuel claddings and core structural materials, power densities and power sizes, and siting options. A look at the fission probabilities (“cross sections”) of selected actinides demonstrates the attractiveness of fast *neutrons* compared to moderated neutrons that dominate the spectrum of today’s LWR. While thermal fission cross sections of fissile U-233 and U-235 and Pu-239 are significantly larger than those for fast fission, their important fission-to-absorption ratio is of the same order but significantly higher for other selected isotopes, in particular atoms heavier than uranium. Large fission-to-absorption ratios are favorable to avoid or minimize the formation of radioactive waste and minor actinides, in particular. Eliminating these isotopes from spent nuclear fuel would reduce drastically the stewardship times of the long-lived wastes (up to a factor 100).

Fast neutron spectra, together with adequate coolants, allow for high neutron economy and reactor designs that are favorable to produce as much or more fissile material than consumed ("breeder reactor") and/or incinerate radioactive waste ("waste or actinides burner"). However, the cores of fast reactors are not in the state of highest reactivity under steady-state operational conditions; changes of physical parameters could lead to disruptive power excursions.

Considered *coolants*, i.e. liquid metals like sodium, lead or lead/bismuth, molten salt (fluorides or chlorides) and gas (helium) are briefly characterized here, for details see [3]. All liquid metals and salts feature good heat storage and transfer capabilities and no need for pressurization for operation in a single-phase mode. But high density and mass may lead to high static loads, notably for lead. All liquids and gas allow for core outlet temperatures of about 510 °C (molten sodium) to almost 600 °C (molten lead, molten salt) or even 850/950 °C (helium), significantly higher than for water. This results in thermodynamic efficiencies for power production clearly above 40 % (rather than 33 % for LWR) and potential use for chemical heat applications.

Current reactors base their *fuel* on metal oxide (UO_2) rather than metals themselves, because the melting point is much higher (2850 °C) and it cannot burn, although its thermal conductivity is very low. Ceramic fuels have the advantage of high heat conductivities and melting points (2700 - 2800 °C) but are more prone to swelling than oxide fuels. Uranium-carbide, most notably in the form of coated micro particles together with ceramic (or graphite) structural material, are regarded as attractive fuel for certain future reactors. Liquid fuels, i.e. dissolved in molten salts, offer numerous operational advantages due to inherently stable self-adjusting reactor dynamics, rapid drain ability into dump-tanks and continuous release of xenon gas that acts as a neutron absorber.

Making fuel, fuel cladding and structural material more resistant to temperature rise and resulting core damage is a promising way to increase the robustness of nuclear reactors against potential accidents. A huge program on "accident tolerant fuel", coordinated by Westinghouse, is focused on high temperature resistant enriched U_3SiC fuel pellets and protecting claddings from oxidation by coating.

Moreover, *thorium* (namely Th-232) is becoming a promising fuel option, for which all uranium fuel cycles apply. Thorium is three to four times more abundant than uranium and has superior physical properties in metallic and oxide states (high melting points, high thermal conductivity, small expansion coefficient). It has more specific energy (200 times more than natural uranium), and produces less nuclear wastes with shorter lifetimes [9]. Th-232 does not undergo fission itself but, on capturing a neutron, it leads to U-233 as final fissile product of the reaction chain. U-233 could be misused for weapon production and, as its forerunner Pa-233 can be separated effectively, the Th-232 fuel is not regarded proliferation proof. Thorium-based technologies are still at early phases with little commercial experience.

Steel alloys dominate the *material for reactor* (pressure) *vessels*; "absolutely" rupture proof pre-stressed concrete reactor pressure vessels are technically feasible.

Nuclear fission enables reactors with high power density and power rating: typical power densities vary from 70 for current LWR to about 290 MW/m^3 for conceptual designs of sodium cooled fast reactors, while those of liquid lead or salt cooled fast reactors are less than half that high and those of gas-cooled thermal reactors are small, in principle. Power ratings follow the economy of scale with 4800 MWth (1600 MWe) of modern large size LWR as a reference point. In principle, high power density and power rating make the reactors more susceptible to loss of coolant/decay heat removal accidents. In other words, limiting the power densities and power rating, together with other means, could provide flexibility to increase the robustness of nuclear reactors.

There is a revival of interest in small and simpler units for electricity production and other purposes. The incentive to develop small (up to 300 MWe) modular reactors (SMR) comes from different sources. There is a strong belief [10] that SMR would

- open additional market sectors, e.g., heat for chemical processes, and, based on enhanced safety characteristics, allow for site flexibility;
- better adapt to low growth rates of energy demand, are more suitable to replace aging fossil-fired plants;
- lower upfront capital cost and ease financing and earlier revenues;
- allow for greater simplicity of design, enable economy of serial production largely in factories and, thus, shorter construction times.

As the inventory of fission products is proportional to the power level, a smaller amount could be released into the environment by smaller-sized reactors under loss of confinement conditions, in principle. However, some question the economic competitiveness of SMR and raise concerns regarding adequacy of the current regulatory system and license ability of some (first-of-its-kind) designs.

Site characteristics are relevant for ensuring that societal risks due to severe nuclear accidents are acceptably low and remote sites are deemed most suitable. However, driven by scarcity of actual remote sites and aspired use of nuclear reactors beyond power production sites closer to consumer centers may have to be permitted. Accordingly, the combination of small, inherently "super-safe" reactors and underground siting has been proposed, the latter allows to protect the plant against extreme external physical impacts.

4. Reactor concepts under development

In what follows, we aim to provide information about reactor concepts and associated states of development by looking into the R&D pipeline. Besides next generation thermal reactors, many prominent reactor concepts are fast reactors that allows them to breed more fissile fuel than they consume or even burn wastes. Most of their proposed designs can use various fuels including spent fuel (SF) from LWR, hence closing the fuel cycle and increases the utilization of uranium significantly compared to current LWR [11]. Most new concepts claim to be inherently safe and highly resistant to proliferation.

4.1 Sodium and lead cooled fast reactors

Heralded as one of the more promising next generation fast breeder reactor concepts, liquid metal cooled reactors (Fig. 2) have a high neutron economy and offer a variety of advantages over conventional. Sodium cooled reactors (*SFR*) in particular, have been in development for more than 60 years. The usual design employs a pool or loop type reac-

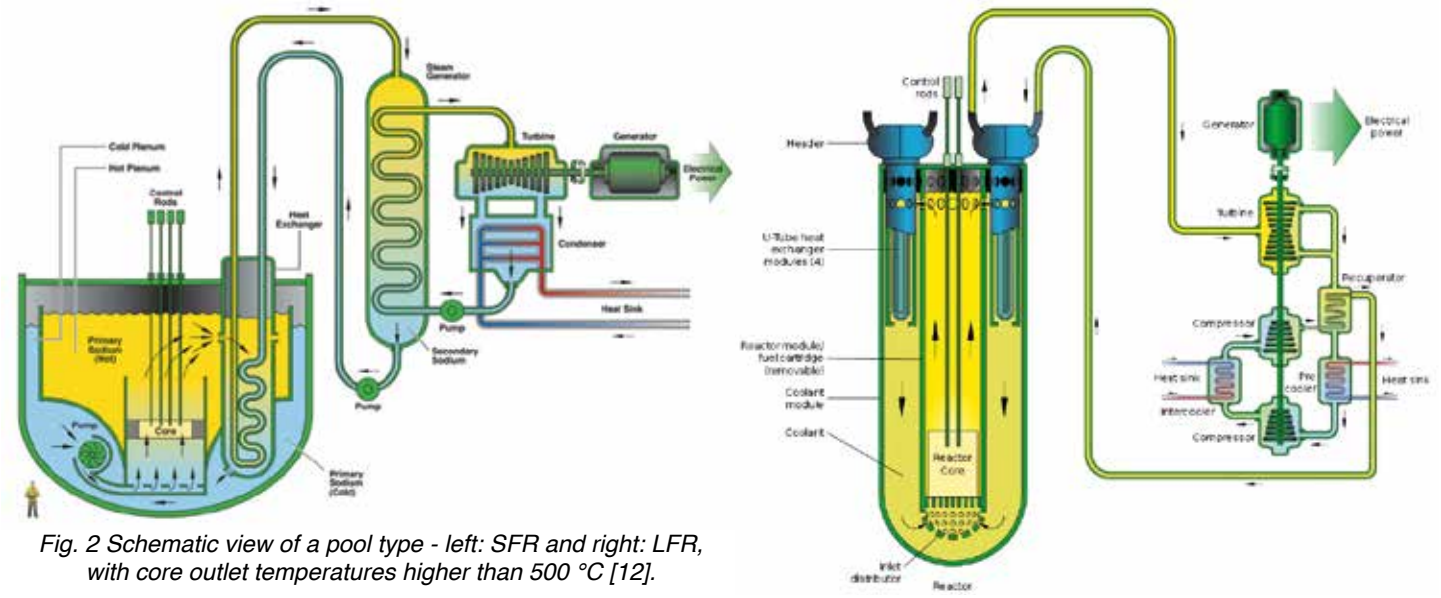

Fig. 2 Schematic view of a pool type - left: SFR and right: LFR, with core outlet temperatures higher than 500 °C [12].

tor filled with molten sodium, an intermediate sodium circuit and a secondary steam generator circuit [3]. Metal oxide fuel (MOX) potentially containing minor actinides is considered as the primary option for larger SFR (600 - 1500 MWe), while metal alloy fuel with minor actinides can also be used for designs in the range of 50 - 600 MWe. All designs use a parfait blanket of fertile material (U-238 and potentially Th-232) in order to increase breeding efficiency. Combined with re-processing techniques which cannot extract plutonium (aqueous re-processing for MOX fuel and pyro-metallurgical for metal alloy fuel), the modern SFR designs are proliferation resistant in this respect. The primary disadvantages of these reactors are the positive void and temperature coefficients (more pronounced in larger cores) and the exothermic reactivity of sodium with water and air.

Lead-cooled reactors (*LFR*) use molten lead or lead-bismuth (Pb-Bi) eutectic as a coolant and share many of the positive characteristics of the SFR. Unlike SFR, the coolant is not chemically reactive with water, making the intermediate coolant loop unnecessary, has a higher boiling point and the positive temperature coefficient is only slightly pronounced due to its neutronic properties [3]. In contrast, the higher melting temperature of the coolant (freezing concerns), Po-210 build-up, corrosive reaction with steel and coolant price (for Pb-Bi) are listed as some of the disadvantages.

Approximately ten liquid metal reactors are expected to be deployed in the near future, out of which PRISM and BREST-OD-300 appear the most promising.

PRISM (Power Reactor Innovative Small Module) is a generation IV SFR under development by GE Hitachi Nuclear Energy. The design comes with two reactor modules, each of 311 MWe power output, using uranium-plutonium-zirconium alloy fuel, which utilizes SF from LWR [13]. Based on the experimental breeder reactor (EBR-II), the design is proven to be both mature and reliable, with additional unique safety features such as negative temperature coefficient (small core size), passive decay heat removal via natural air circulation, and digital instrumentation and control. PRISM is in an advanced stage and as of 2019 has entered the US Versatile Test Reactor program, which aims to build a fast-breeder reactor by 2026 [14].

BREST-OD-300 is a generation IV, 300 MWe LFR developed by RDIPE in Russia. It is a pool-type reactor with passive decay heat removal using natural air circulation. The fuel used is uranium-plutonium mononitride (PuN-UN) mainly comprised of SF from LWR. The design is claimed to be resistant to loss-of-coolant and heat removal accidents, while the small operating reactivity margin prevents power excursions in normal operating conditions [15]. The reactor is in an advanced stage and construction was approved in 2016, with the first plant expected to be operating by 2025 [16]. A larger 1200 MWe version is planned to be built if operation of BREST-OD-300 proves to be successful.

4.2 Molten salt-cooled thermal and fast reactors

Molten salt reactor (*MSR*) designs have been of interest since the 1960s, with one experimental reactor (MSRE) in the USA, operable from 1965 to 1969. The main coolant is a molten salt mixture which can have different properties depending on the salt used (fluoride, chloride), while lithium salts with higher boiling points are preferable (> 1400 °C) as they allow operating at higher temperatures (750 - 900 °C). These reactors can operate with thermal or fast neutron spectra and use solid fuel or fuel dissolved into the coolant, which is the preferable option [3]. Both uranium or thorium-based fuel can be used, optionally with added minor actinides, with the reactor operating as a breeder or a waste burner. The next generation designs envision an unpressurized breeder or burner MSR with fuel dissolved in the coolant. The coolant is constantly circulated through the core and chemical processing plant, in which volatile fission products are separated and the fuel concentration is controlled (Fig. 3). In case of overheating, a freeze plug melts and dumps the coolant into tanks, which immediately stops the fission reaction. The decay heat from the tanks is passively cooled, making the design safe in station blackout scenarios. Main drawbacks of MSR are the corrosive properties of the coolant and potential criticality spikes.

There are multiple MSR under development, with the Danish SWaB (Seaborg Waste Burner) as one of the most promising concepts, designed as a modular reactor which uses SF and thorium. The reactor has a reliable passive overflow system which would dump the fuel in both overheating and prompt criticality scenarios [17]. Even in the worst-case scenarios, such as meltdown due to failure of the system to dump the fuel, the company claims that a redundant dump tank and a secondary barrier would prevent fission products

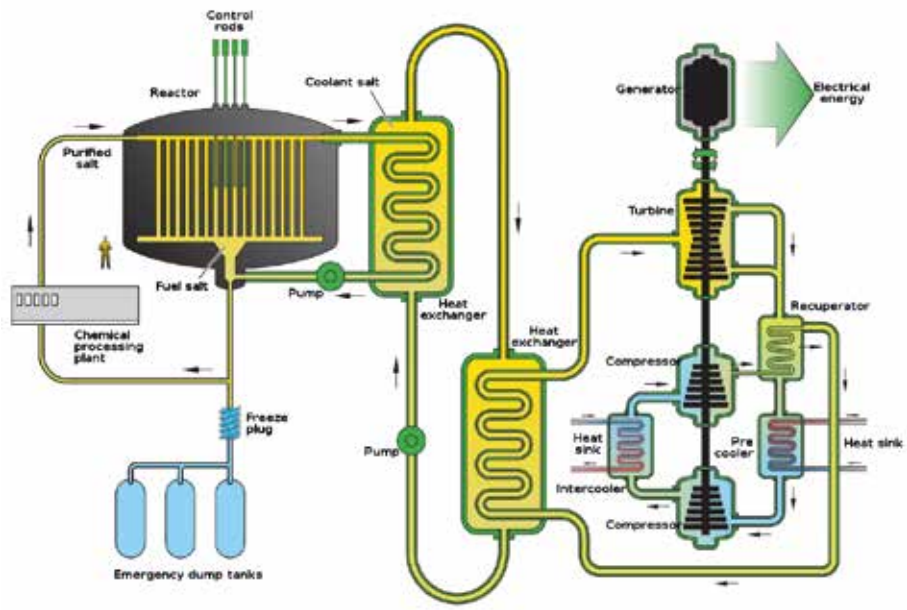

Fig. 3 Schematic view of MSR with online reprocessing, intermediate molten salt circuit and a steam cycle [12].

release to the environment. Although promising, the design is still in a very early stage of development.

4.3 High temperature gas-cooled thermal reactors

Modern high temperature gas-cooled reactor (*HTR*) designs focus on using graphite as moderator and helium as coolant (with inert properties). The high operating temperatures could also open new perspectives for nuclear power, such as cogeneration and hydrogen production [3][18]. The fuel in the form of ceramic pebbles is comprised of thousands of TRISO coated particles embedded in a graphite matrix. The TRISO coated particles consist of a lightly enriched (< 20 %) uranium kernel, a porous pyrolytic graphite layer to accommodate for fuel expansion, an inner and outer dense pyrolytic graphite layer and a silicon carbide (SiC) layer in between for fission products retention (Fig. 4a). HTR offers a range of advantages, such as pronounced negative temperature reactivity coefficient, continuous refueling, fission products retention up to fuel temperatures of about 1600 °C. Together with use of heat storage and convection capabilities, these reactors are deemed inherently safe. However, the concept is not without disadvantages: standard measuring equipment cannot be placed inside the pebble bed core and reprocessing of the ceramic fuel elements is very difficult, raising concerns about the increasing amount of nuclear waste. Multiple prototypes employing this technology were taken into operation, such as the AVR (Germany, 1966), THTR-300 (Germany, 1983) and HTR-10 (China, 2003).

The HTR-PM (pebble-bed modular) reactor (Fig. 4b) is currently under construction in Shindao Bay, China, and expected to become operational in 2020. The design specifies that two 250 MWth reactors, intended to operate at temperatures of 750 °C, will be connected to power a single 210 MWe turbine [18]. The reactor relies on inherent safety features and use of passive cooling systems for decay heat removal, practically eliminating the danger of station blackout events (large grace period). The main vulnerability of the design is that potential unrestricted air or water ingress could cause graphite corrosion.

4.4 Accelerator-driven subcritical systems

Accelerator-driven systems (*ADS*) are novel concepts comprised of a subcritical reactor and an external neutron source, usually a high-intensity proton accelerator [3]. The proton beam is focused on a metal target and produces neutrons by spallation. As the reactor is incapable of self-sustaining fission reactions, the chain reaction stops by turning off the accelerator. Therefore, these systems do not require the installation of control rods and eliminate the possibility of reactivity induced accidents. The reactor is conceptualized as a lead or lead-bismuth (Pb-Bi) cooled fast breeder reactor, introduced before. These characteristics make the ADS perfect for the burning of minor actinides (transmutation) which greatly reduces the husbandry times of nuclear waste.

One of the more promising concepts currently in development is MYRRHA (Fig. 5), a proposed actinide burner developed by the Belgian Centre for Nuclear Research. The design couples a subcritical (multiplication factor 0.95) Pb-Bi cooled fast reactor with a proton accelerator, focused on a liquid Pb-Bi spallation target. With a total budget of 1.6 billion euros, the system is expected to be commissioned by 2036 [19].

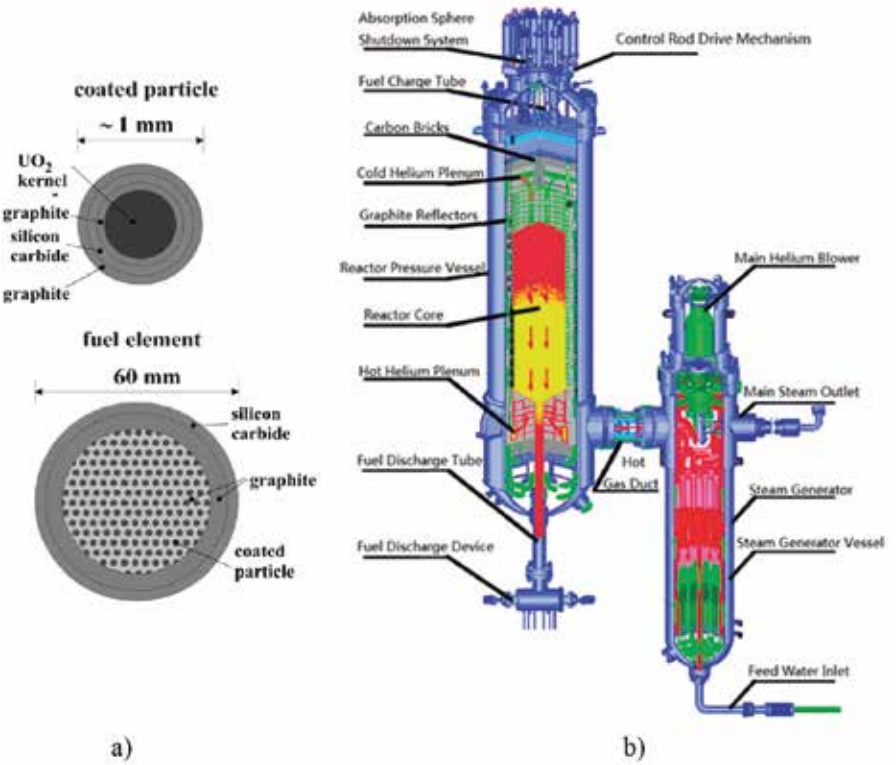

Fig. 4 Schematic view of HTR - a) TRISO coated particle and fuel element and b) HTR-PM reactor design [18].

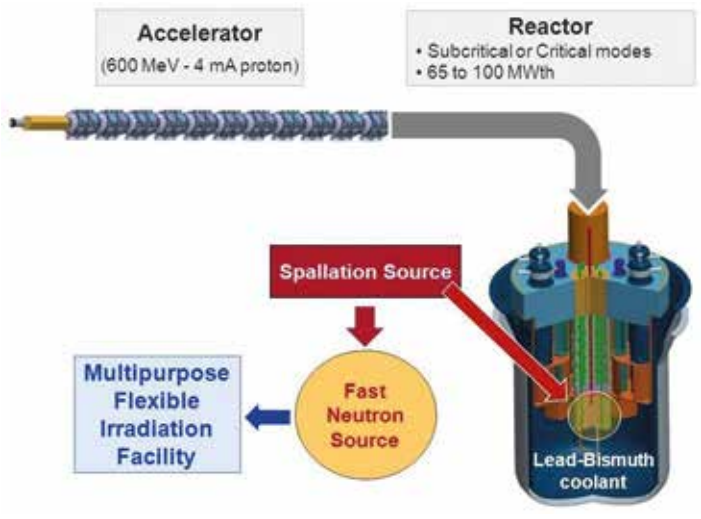

Fig. 5 Schematic view of MYRRHA (Multi-purpose Hybrid Research Reactor for High-tech Applications) [3].

4.5 Small-medium sized, modular reactor concepts

Following the expected benefits of small modular reactors (*SMR*) different concepts are currently under development worldwide (Fig. 6). They include smaller versions of all reactor types, including reactors with thermal and fast neutron spectrum; the most promising "revolutionary" designs discussed before are often considered as SMR.

Additional designs of interest are LWR-based SMR, which have the lowest technological and regulatory risk. The NuScale project in the USA appears to be in a well-advanced stage and initial deployment is expected in 2026. The 60 MWe reactors are based on mature PWR designs, with technological advancements which claim to make the reactor inherently safe, such as small size, small fuel and fission product inventory (1/20 of normal PWRs), containment immersed in the cooling pool, etc. [21]. Additionally, up to 12 reactors can be submerged in one cooling pool, still allowing power generation of 720 MWe.

Another interesting concept are the floating SMR, built at shipbuilding facilities and towed to designated areas where they could provide electricity, district heating and seawater desalination, especially in developing countries. The first plant of this kind is Akademik Lomonosov, recently commissioned in Russia. This plant is powered by two 35 MWe PWR, based on the KLT-40 marine propulsion reactor, with passive decay heat removal, modernized active safety systems and instrumentation [22].

5. Evaluation of selected candidate concepts against key requirements

The results of a concept-by-concept comparison indicate a high potential for far-reaching improvements compared to the most advanced LWR (Generation III+) as the benchmark. As can be can be seen from Table 1, none of the best versions, i.e. small sized in general, of the candidate concepts fully meet all requirements convincingly, yet [3][23]. Thermal helium cooled reactors (HTR-PM) come closest, promising inherent robustness against severe accidents and largely avoiding long-lived radio-isotopes when using thorium fuel. With respect to burning waste, molten salt fast reactors promise to do best but appear most susceptible to reactivity-induced accidents, as are all liquid metal cooled fast reactors are, albeit to different degrees. The only exception are the accelerator-driven systems (ADS), which are inherently resistant to RIA due to their subcritical core design. There is also a potential of new concept specific accidents, such as overcooling/freezing of coolant, chemical reactions following coolant outflows after leaks or air/water ingress into hot graphite cores, which deserve special attention.

All concepts seem to have limited capabilities to achieve the goal of reducing proliferation risk or even to maintain the current level, mainly due to partially elevated and/or significantly increased enrichment or significantly heightened by the need for off-site reprocessing.

It is also important to note that revolutionary designs and technologies often start from scratch and introduce new man-machine interfaces and tend to represent a jump in complexity. The molten salt cooled systems with dissolved fuel, fission products, and off-gas systems may serve as example; some features of coolants, e.g., production of activation products, chemical toxicity, non-transparency, freezing at high temperatures, may require complex operations and maintenance procedures [4].

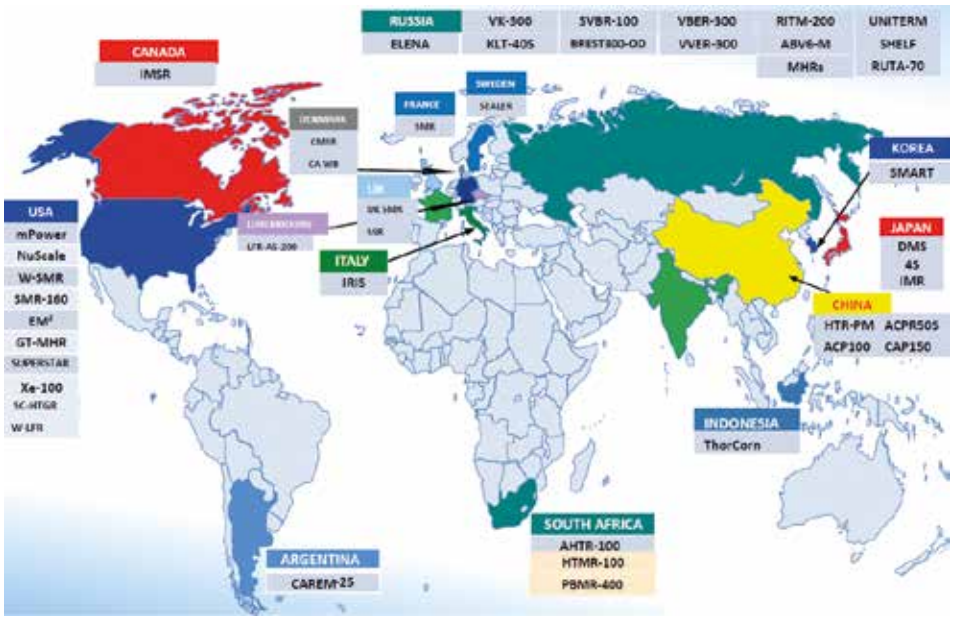

Fig. 6 World map of small and medium reactor designs under development [20].

6. Conclusions

The global demand of energy, of electricity in particular, is expected to grow, simultaneously confronted by the requirement of de-carbonization. Most countries base their future strategies on "renewables" while there are growing concerns that renewables alone will be adequate and sufficient. Diversification and use of low-carbon energy sources according to their merits seem to be a prudent principle. Nuclear energy has the potential to become an asset in a future energy mix. However, its prospects are dim in many parts of the world and major barriers including risk aversion must be overcome to make its use acceptable to the public which current technologies barely achieve.

Therefore, we set up key requirements

Table 1 Ranking from excellent (5) to neutral to very poor (1) of candidate reactor concepts against key requirements with the generation III+ EPR as the benchmark

Key requirements	***Candidate reactor concepts – varying coolant, selected designs in brackets***					
	Water – thermal (large EPR)	Sodium – fast (PRISM)	Molten Salt – fast (SaWB)	Helium – thermal (HTR-PM)	Lead – fast (BREST-OD-300)	ADS (MYRRHA)
Elimination of Reactivity Induced Accidents	**4**	**2**	**1**	**5**	**2 - 3**	**5**
Resistance to Loss of Active Core Cooling	**1**	**2**	**3**	**5**	**2 - 3**	**3**
- avoid exceeding critical temperatures	1	n.a.	n.a.	5	n.a.	n.a.
- avoid high fission product inventory	1	4 [1]	5 [2]	4 [1]	4 [1]	4 [1]
- provide sufficient heat storage & transfer capacity	4	5	4	4	5	5
Structural Integrity	**2**	**4**	**4**	**5**	**4**	**4**
- avoid high operating pressure	1	4 [3]	5	4	4 [3]	4 [3] [4]
[suitability of underground siting]	[2]	[?]	[5] [4]	[5] [4]	[4]	
Use Non-chemically Reactive / Non-Toxic Materials	**4**	**1** [5]	**2** [5] (non-stable)	**5**	**4**	**4**
Avoid Long-lived Radioisotopes	**1**	**4**	**5**	**4**	**5**	**5**
Enhance Proliferation Resistance	**4**	**2**	**2**	**3**	**2**	**2**
- avoid high enriched uranium	5	2 [6]	2 [6]	2-3	2 [6]	2 [6]

[1] due to small power size
[2] in case of dispersed fuel & due to small power size
[3] not pressurized but high static load
[4] foreseen
[5] intermediate cycle (IHX) foreseen
[6] close to / above HEU lower limit

and recommend a fundamental shift towards designs that incorporate passive and inherent safety features, are less sensitive to stable operating conditions and apply fuel cycle concepts that are more sustainable and reduce husbandry times of nuclear wastes to historical time-scales. Novel reactor designs with coolants different from water, thermal or fast spectrum, the latter allowing for fuel breeding and waste burning, and fuel cycle concepts are under development which indicate a high potential for far-reaching improvements compared to the most advanced current designs. However, none of the best versions of the candidate concepts fully meet all requirements convincingly, yet, while small sized concepts deem favorable, in general, while thermal helium cooled reactors (HTR-PM) come closest, promising inherent robustness against severe accidents and largely avoiding long-lived radio-isotopes when using thorium fuel. Boosted R&DD appear necessary, aiming at further improving some essential characteristics and features of evaluated concepts and mastering some jumps in complexity as well as to shorten commercial deployment times to ten to twenty years from now.

References

[1] BP (2019) BP Statistical Review of World Energy 2019, 68th edition. https://www.bp.com/content/dam/bp/business-sites/en/global/corporate/pdfs/energy-economics/statistical-review/bp-stats-review-2019-full-report.pdf
[2] OECD-IEA (2019) World Energy Outlook 2019. https://www.iea.org/reports/world-energy-outlook-2019
[3] Sornette, D., Kröger, W. and Wheatley, S. (2019) New Ways and Needs for Exploiting Nuclear Energy. Springer.
[4] Buongiorno, J., Corradini, M., John, P., & Petti, D. (2018). The Future of Nuclear Energy in a Carbon-Constrained World. Massachusetts Institute of Technology, 26.
[5] Greenpeace (2015) The Energy [R]evolution 2015. http://www.greenpeace.org/international/en/campaigns/climate-change/energyrevolution/
[6] IAEA (2019) Preliminary Nuclear Power Facts and Figures for 2019. https://www.iaea.org/newscenter/news/preliminary-nuclear-powerfacts-and-figures-for-2019
[7] OECD-NEA and IAEA (2018) Uranium 2018: Resources, Production and Demand. NEA No. 7413. https://www.oecd-nea.org/ndd/pubs/2018/7413-uranium-2018.pdf
[8] Hirschberg, S. and Burgherr, P. (2015) Sustainability Assessment for Energy Technologies. Handbook of Clean Energy Systems.
[9] Kiplinger, J. L. and Ramos, O. Jr. (2011) Th-ING: A Sustainable Energy Source. https://www.lanl.gov/science/NSS/issue2_2011/story6full.shtml
[10] World Nuclear Association (WNA) (2020) Small Nuclear Power Reactors. https://www.world-nuclear.org/information-library/nuclear-fuel-cycle/nuclear-power-reactors/small-nuclear-power-reactors.aspx
[11] Tsvetkov, P., Waltar, A. and Todd, D. (2012) Sustainable Development of Nuclear Energy and the Role of Fast Spectrum Reactors. In Fast Spectrum Reactors (pp. 3 - 22). Springer, Boston, Massachusetts.
[12] Generation IV International Forum (2002) A Technology Roadmap for Generation IV Nuclear Energy Systems.
[13] Tripplet, B. S., Loewen, E. P. and Dooies, B. J. (2010) PRISM: A Competitive Small Modular Sodium-Cooled Reactor. Nuclear Technology, 178:2, 186-200. https://doi.org/10.13182/NT178-186
[14] GE Hitachi (2018) GE Hitachi and PRISM Selected for U.S. Department of Energy's Versatile Test Reactor Program. https://www.genewsroom.com/press-releases/ge-hitachi-and-prism-selected-us-department-energys-versatile-test-reactor-program
[15] IAEA BREST-OD-300. https://aris.iaea.org/PDF/BREST-OD-300.pdf
[16] Nuclear Engineering International (2019) Titan-2 Contracted to Build Russia's Brest 300 Reactor. https://www.neimagazine.com/news/newstitan-2-contracted-to-build-russias-brest-300-reactor-7527297/
[17] Seaborg Technologies (2015) Seaborg Wasteburner. Molten Salt Reactor. Whitepaper SEAB-WP-2015-001. http://citeseerx.ist.psu.edu/viewdoc/download?doi=10.1.1.712.5069&rep=rep1&type=pdf
[18] Zhang, Z. et al. (2016) The Shandong Shidao Bay 200 MWe High-Temperature Gas-Cooled Reactor Pebble-Bed Module (HTR-PM) Demonstration Power Plant: An Engineering and Technological Innovation. Engineering 2 (2016) 112–118. Elsevier. https://doi.org/10.1016/J.ENG.2016.01.020
[19] MYRRHA Project (2020) MYRRHA Phased implementation. https://www.myrrha.be/myrrha-project/
[20] Reitsma, F. (2019) The Status of Different SMR Technologies and the Role of The IAEA to Support its Member States in SMR Technology Development - IAEA Atoms for Peace and Development presentation. https://wins.org/wp-content/uploads/2018/11/3.-Frederik-Reitsma_IAEA_SMRs_WINS_Reitsma_5March2019.pdf
[21] Black, G. and Peterson, S. (2019) Economic Impact Report: Construction and Operation of a Small Modular Reactor Electric Power Generation Facility at the Idaho National Laboratory Site, Butte County, Idaho. Idaho Policy Institute, Boise State University.
[22] IAEA (2013) KLT-40S. https://aris.iaea.org/PDF/KLT-40S.pdf
[23] Kröger, W., Sornette, D. and Ayoub, A. (2020) Towards Safer and More Sustainable Ways for Exploiting Nuclear Power. World Journal of Nuclear Science and Technology. doi:10.4236/wjnst.2020.103010

Progress in Physics (76)

Atomic buckling in silicene determined with sub-Ångstrom precision by atomic force microscopy

Rémy Pawlak, Ernst Meyer, University of Basel, Switzerland
Jorge Iribas Cerda, Instituto de Ciencia de Materiales de Madrid (ICMM), Madrid, Spain

Introduction

Since the first exfoliation of a single graphene layer from graphite in 2004 [1], mono-species two dimensional materials, generically termed Xenes [2] have attracted a tremendous interest leading to the synthesis of silicene [3], germanene [4], stanene [5] and many others [2, 6]. In contrast to the flat sp^2 nature of graphene, most Xenes exhibit an intrinsic buckling at the atomic scale due to their larger bond lengths which impede an efficient overlap, thus promoting a mixture of sp^2/sp^3 bondings. Rather than a drawback, this lack of flatness is recognized as an opportunity to achieve exciting quantum phases, particularly the quantum spin Hall (QSH) [7-9]. Indeed, the emergence of such topological properties in honeycomb Xene lattices depends on the strength of the spin-orbit coupling (SOC), which can be greatly enhanced using heavy elements in contrast to graphene. Atomic buckling thus becomes a pivotal parameter as it could significantly enhance the SOC by the corrugation [10]. To date, quantifying atomic buckling of X-ene lattice using diffraction techniques is severely restricted by their complex restructuring at surfaces or the presence of defects. On the other hand, height estimation using scanning probe techniques such as scanning tunneling microscopy (STM) is often hampered by the convolution of topographic and electronic features.

In the present article, we demonstrate that low-temperature atomic force microscopy with CO-terminated tips assisted by density functional theory enable an in-depth structural analysis of the various silicene structures on Ag(111). Our work published in PNAS is the result of an intense collaboration between the experimental group of Prof E. Meyer at the University of Basel and theoretical inputs from Dr. J. I. Cerda from the Instituto de Ciencia de Materiales de Madrid (ICMM). We believe that such investigation will help in foreseeing the precise structural characterization of analogous 2D materials where atomic buckling defects could lead to novel exotic properties.

Low-temperature force spectroscopy

These past decades, many Swiss Institutions such as IBM Rüschlikon, University of Basel or EMPA Dübendorf have pushed atomic force microscopy (AFM) imaging technique operated at low temperature with functionalized CO tips to unprecedented lateral resolutions, opening new avenues into the real-space characterization at surfaces of aromatic molecules [11-16] and 2D materials [17, 18]. Additionally, force spectroscopy further enables one to measure tip – sample forces [14] allowing to assess the atomic height variations [19]. In this context, AFM imaging and force spectroscopy combined with numerical calculations offer new opportunities to disentangle structural and electronic properties at the atomic level, notably in epitaxial Xenes,

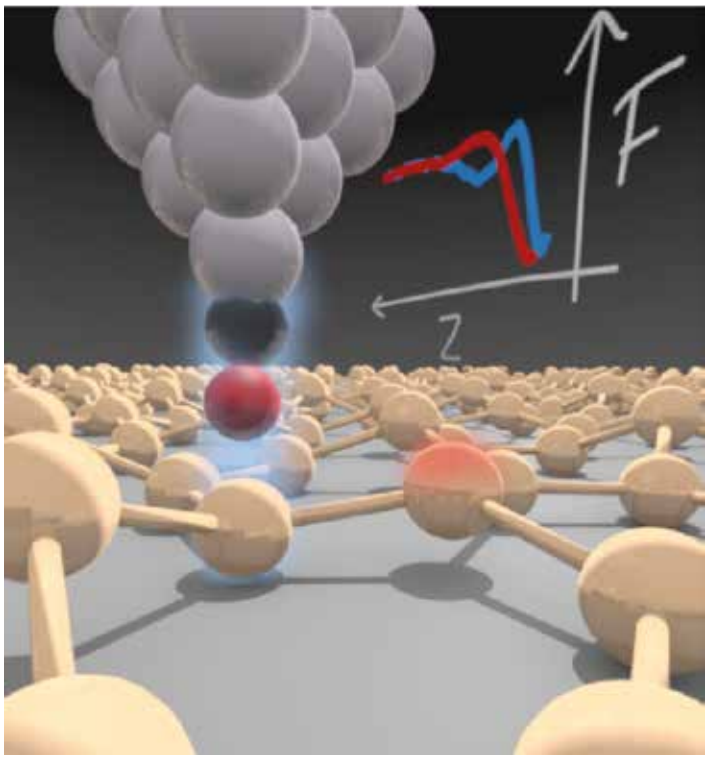

Figure 1. Artistic view of the experimental method employed to estimate the atomic buckling with sub-Ångstrom precision in silicene lattices on Ag(111). An AFM tip terminated with a single carbon monoxide (CO) molecule probes the interaction forces between tip and sample. A dip in the force-retraction curve F(Z) (background curve) is the fingerprint of the relative height of the probed atom compared to the neighboring ones (blue halo versus red halo).

specifically their intrinsic atomic buckling with sub-Ångstrom resolution.

Silicene: a paradigm of buckled Xenes

Since its first growth on Ag(111) by Vogt *et al.* in 2012 [3], the silicene properties have been widely examined using STM [3, 20-24] or angle-resolved photoemission spectroscopy (ARPES) [3, 25-27] as well as by extensive density functional theory (DFT) calculations [3, 22, 28-30]. Silicene adopts three atomically thin honeycomb structures on Ag(111) that corresponds to Si/Ag commensurate lattices: (4×4), (2√3×2√3)R30° and (√13×√13)R13.9°, denoted in the following 4×4, 2√3, and √13, respectively. The former is the most studied one and a general consensus now exists on its atomic and electronic structure [3].

To benchmark our experimental method, we first focused [31] on accurately characterizing the 4×4 phase. Figures 2A and B show experimental STM and constant-height AFM images of the 4×4 phase acquired at 4,5 K. Both images show a hexagonal arrangement of triangular patterns (dashed lines), which sides are 3,75 ± 0,05 Å. The theoretically optimized structure is displayed in Figure 1C. The most

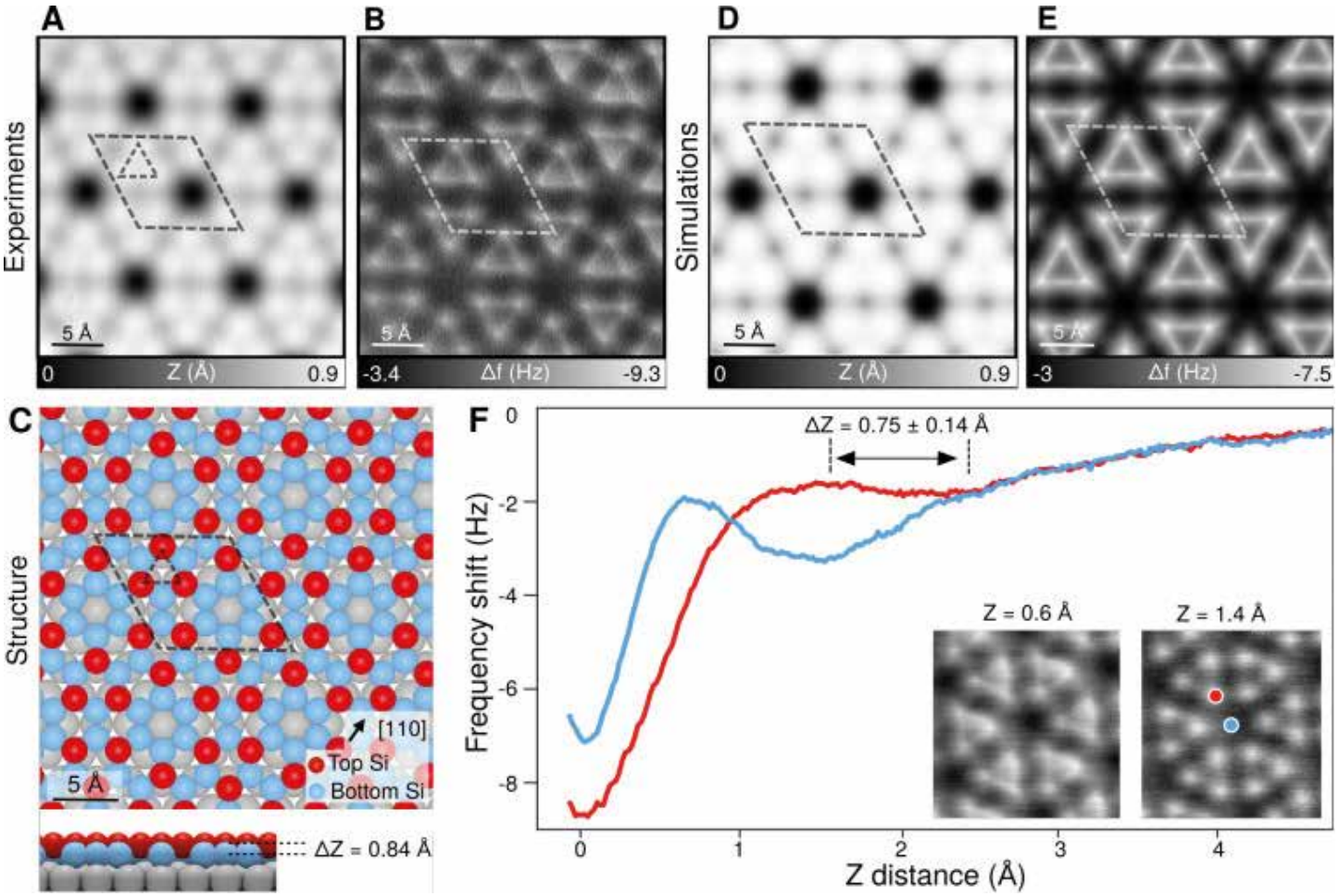

Figure 2. The 4×4 silicene lattice on Ag(111). (A and B) Experimental STM topography and constant-height AFM image acquired with CO-terminated tips at 4,5 K. (C) Representations of the 4×4 silicene structure optimized by DFT. The red and blue atoms are upmost and downmost silicon atoms of the lattice, respectively. (D and E) Simulated STM topography and AFM images from the relaxed structure. (F) Experimental force spectroscopic measurement, Δf(Z), above the 4×4 upmost (red) and downmost (blue) atoms. The vertical dashed lines show the Z positions of upmost/downmost Si atoms allowing an estimate of the buckling magnitude ΔZ. Insets are constant-height AFM images acquired at Z = 0,6 Å and Z = 1,4 Å, respectively. Reproduced from Pawlak et al. PNAS, 117, 228-237 (2020). © 2020 National Academy of Sciences.

protruding Si atoms colored in red atoms form the triangles observed in both STM/AFM images. Their side lengths are 3,86 Å while the atomic buckling obtained by comparing the upmost (red) and downmost (pale blue) Si atoms is 0.84 Å. From the calculated lattice, we computed the associated STM/AFM images (Figures 1D and E) that both indicate a good agreement with their experimental counterparts. More importantly, it allows us to identify the triangular contrast in the AFM images caused by only three upmost Si atoms in one buckled hexagonal ring. Although the 4×4 silicene lattice is a closed-packed honeycomb structure (like graphene), its intrinsic atomic buckling prevents to resolve by STM/AFM all the Si atoms of the silicene hexagons (unlike carbon rings in graphene). Thus, each triangle in the following images is associated to a buckled Si hexagonal ring.

To experimentally quantify the atomic buckling, we then performed force spectroscopic measurements above the 4×4 silicene phase. Site-dependent frequency shift curves as a function of tip – sample separation Δf(Z) were acquired above the upmost (red) and downmost (blue) Si atoms of the structure (Figure 2C and inset Figure 2F). At relative close tip – sample distances (below Z = 2,5 Å), each curve shows a “local minimum” followed by a “bump” arising from specific interactions between the front end oxygen atom of the CO-terminated tip apex and the probed Si atom of the silicene structure. The positions in Z of the dips in principle give a good estimate of the relative heights of the corresponding atoms with respect to the tip – sample distance. We extracted the upmost atoms heights as the dip position in the red curve to be Z = 2,42±0,08 Å while the lower Si atoms (blue curve) is at Z = 1.67 ± 0,05 Å. The difference of relative height ΔZ is then 0,75 Å in excellent agreement with our DFT calculations (Figure 2C) and previous results [3, 22, 32]. These observations are further confirmed by constant-height AFM images (insets of Figure 2F).

Local symmetry due to atomic buckling

Using the same strategy, the atomic buckling of the 2√3 and √13 silicene structures were characterized combining force spectroscopy and DFT calculations. By fitting the force spectroscopic curves of different atoms with a Coulomb-Buckingham potential [31], we precisely estimated the buckling magnitude in each silicene phase ranging from 0,75 ± 0,14 Å for the 4×4, 0,97 ± 0,16 Å for the 2√3 and 0,98 ± 0,32 Å for the √13. We also found out that atoms of the 2√3 and √13 phases possess three and four buckling heights in their structures, respectively. More details of the spectroscopic analysis can be found in our work [31].

Not only the relative heights of the buckled atoms is important (i.e. in the Z direction) but also their lateral positions

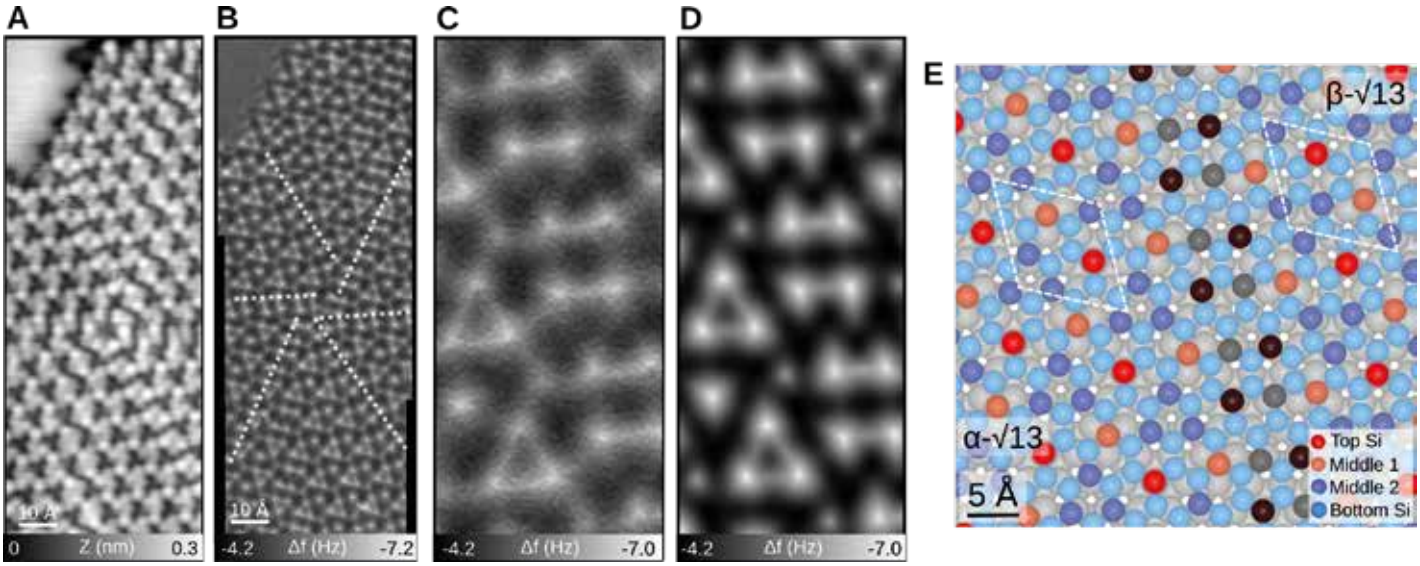

Figure 3. Local symmetry in silicene induced by variation of buckling. (A and B) Experimental STM and AFM images of the √13 moiré superstructure composed of line defects (white dashed lines) emerging from a vortex-like center. (C) Zoom-in AFM image of the line defect revealing square-like patterns and (E) Simulated AFM image obtained from the relaxed DFT structure shown in (E). According to the DFT structure, the line structure consists of a boundary between α–√13 and β–√13 chiral domains. Reproduced from Pawlak et al. PNAS, 117, 228-237 (2020). © 2020 National Academy of Sciences

within the silicene lattice. Indeed, we observed that Si atoms of similar buckling heights are precisely ordered which can lead to complex silicene restructuring. This is particularly exemplified by the √13 silicene structure (Figures 3A and B) that systematically shows vortices formed by the convergence of six defected lines (indicated by white dashed lines in Figure 3B). These boundaries separate adjacent domains of triangular features pointing in opposite directions (denoted α– and β–√13 structures as calculated by DFT of Figure 3E). Each supercell is characterized by a triangle with edges 3,6 Å long (dark blue atoms), which corresponds to a buckled Si hexagonal ring. The brighter protrusion in the AFM image of Figures 3B and C corresponds to the most protruding atom (red atom) in Figure 3E, while the second less intense bump (only observed by AFM) coincides with intermediate buckling heights (orange in Figure 3E). Despite the complexity of the pattern, the √13 lattice displays a clear *p3* symmetry with three possible rotation axes: in the triangle's epicenter as well as in either of the 2 bumps. Following symmetry arguments, we concluded to the coexistence of only two inequivalent √13 domains (i.e. α– and β–√13) that are associated by an inversion of the silicene adlayer. Energetically, the stability of these two structures is within 10 meV.

Looking now at the line defects (Figure 3C), a typical square pattern containing four maxima linked by pairs along the transversal direction. The distance between the paired atoms is 3.8 Å, thus slightly longer than the triangle sides, while the pairs are separated by 4.0 Å. Figure 3E presents the DFT relaxed structure that matches the experimental AFM image, as shown by the corresponding simulated AFM image of Figure 3D. The line defects appears to induce a large restructuring at the boundaries between the two √13 domains. However, the silicene film remains a continuous honeycomb layer without truncation and exhibits only small deformations due to a compressive strain. Note that these superstructures are stabilized on areas of several hundreds of nanometers.

Observing disordered silicene structures at domain boundaries

Interestingly, we also analyzed by AFM defected regions and boundaries between adjacent domains (Figure 4), that allow us to comment on long-standing debates of the silicene community. Indeed, previous works have reported the presence in STM images of dark regions surrounding the silicene domains which were attributed to Si-Ag alloys. Additionally, silicene domains always appear by STM topographic images embedded into the surface. These works raised numerous questions suggesting the existence of a silicon alloy instead of a true silicene adlayer. Thank to our accurate structural analysis and looking at the excellent agreement between theory and experiments, we can firmly conclude that these phases only contains Si atoms lying at

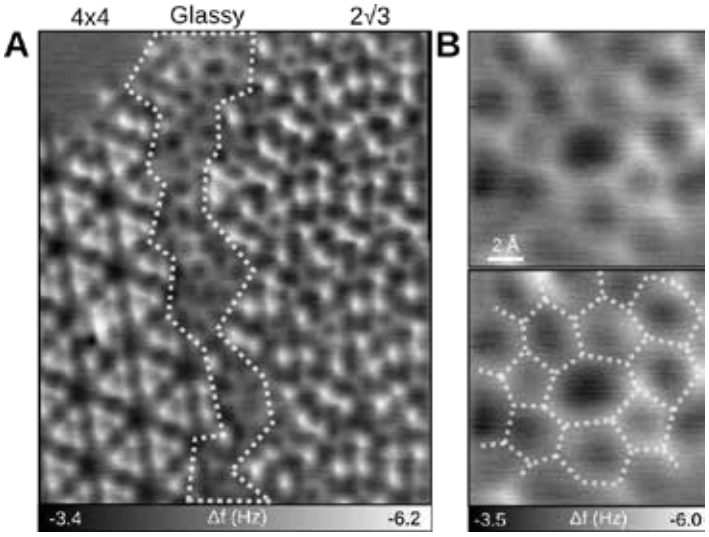

Figure 4. Imaging defects in silicene. (A) Constant-height AFM image of a grain boundary between a 4×4 and a 2√3 domain. The boundary region is delimited with white dashed lines. (B) Zoom-in AFM image of this region revealing buckled and highly distorted hexagonal, pentagonal, and heptagonal motifs (marked by white dashed lines in bottom image). Reproduced from Pawlak et al. PNAS, 117, 228-237 (2020). © 2020 National Academy of Sciences.

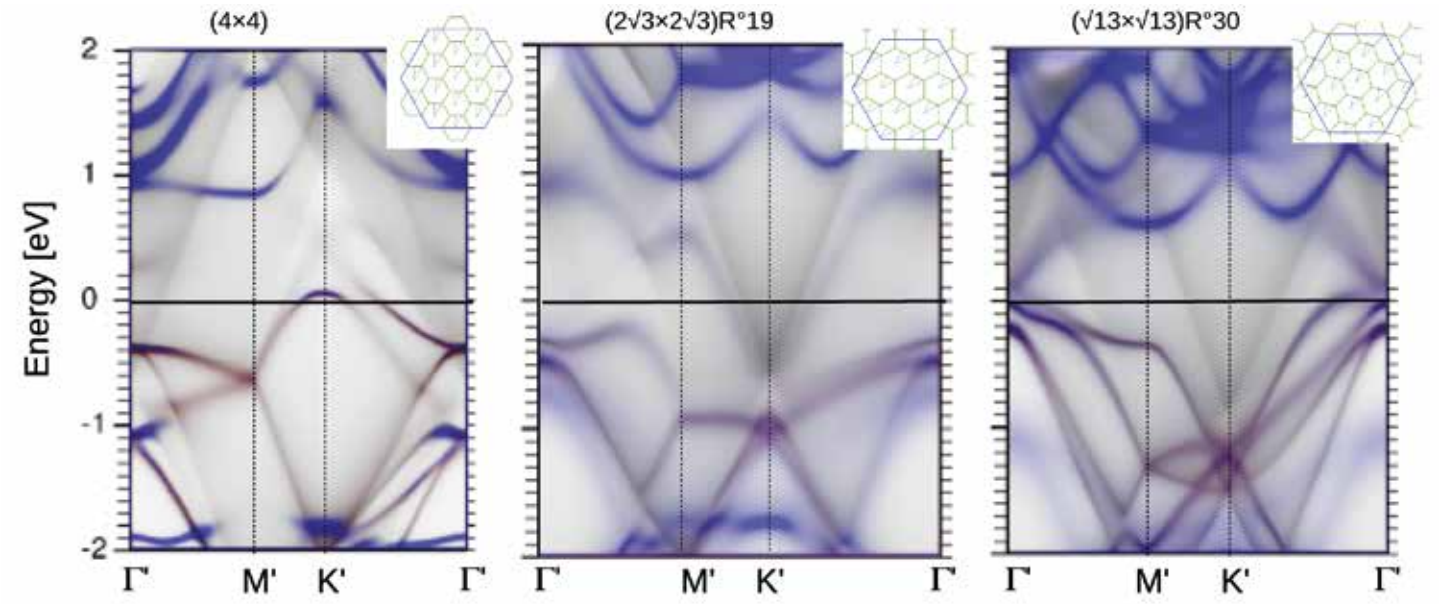

Figure 5. Calculated electronic structure of the silicene phases. (A-C), Partial density of states PDOS(k, E) projected on the surface most atoms along G0-M0-K0 for the 4×4, 2√3 and √13 silicene phases on Ag(111), respectively. Si (blue) and first Ag layer (red) projections have been superimposed on top of the second and third Ag layers (gray). Insets shows the corresponding supercells' BZ in an extended zone scheme (light green hexagons), the k-path in each case (thin solid triangles) and the Ag(111) BZ (blue). Reproduced from Pawlak et al. PNAS, 117, 228-237 (2020). © 2020 National Academy of Sciences.

0.18 Å above the silver surface [31]. Furthermore, Figure 4A shows a constant-height AFM image of a such dark STM region (white dashed line in Figure 4B) between a 4×4 and a 2√3 silicene domains on Ag(111). It reveals the signature of multiple structural motifs indicating a "glassy-like" silicene region where buckled hexagons, pentagons, and heptagons appear interconnected, in line with other Si structures where non-hexagonal motifs have been predicted [37-39].

Electronic properties of silicene on Ag(111)

From the silicene structure determined with sub-Ångstrom precision, we computed their band structure including the silver substrate (Figure 5) [31] . In each map, the projections on the Si atoms (blue) and the first Ag layer (red) have been superimposed on top of those corresponding to the subsurface Ag layers (gray). Despite the profusion of bands across the Brillouin zones (BZs) due to backfolding and apart from a few faint resonances crossing EF, all phases show a clear gap in the π bands. No sign of any Dirac cones localized within the silicene sheet appears in any of the phases, since all surface bands in the -2 to +1eV region have a strong Si-Ag1 hybridization with parabolic dispersions due to covalent bonding (in contrast with the linear metal bands). This observation is in line with previous experimental observations of silicene on Ag(111) [25, 26, 29, 30, 33-36]. We also emphasize that calculated band structures of the free-standing silicene structure phases (excluding the silver substrate) concluded the presence of Dirac cones in all the phases. Our results thus underlines, not only the pivotal role of atomic buckling in the electronic properties of silicene, but also the importance of developing novel synthesis processes or exfoliation methods towards nonconductive substrates to preserve their electronic character.

Conclusion

Our AFM/DFT-based approach is self-contained to characterize accurately the structure of silicene and other mono-element Xenes at surfaces with high lateral resolution. Importantly, local atomic bucklings can be determined with sub-Ångstrom precision independent of their structural complexity. We are thus convinced that such systematic investigation will help in foreseeing the precise structural characterization of analogous 2D materials where atomic buckling defects could lead to novel exotic properties [2].

Acknowledgment

Financial support from the Swiss National Science Foundation (SNF), the Swiss Nanoscience Institute (SNI) and the Spanish MINECO under Grant Nos. MAT2015-66888-C3-1R and RTI2018-097895-B-C41 is gratefully acknowledged. We also thank the European Research Council (ERC) under the European Union's Horizon 2020 research and innovation programme (ULTRADISS grant agreement No 834402).

References

[1] A. K. Geim & K. S. Novoselov. The rise of graphene. *Nat Mater* **6**, 183-191 (2007).
[2] A. Molle, J. Goldberger, M. Houssa, Y. Xu, S. C. Zhang & D. Akinwande. Buckled two-dimensional Xene sheets. *Nat Mater* **16**, 163-169 (2017).
[3] P. Vogt, P. D. Padova, C. Quaresima, J. Avila, E. Frantzeskakis, M. C. Asensio, A. Resta, B. Ealet & G. L. Lay. Silicene: compelling experimental evidence for graphene like two-dimensional silicon. *Phys. Rev. Lett* **108**, 155501 (2012).
[4] M. E. Dávila, L. Xian, S. Cahangirov, A. Rubio & G. L. Lay. Germanene: a novel two-dimensional germanium allotrope akin to graphene and silicene. *New J Phys* **16**, 095002 (2014).
[5] F. F. Zhu, W.-J. Chen, Y. Xu, C.-L. Gao, D.-D. Guan, C.-H. Liu, D. Qian, S.-C. Zhang & J.-F. Jia. Epitaxial growth of two-dimensional stanene. *Nat. Mater.* **14**, 1020-1025 (2015).
[6] G. Bihlmayer, J. Sassmannshausen, A. Kubetzka, S. Blügel, K. von Bergmann & R. Wiesendanger. Plumbene on a Magnetic Substrate: A Combined Scanning Tunneling Microscopy and Density Functional Theory Study. *Phys. Rev. Lett* **124**, 126401 (2020).
[7] C.-C. Liu, W. Feng & Y. Yao. Quantum spin Hall effect in silicene and two-dimensional germanium. *Phys. Rev. Lett* **107**, 076802 (2011).
[8] M. Ezawa. Topological insulators in silicene: Quantum hall, quantum spin hall and quantum anomalous hall effects. *AIP Conference Proceedings* **1566**, 199 (2013).
[9] F. e. a. Reis. Bismuthene on a SiC substrate: A candidate for a high-temperature quantum spin Hall material. *Science* **357**, 287- 290 (2017).

[10] Z.-Q. Huang, C.-H. Hsu, F.-C. Chuang, Y.-T. Liu, H. Lin, W.-S. Su, V. Ozolins & A. Bansil. Strain driven topological phase transitions in atomically thin films of group IV and V elements in the honeycomb structures. *New Journal of Physics* **16,** 105018 (2014).
[11] L. Gross, F. Mohn, N. Moll, P. Liljeroth & G. Meyer. The chemical structure of a molecule resolved by atomic force microscopy. *Science* **325**, 1110-1114 (2009).
[12] L. Gross. Recent advances in submolecular resolution with scanning probe microscopy. *Nature Chemistry* **3**, 273-278 (2011).
[13] R. Pawlak, S. Kawai, S. Fremy, T. Glatzel & E. Meyer. Atomic-Scale Mechanical Properties of Orientated C_{60} Molecules Revealed by Noncontact Atomic Force Microscopy. *ACS Nano* **5**, 6349-6354 (2011).
[14] S. Kawai, A. Sadeghi, T. Okamoto, C. Mitsui, R. Pawlak, T. Meier, J. Takeya, S. Goedecker & E. Meyer. Organometallic Bonding in an Ullmann-Type On-Surface Chemical Reaction Studied by High-Resolution Atomic Force Microscopy. *Small* **12**, 5303-5311 (2016).
[15] S. Kawai, V. Haapasilta, B. D. Lindner, K. Tahara, P. Spijker, J. A. Buitendijk, R. Pawlak, T. Meier, Y. Tobe, A. S. Foster & E. Meyer. Thermal control of sequential on-surface transformation of a hydrocarbon molecule on a copper surface. *Nature Communications* **7**, 12711 (2016).
[16] P. Ruffieux, S. Wang, B. Yang, C. Sánchez-Sánchez, J. Liu, T. Dienel, L. Talirz, P. Shinde, C. A. Pignedoli, D. Passerone, T. Dumslaff, X. Feng, K. Müllen & R. Fasel. On-surface synthesis of graphene nanoribbons with zigzag edge topology. *Nature* **531**, 489-492 (2016).
[17] S. Kawai, S. Nakatsuka, T. Hatakeyama, R. Pawlak, T. Meier, J. Tracey, E. Meyer & A. S. Foster. Multiple heteroatom substitution to graphene nanoribbon. *Sci Adv* **4**, eaar7181 (2018).
[18] S. Mishra, D. Beyer, K. Eimre, S. Kezilebieke, R. Berger, O. Gröning, C. A. Pignedoli, K. Müllen, P. Liljeroth, P. Ruffieux, X. Feng & R. Fasel. Topological frustration induces unconventional magnetism in a nanographene. *Nature Nanotechnology* **15**, 22-28 (2020).
[19] Y. Sugimoto, P. Pou, M. Abe, P. Jelinek, R. Pérez, S. Morita & O. Custance. Chemical identification of individual surface atoms by atomic force microscopy. *Nature* **446**, 64-67 (2007).
[20] B. Feng, B. Feng, Z. Ding, S. Meng, Y. Yao, X. He, P. Cheng, L. Chen & K. Wu. Evidence of Silicene in Honeycomb Structures of Silicon on Ag(111). *Nano Lett* **12**, 3507 (2012).
[21] L. Chen, C. Liu, B. Feng, X. He, P. Cheng, Z. Ding, S. Meng, Y. Yao & K. Wu. Evidence for Dirac Fermions in a Honeycomb Lattice Based on Silicon. *Phys. Rev. Lett* **109**, 056804 (2012).
[22] C.-L. Lin, R. Arafune, K. Kawahara, N. Tsukahara, E. Minamitani, Y. Kim, N. Takagi & M. Kawai. Structure of Silicene Grown on Ag(111). Appl. Phys. Exp 5, 045802 (2012).
[23] H. Jamgotchian, Y. Colignon, N. Hamzaoui, B. Ealet, J. Y. Hoarau, B. Aufray & J. P. Bibérian. Growth of silicene layers on Ag(111): unexpected effect of the substrate temperature. *J. Phys.: Cond. Matt* **24**, 17 (2012).
[24] R. Arafune, K. K. C.-L. Lin, N. Tsukahara, E. Minamitani, Y. Kim, N. Takagi & M. Kawai. Structural transition of silicene on Ag(111). *Surf. Science* **608**, 297 (2013).
[25] D. Tsoutsou, E. Xenogiannopoulou, E. Golias, P. Tsipas & A. Dimoulas. Evidence for hybrid surface metallic band in (4×4) silicene on Ag(111). *Appl. Phys. Lett* **103**, 231604 (2013).
[26] Y. Feng, D. Liu & B. Feng. Direct evidence of interaction-induced Dirac cones in a monolayer silicene/Ag(111) system. *Proc. Natl. Acad. Sci. USA*, (2016).
[27] P. M. Sheverdyaeva, P. M. Sheverdyaeva, S. K. Mahatha, P. Moras, L. Petaccia, G. Fratesi, G. Onida & C. Carbone. Electronic States of Silicene Allotropes on Ag(111). *ACS Nano* **11**, 975 (2017).
[28] H. Enriquez, S. Vizzini, A. Kara, B. Lalmi & H. Oughaddou. Silicene structures on silver surfaces. *J. Phys.: Condens. Matter* **24**, 314211 (2012).
[29] Z.-X. Guo, S. Furuya, J.-I. Iwata & A. Oshiyama. Absence of Dirac Electrons in Silicene on Ag(111) Surfaces. *J. Phys. Soc. Japan* **82**, 6 (2013).
[30] E. Scalise, M. Houssa, G. Pourtois, B. van den Broek, V. Afanas'ev & A. Stesmans. Vibrational properties of silicene and germanene. *Nano Research* **6**, 19-28 (2013).
[31] R. Pawlak, C. Drechsel, P. D'Astolfo, M. Kisiel, E. Meyer & J. I. Cerda. Quantitative determination of atomic buckling of silicene by atomic force microscopy. *Proc Natl Acad Sci USA* **117**, 228 (2020).
[32] A. Curcella, R. Bernard, Y. Borensztein, A. Resta, M. Lazzeri & G. Prevot. Determining the atomic structure of the (4 × 4) silicene layer on Ag(111) by combined grazing-incidence x-ray diffraction measurements and first-principles calculations. *Phys Rev B* **94**, 165438 (2016).
[33] J. Sone, T. Yamagami, Y. Aoki, K. N. &. H. Hirayama. Epitaxial growth of silicene on ultra-thin Ag(111) films. *New J. Phys* **16**, 095004 (2014).
[34] G. Prévot, R. Bernard, H. Cruguel & Y. Borensztein. Monitoring Si growth on Ag(111) with scanning tunneling microscopy reveals that silicene structure involves silver atoms. *App. Phys. Lett* **405**, 213106 (2014).
[35] Y. Borensztein, A. Curcella, S. Royer & G. Prévot. Silicene multilayers on Ag(111) display a cubic diamondlike structure and a 3×3 reconstruction induced by surfactant Ag atoms. *Phys. Rev. B* **92**, 155407 (2015).
[36] R. Bernard, Y. Borensztein, H. Cruguel, M. Lazzeri & G. Prévot. Growth mechanism of silicene on Ag(111) determined by scanning tunneling microscopy measurements and ab initio calculations. *Phys. Rev. B* **92**, 045415 (2015).
[37] S. Li, Y. Wu, Y. Tu, Y. Wang, T. Jiang, W. Liu & Y. Zhao. Defects in Silicene: Vacancy Clusters, Extended Line Defects, and Di-adatoms. *Sci. Rep* **5**, 7881 (2015).
[38] D. Ghosh, P. Parida & S. K. Pati. Stable line defects in silicene. *Phys. Rev. B* **92**, 195136 (2015).
[39] J. I. Cerdá, J. Sławińska, G. L. Lay, A. C. Marele, J. M. Gómez- Rodríguez & M. E. Dávila. Unveiling the pentagonal nature of perfectly aligned single-and double-strand Si nanoribbons on Ag(110). *Nat. Comm* **7**, 13076 (2016).

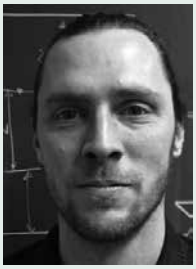

Rémy Pawlak has been a senior scientist at the University of Basel since 2017 in the group of Prof. Dr. E. Meyer, that he joined as postdoctoral fellowship in 2010. He is working on atomic and molecular characterization and their manipulation by scanning tunneling microscopy (STM) and atomic force microscopy (AFM) in cryogenic environment. He studied at the Aix-Marseille University, where he received his PhD in Physics and nanosciences in 2010 for the growth of supramolecular and polymerized molecular networks at surfaces studied by STM/AFM.

Ernst Meyer is professor of physics at the University of Basel since 1997. His main interests are nanomechanics experiments with a focus on atomic friction and energy dissipation. The transition from metallic to superconductive phase was observed by non-contact friction experiments. High resolution force microscopy is an important tool to characterize surfaces or molecular aggregates. Experiments with graphene nanoribbons and metallic nanowires were performed to get further insight into the mechanical, electrical and magnetic properties of these assemblies.

Jorge Iribas Cerdá is a staff senior researcher at Materials Science Institute of Madrid (ICMM-CSIC) since 2012. His main research interest is the theoretical understanding of surface and interface properties from DFT and post-DFT formalisms, some of them developed and implemented by himself along the last two decades. He counts with a long expertise in the simulation of STM images explicitly including the tip apex; a tool that has allowed the resolution of a number of complex surface structures. Currently he is intensely involved in spin-orbit related phenomena.

Progress in Physics (77)

Focal Mography – an optical method for label-free detection of biomolecular interactions

Christof Fattinger, Roche Innovation Center Basel, Andreas Frutiger, Iino Biotech AG & ETH Zürich

Abstract:

Focal mography is a new method for label-free molecular interaction analysis in crude samples. In contrast to refractometric optical sensors, focal mography is insensitive to nonspecific molecular interactions. This unique property is achieved with a special 2D nanopattern of molecular binding sites on a chip, termed mogram. A mogram is designed such that molecules bound to it diffract light constructively into a focal spot. The intensity of the focused light is measured to quantify the amount of bound molecules. In biological samples, highly abundant off-target molecules readily adsorb to the surface of the sensor. Yet, this process is completely random and the off-target molecules do not bind to the ordered binding sites of the mogram. Thus, their scattering is uniform in all spatial directions and therefore they hardly contribute to the measured light intensity in the narrow solid angle of the focal spot.

1. Introduction

Specific biomolecular interactions in crowded environments are central to life on the molecular scale. Label-free biomolecular interaction analysis is widely used for the study of biomolecular interactions and processes [1, 2]. The detected biomolecular interaction is directed by a molecular recognition [3, 4]. The recognition leads to specific binding of a distinct biomolecule to another distinct biomolecule [3, 4]. Ideally, we would like to observe the two molecules during complex formation. We can see such dynamic phenomena of large individual biomolecules in highly dilute solutions [5]. Yet, in crowded solutions this is impossible. The only way to see dynamic phenomena in real-life, crowded biological environments is to observe the interactions amongst two ensembles of biomolecules. To achieve this, we use the coherent detection of the refractive index changes that are induced by the spatial immobilization of biological matter through molecular interactions. This physical detection principle is termed “focal mography” (“mography” in short) [6, 7, 8]. In this article, we explain focal mography, its implications and some of its possible applications.

In short, mography is a new analytical method for the robust and sensitive label-free detection of biomolecular interactions without the use of additional fluorescent labels [6, 7, 8]. Its working principle is illustrated in Figure 1. A mogram is a coherent assembly of binding sites on a chip that form the blueprint of a diffractive lens. Biomolecules that bind to the mogram diffract laser light into a diffraction-limited focal spot, the focus of the mogram. The diffracted intensity in the focal spot correlates quadratically with the adsorbed mass and hence with the number of biomolecular interactions on the mogram. The focal spot monitors the collective binding activity on the entire coherent assembly. Mography is therefore a technique to directly “see” an ensemble of molecules in action.

Being able to see biomolecular processes unfold in real time allows us to understand the mechanisms of life as well as disease. As an ensemble, we envision a very small amount of one type of a biological molecule – the specimen - typically a few pg or less. The specimen shall be detected by a specific biomolecular interaction. This is achieved by the binding of the molecules in the specimen to predefined binding sites through a specific biomolecular interaction. The formation of molecular recognition complexes can be detected optically because biological matter has a significantly higher refractive index than the surrounding aqueous solution, which is mainly water [9]. A biomolecule in water is therefore a pure phase object. Frits Zernike already realized that it is the phase retardation of light induced by the specimen - not the absorption of light [10] - that is the relevant physical quantity for observation of a small biological specimen under the microscope. Based on this insight, Zernike introduced phase contrast microscopy in 1934 [10, 11]. Upon complex formation, the local refractive index increase induced by the binding of molecules leads to an increase in the scattering strength of the individual molecular recognition complexes. However, as mentioned above the signal of an individual

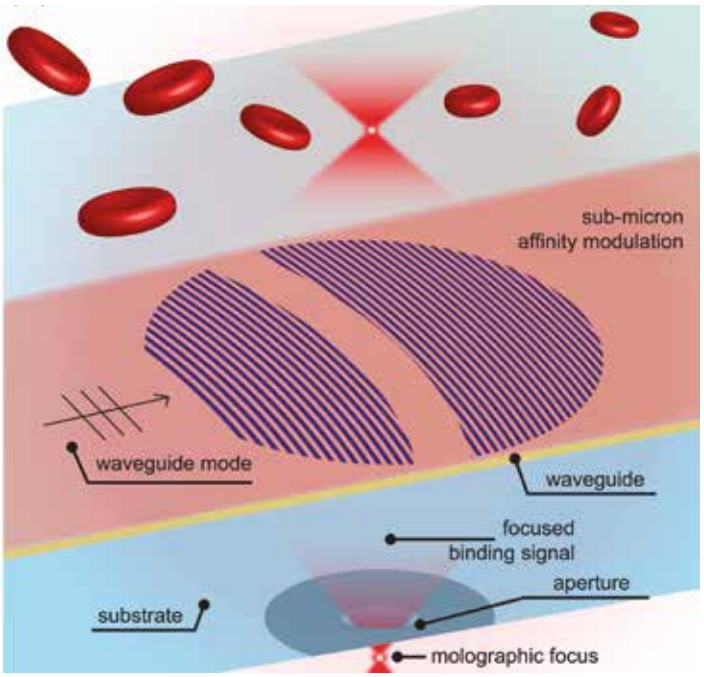

FIG. 1. Focal mography incorporates the essentials of a highly sensitive diffractometric biosensor: A submicrometer affinity modulation formed by specific binders is exposed to a biological sample (e.g., blood). The mode of a high-refractive-index waveguide provides perfect dark-field illumination of the molecules in the vicinity of the sensor surface and enhances the light intensity. The shape of the pattern acts as a diffractive lens, which concentrates the diffracted signal into a focal spot, whereas the background intensity is diluted over the entire solid angle. For efficient spatial filtering, the aperture of the optical system is matched to that of the mogram. (Figure reproduced from [8])

recognition complex is too small to be detected. Only the coherent addition of the individual scattering signals in an ensemble of recognition complexes is detectable.

In principle, label-free optical detection of a specimen of a few pg or less can be achieved by two approaches: One could imagine the specimen to be densely packed as it was the case in Zernike's experiments. This specimen would have a size in the range of one wavelength of visible light. The scattering of light by the dense specimen (i.e. a nanoparticle composed of biomolecules, e.g. proteins or DNA) is visible as a point scatterer under a microscope with dark-field illumination or by phase contrast microscopy. However, a densely packed specimen is completely unsuited for the study of molecular recognition, because molecular recognition requires diffusional accessibility of the binding sites. The second approach is to configure the specimen in a coherent assembly of molecules such that the phases of light scattered by the diffractometric phase object add constructively. A prerequisite for this detection scheme is sufficient coherence of the utilized light source. In a coherent assembly of recognition sites, the sites are spread over distances of many wavelengths (100-1000). Therefore, the recognition sites are sufficiently disperse that they are accessible to the specimen by diffusion. Thus, only a disperse (not densely packed) coherent assembly of molecular recognition complexes is suitable for the detection of biomolecular interactions.

A mologram comprises a blueprint of a particular coherent assembly of molecules. Namely, one that arranges the recognized biological molecules into a focusing diffractometric phase object. The phase object generates a diffraction limited focus from an incident laser beam in close proximity to the chip. The phase object constitutes a "molecular hologram", termed "mologram" in short. A typical diameter of a mologram is 50 μm to 500 μm. A saturated (i.e. fully bound) mologram consists of typically a few pg to 1 ng of bound biological molecules. Therefore, even in the saturated state the biological molecules are only loosely packed and enough open space between the molecules is left. The open space is crucial for the analysis of biomolecular interactions, because (i) molecules can diffuse freely and (ii) the recognition complexes do not influence another to avoid multivalency or avidity effects [12].

2a. Method description: Synthesis of mologrames

The synthesis of mologrames on a planar optical waveguide on a chip succeeds with properly designed surface chemistry and reactive immersion lithography (RIL) [7]. The RIL process is explained in Figure 2. It allows the creation of the biomolecular recognition structure of the mologram on a light-sensitive non-fouling graft copolymer layer [7]. The synthesis of mologrames avoids steric hindrance between the binding sites of the mologram that would occur from overcrowding of molecules in the coherent mologrephic assembly on the chip [7]. The copolymer layer contains photoactivatable functional groups for patterning of the recognition sites of the mologram under immersion by exposure to light [7]. The RIL process enables tuning of surface chemistries specific to the desired analytical application. It is important

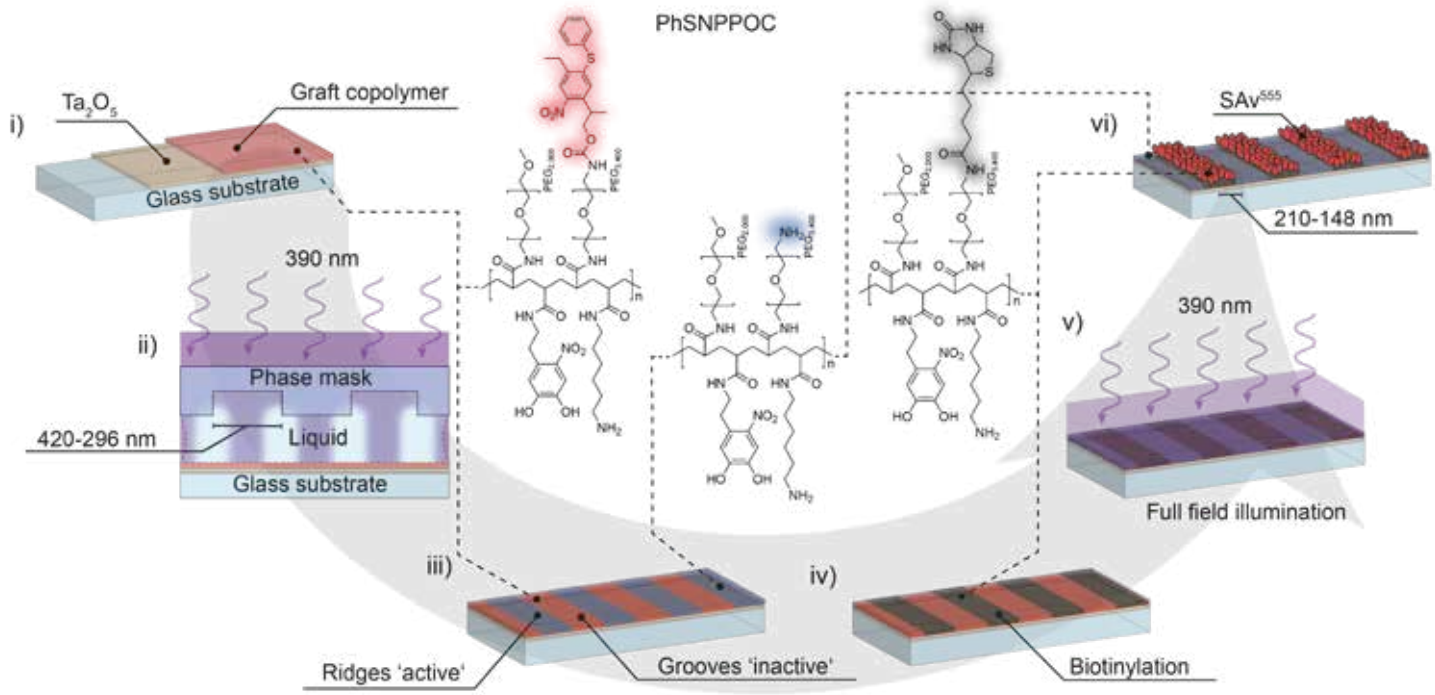

FIG. 2. Schematic illustration of the reactive immersion lithography (RIL) process used in mologrephy, cf. [7]. For a better understanding, the copolymer structures at different stages of the process are connected via dashed lines. (i) The 145 nm metal oxide (Ta_2O_5) waveguide layer is coated with a thin photosensitive graft copolymer layer containing PhSNPPOC protected amino-PEG_{3400} polymer. (ii) Phase mask technology is used for activation of the monolithic photosensitive layer. The physics of the phase mask lithography process results in structures with half the period of the phase mask (420–296 nm). This allows the creation of the nanostructures (210–148 nm line width) of the mologram. (iii) Induced activation contrast after photolithography. Activated areas are termed 'ridges' and inactive areas 'grooves'. (iv) Further functionalization with amine reactive compounds leads to the desired binding properties (chemical functionalization). NHS-biotin for streptavidin (SAv) binding. (v) To minimize the difference in nonspecific binding between grooves and ridges, or to realize backfilling of the mologram, the remaining PhSNPPOC groups are photocleaved. Additional passivation (not shown) can be obtained by amine reactive blocking reagents, for example, NHS-PEG. (vi) The mologrephic signal is generated by binding of SAv. (Figure reproduced from [7])

to note that the used photolithography at a wavelength of 390 nm, at the energy doses used, does not induce refractive index modulations in the copolymer layer [7]. The RIL process was characterized in detail with simulations and stimulated emission and depletion (STED) microscopy [7 and Supplemental Material].

The detection limit of molography can be improved by image reversal reactive immersion lithography [13]. The image reversal RIL process enables the formation of inverse molograms, which exhibit a larger analyte efficiency (i.e. higher quality) compared to standard molograms and therefore require less analyte to achieve a certain molographic signal [13]. As a result, inverse molograms decrease the detection limit of molography whenever the number of molecules available to the sensor is limited. This is the case in most diagnostically relevant applications, which operate either under conditions where the sensor does not equilibrate on a reasonable timescale or in the mass-sensing regime (analyte depletion) [13].

2b. Method description: Read-out of molograms

In this subsection we discuss and exemplify the findings of two publications on molography in journals of the American Physical Society [6, 8].

We imagine a special hologram with three properties: (1) the hologram uses its entire diffractive power for reconstruction of just one image point, a diffraction-limited focal spot that is located in the area of first order diffraction of the incident laser beam. (2) The imagined hologram diffracts a tiny portion of the incident laser beam into its single image point, the diffraction-limited focal spot, and, (3) the hologram is illuminated by evanescent light and its single image point is observed in dark field illumination. In the eyes of a physicist, it is evident that the diffractive power of such a hologram can be extremely weak without loss of its optical function, i.e. the reconstruction of just one first order diffraction focus. The amount of optical material in such a hologram that is required to unambiguously detect a change in the diffracted intensity lies below 10 fg [8]. This is a very small quantity for the detection of a specific molecule in an analytical application. We have shown that a molecular hologram with the described properties can be synthesized [7, 8, 13]. Molography combines the physics of a molecular hologram with the specific recognition between biomolecules [3, 4] to create a small biooptical element for analytical purposes. Dark field illumination of the molograms on a chip is achieved with the evanescent light of a waveguide mode propagating along the surface of the chip [6, 7, 8].

The readout of molograms is based on the analysis of the light in the foci of the molograms [6, 7, 8]. This is achieved in real time by imaging the molographic foci on a photodetector array. The molographic signal in the image plane of a mologram is embedded in a weak background originating from stray light [8]. This background is mainly caused by small non-coherent irregularities in the substrate and the substrate-cover interface. [8]. Due to the random phase and magnitude of the scattered light from the irregularities and non-coherently distributed molecular imperfections the background constitutes a speckle pattern. On the other hand, the diffraction of light by bound molecules at the recognition sites of the mologram is a coherent process with a defined spatial frequency. In molography, the image plane of the mologram constitutes a Fourier plane and we can therefore employ spatial frequency filtering of this image to separate the molographic signal from the speckle background [8]. The quantification of the molographic signal in this speckle pattern is discussed in detail in reference [8].

From the viewpoint of a physicist, molography can also be understood as a chemical radio [8]. The transmission of radio signals is based on the modulation of an rf carrier signal and the subsequent demodulation at the receiver. Molography applies this principle at optical frequencies to the transmission of chemical signals. Molecules recognize the affinity modulation in the mologram and interact with it. The molecular interaction renders a coherent molecular pattern in the form of a diffractive lens. This diffractive lens modulates the momentum of the guided mode with the spatial frequency of the mologram. The demodulation in k-space is performed by Fourier optics and the molographic signal is separated from the carrier wave in the focal plane of the molographic lens. Molography enables the transmission of chemical signals (e.g. binding information) from coherently ordered molecules in the mologram to a detection point in space (the focus of the mologram).

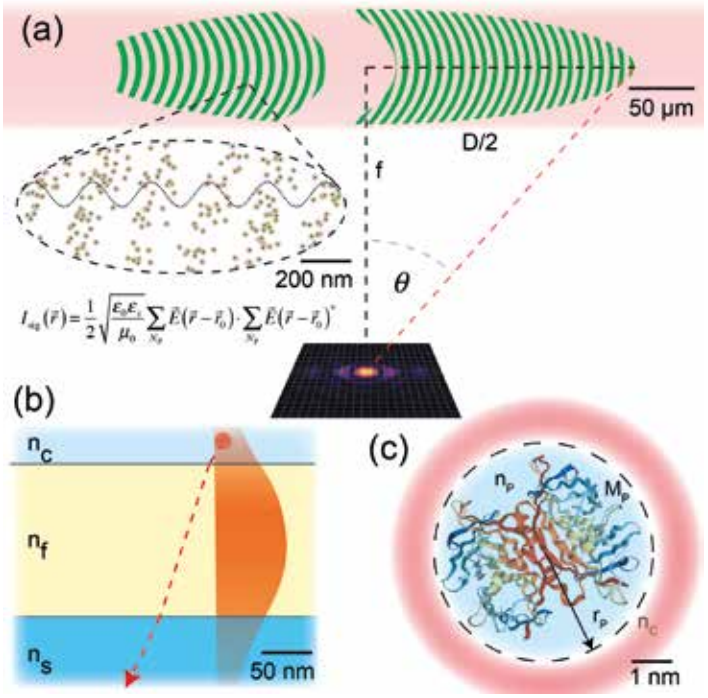

FIG. 3. Simulation of molographic foci, cf. [8]. (a) The molographic signal emerges from the superposition of the scattered electric fields of many individual protein molecules on the surface of the waveguide [proteins are not drawn to scale but their number density corresponds to 2.6 pg/mm^2]. This field is computed for every pixel on a specified screen in the focal plane of the mologram. (b) The scattered field is calculated by modeling the proteins as Rayleigh scatterers excited by the evanescent field of the waveguide mode, which is obtained by solving the eigenvalue problem of the slab waveguide. n_c, n_f and n_s are the refractive indices of cover, film, and substrate, respectively. (c) The optical properties necessary to determine the polarizability of the protein dipole, i.e., refractive index and radius, can be calculated from its molecular mass and the refractive-index increment for proteins in water. (Figure reproduced from [8])

3. Applications of molography

Possible applications of molography are vast. They range from the investigation of a specific biomolecular interaction in basic biological research to the diagnosis of a critical health condition in an emergency. To illustrate and to explain the broad applicability of molography we discuss a recently published new method for quantification of molecular interactions in living cells in real time [14]. The method is termed "cell-based molography". It enables investigations of membrane proteins in their natural environment [14]. The ability to examine biomolecular interactions in living cells in a physiologically relevant context is crucial to the understanding of cellular processes and emanating drug discovery efforts.

In cell-based molography [14], cells plated on a molographic sensor chip spread and adhere under standard tissue culture conditions. Thereby the targeted membrane protein in the plasma membrane of the living cells is aligned by a "template mologram" on the surface of the chip. In doing so, the membrane protein molecules transfer the molographic pattern on the chip to the inside of the cell, forming a "transmembrane mologram" (cf. Fig 4b). The transmembrane mologram has the following key characteristics: The coherently arranged membrane protein molecules under study remain in their natural environment but become visible through their coherent arrangement inside the cell membrane. They create a diffraction-limited spot of light, the focus of the transmembrane mologram. Molecules interacting with their intra- or extracellular domains diffract light into this spot.

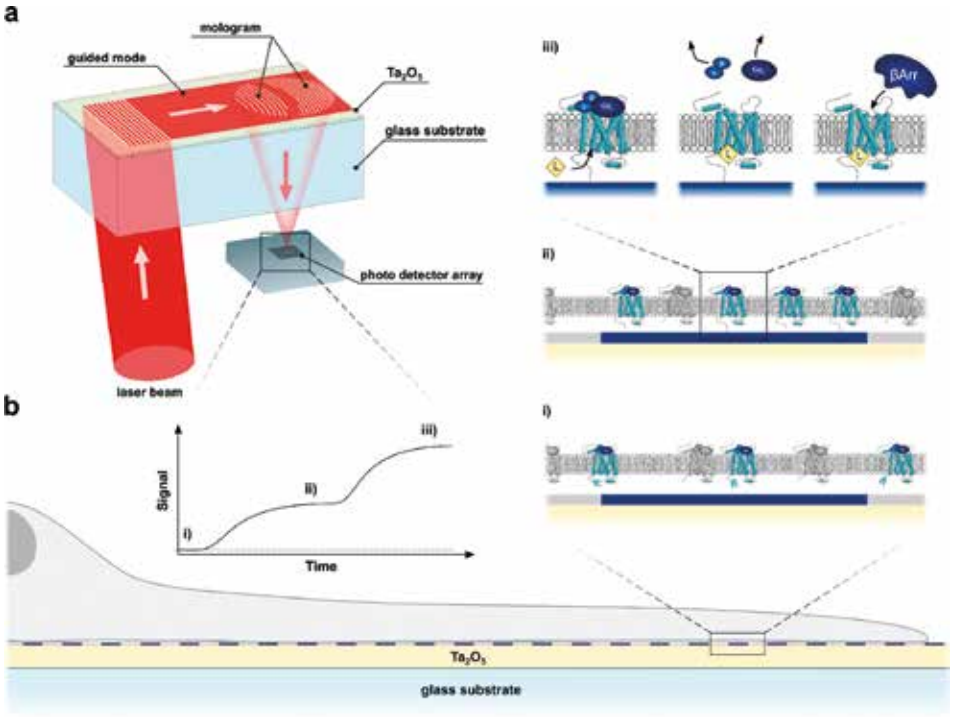

FIG. 4. Illustration of the working principle of cell-based molography, cf. [14]. (a) A single-mode optical waveguide with graft copolymer layer serves as a sensor chip. The guided mode is diffracted at the biomolecules comprising the mologram and forms a diffraction-limited focal spot. Molecules that bind to the mologram contribute to the light intensity in the focal spot, whereas other molecules in the sample do not contribute to this signal. The light intensity scales quadratically with the number of molecules bound to the mologram. The time course of the light intensity is monitored with a photodetector array. (b) Reactive immersion lithography (RIL) is used to generate a template mologram capable of ordering the membrane protein of interest in the adherent cells on the mologram. The autoreactive SNAP-tag protein is fused to the extracellular side of the membrane protein of interest, here a transmembrane spanning, G protein coupled receptor. The SNAP-tag permits one to arrange the target receptor to the template mologram on the sensor chip by covalent binding to the SNAP-tag substrate. Cells are plated onto the sensor chip. (i) Target and off-target proteins expressed in the cells diffuse freely within the plasma membrane. (ii) The randomly distributed target receptors are localized to the mologram on the chip via the extracellular SNAP-tag, leading to a spatial organization of the receptors within the cell membrane. As a result, the mologram is transferred from the surface of the chip into the plasma membrane of the cell, establishing a transmembrane mologram. The number of receptors that are arranged in this fashion can be controlled by the number and therefore the density of SNAP-tag binding sites on the template mologram. Unbound as well as off-target receptors stay randomly distributed. (iii) Refractive index changes at the arranged proteins of interest change the molographic signal. Such refractive index changes are caused either by a local mass change through ligand binding (left), dissociation (middle), or association (right) of cytosolic proteins but also by local changes in ion concentration caused by water or ion influx through a membrane channel. Other molecular interactions, e.g., binding at off-target membrane proteins do not contribute to the molographic signal because they are incoherent. (Figure reproduced from [14])

Cell-based molography uses a membrane protein nanopattern, the transmembrane mologram within adherent cells, to eliminate disturbing cross-sensitivities in the assay [14]. The required specificity of the molecular detection is achieved by spatially ordering a membrane protein of interest into a coherent pattern of fully functional membrane proteins in the cell membrane on the surface of a sensor chip [14]. Thereby, molecular interactions with the coherently ordered membrane protein become visible in real time, while nonspecific interactions and holistic (i.e. cell shape) changes within the living cell remain invisible [14]. Examples of nonspecific interactions are off-target proteins that interact with non-ordered membrane molecules or the membrane itself as well as other molecules distributed within the cell.

The evanescent field of the guided mode limits the sensitive volume above the surface of the sensor chip to a thin layer of approximately 80 nm thickness. Within this sensitive volume, cell-based molography probes all interactions of molecules with the transmembrane protein in the transmembrane mologram in real time in a living cell.

4. Conclusion and outlook

Thanks to advances in photolithography and nonfouling, photoactivatable surface chemistry, it has become possible to apply the holographic principle to sensitive molecular detection. Such molecular holograms, termed mologrames, can be used for analysis of biomolecules in complex biological samples. In molography, biomolecules on a chip become apparent through diffraction, their coherent signal stand-

ing out from the speckle background generated by randomly arranged scatterers. The mologramphic signal is hardly affected by changes in refractive index due to temperature gradients, buffer changes, or nonspecific bindings, which all are largely incoherent with respect to the mologramphic pattern.

The processes of life are naturally dynamic in space and time on the intermolecular and the intramolecular level. The amount of biomolecular interactions that may be discovered in the future is huge. Being able to see and to follow biological interactions unfold in time allows us to understand the mechanisms of life as well as disease. Mologramphy allows not only the discovery of biomolecular interactions but also to investigate and to characterize them in complex environments and even within living cells. Mologramphy widens our analytic capabilities for the investigation of biomolecular interactions in a broad range of possible applications.

Acknowledgements

Christof Fattinger (CF) acknowledges Janos Vörös (JV), Klaus Peter Stengele, Volker Gatterdam, Andreas Frutiger, Yves Blickenstorfer, Thomas Lübbers, Dieter Heindl, Cla Duri Tschannen, Andreas M. Reichmuth, Fridolin Treindl, Silvio Bischof, Matthias Lauer and Markus Müller for their contributions to the development of mologramphy. The first experimental realization of mologramphy was accomplished at ETH Zürich in a fruitful collaboration between JV and CF. Without this collaboration, which was enabled and financed by Roche, the mologramphy method would still be in its infancy. The development of mologramphy at ETH and Roche resulted in the foundation of a joint ETH-Roche spinout company – lino Biotech AG - for commercialization of mologramphy. Finally yet important, CF thanks Bernhard Braunecker for the invitation to contribute with this article to the *SPG Mitteilungen*.

References

[1] J. Homola, “Surface plasmon resonance sensors for detection of chemical and biological species,” Chem. Rev. **108**, 462 (2008).
[2] X. Guo, “Surface plasmon resonance based biosensor technique: a review,” J. Biophotonics **5**, 483 (2012).
[3] S. H. Gellman, “Introduction: Molecular Recognition,” Chem. Rev. **97**, 1231 (1997).
[4] R. Baron, J. A. McCammon, “Molecular recognition and ligand association,” Annu. Rev. Phys. Chem. **64**, 151 (2013).
[5] M. Piliarik, V. Sandoghdar, “Direct optical sensing of single unlabelled proteins and super-resolution imaging of their binding sites,” Nat. Commun. **5**, 4495 (2014).
[6] C. Fattinger, “Focal mologramphy: Coherent microscopic detection of biomolecular interaction,” Phys. Rev. X **4**, 031024 (2014) and the corresponding Viewpoint: G. Binnig, “Coherent signal picks out biomolecular interactions,” Physics **7**, 84 (2014).
[7] V. Gatterdam, A. Frutiger, K-P. Stengele, D. Heindl, T. Lübbers, J. Vörös, and C. Fattinger, “Focal mologramphy is a new method for the in situ analysis of molecular interactions in biological samples,” Nat. Nanotechnol. **12**, 1089 (2017).
[8] A. Frutiger, Y. Blickenstorfer, S. Bischof, C. Forró, M. Lauer, V. Gatterdam, C. Fattinger, and J. Vörös, “J. Principles for Sensitive and Robust Biomolecular Interaction Analysis: The Limits of Detection and Resolution of Diffraction-Limited Focal Mologramphy,” Phys. Rev. Applied **11**, 014056 (2019).
[9] T. L. McMeekin, M. L. Groves, N. J. Hipp, “Refractive Indices of Amino Acids, Proteins, and Related Substances.” In Amino Acids and Serum Proteins; American Chemical Society, 1964; Vol. 44, Advances in Chemistry, chapter 4, pp. 54–66.
[10] F. Zernike, “How I Discovered Phase Contrast,” Science **121**, 345 (1955).
[11] K. Michel, “Das Phasenkontrastverfahren und seine Eignung für zytologische Untersuchungen," Naturwissenschaften **37**, 52 (1950).
[12] M. Mammen, S.-K. Choi, G. M. Whitesides, “Polyvalent Interactions in Biological Systems: Implications for Design and Use of Multivalent Ligands and Inhibitors,” Angew. Chem. Int. Ed Engl. **37**, 2754 (1998).
[13] A. Frutiger, C. D. Tschannen, Y. Blickenstorfer, A. M. Reichmuth, C. Fattinger, and J. Vörös, “Image reversal reactive immersion lithography improves the detection limit of focal mologramphy,” Opt. Lett. **43**, 5801 (2018).
[14] A. M. Reichmuth, M. Zimmermann, F. Wilhelm, A. Frutiger, Y. Blickenstorfer, C. Fattinger, M. Waldhoer, and J. Vörös, “Quantification of Molecular Interactions in Living Cells in Real Time using a Membrane Protein Nanopattern,” Anal. Chem. **92**, 8983 (2020).

Zernike’s phase contrast method of observation (1932)

When imaging a biological phase object $u(x,y) = \exp(i\,\phi(x,y))$ a clearly visible increase in contrast can be achieved either by selective staining of the sample, or more efficiently, by installing a phase plate $A = a\exp(i\,\alpha)$ in the pupil plane of the microscope objective. The zeroth diffraction-order of the phase object does not carry information about the object. The phase plate should cover only the zeroth diffraction-order of the object-function and should damp it. The damping reduces the amplitude of the zeroth diffraction-order and balances it to the amplitude of the diffracted waves. The phase plate in the pupil of the objective causes a phase shift between the zeroth order and the higher diffraction-orders of the object-function, which carry the object information. The phase shift α within the object wave leads - after the second Fouriertransformation from the pupil to the image plane - to an intensity variation by the interference term $I(x,y) = C\,[a^2 \pm 2a\,\phi(x,y)]$ with C a constant and $\alpha = \pm\,\pi/2$. Thus, the invisible phase function ϕ in the object plane is observable as intensity contrast variation in the image plane.

(Born & Wolf, "Principles of Optics", Pergamon Press, 1975, p. 424 ff)

Cryo Electron Microscopy reaches atomic resolution for the 3D structure of proteins

Holger Stark, MPI for Biophysical Chemistry, Göttingen

Cryo-EM is a technique that is capable of solving the three-dimensional structure of proteins by computational analysis of large amounts of electron microscopic images obtained from flash frozen and ice embedded protein molecules. The method is based on an instrument that has been invented by Ernst Ruska already in the 1930's and improved ever since. Initially, the electron microscope has been regarded entirely useless for biological research, mainly because of the expected beam damage by the electron radiation and the fact that electron microscopes require operation in high vacuum. Nevertheless, improvements in microscope hardware, specimen preparation techniques and computational image analysis techniques made it finally possible to establish cryo-EM as a structural biology tool that is capable of solving 3D structures of proteins at resolutions that allow atomic model building. This brought cryo-EM up to the level of NMR and X-ray crystallography as structure solving technique. A substantial amount of the required technological advancements happened only in the last 10 years leading to what is today known as the resolution revolution in cryo-EM. The importance of the unleashed potential of cryo-EM for structural biology led to the Nobel prize award in Chemistry in 2017.

Two European laboratories have now announced to have pushed the resolution limits of cryo-EM even further. In both cases novel electron microscopic hardware was used to reach true atomic resolution structure determination of proteins and the visualization of hydrogen atoms. Atomic resolution can be defined as the resolution level that is needed to visualize each atom within the protein separated from all other atoms in the three-dimensional density map. Atoms are indeed shown to be separated in this most recent work approaching resolutions of 1 Å (1.15 and 1.22 Å respectively). At this resolution the map interpretation becomes much more direct without the need of prior chemical knowledge about proteins that is normally required for atomic model building at lower resolution (in the 3 ± 0.5 Å range). The benefit of such high resolution is the increased accuracy that allows small deviations from normal protein chemistry to be interpreted directly. It is well known from enzymology that such deviations from expected chemistry drive chemical reactions in proteins which makes this resolution improvement very important to understand protein function. Any increase in resolution also goes along with an increase of water and ions that can be observed in the density map. This is highly relevant because they also play very important roles in protein chemistry. Obviously, such an increase in the level of understanding of protein architecture and function at high resolution is also essential for the development of drugs that directly interfere with the structure and function of their protein targets. This next step towards higher resolution structure determination will make cryo-EM increasingly more interesting and important for pharmacologically relevant studies that are aimed at the development of new and better drugs.

The two laboratories used different electron microscopic hardware improvements to reach this next step in cryo-EM technology. One of the microscopes was equipped with a novel cold field emission electron source, an energy filter and the latest high-end direct electron detector. The other microscope used an additional monochromator in combina-

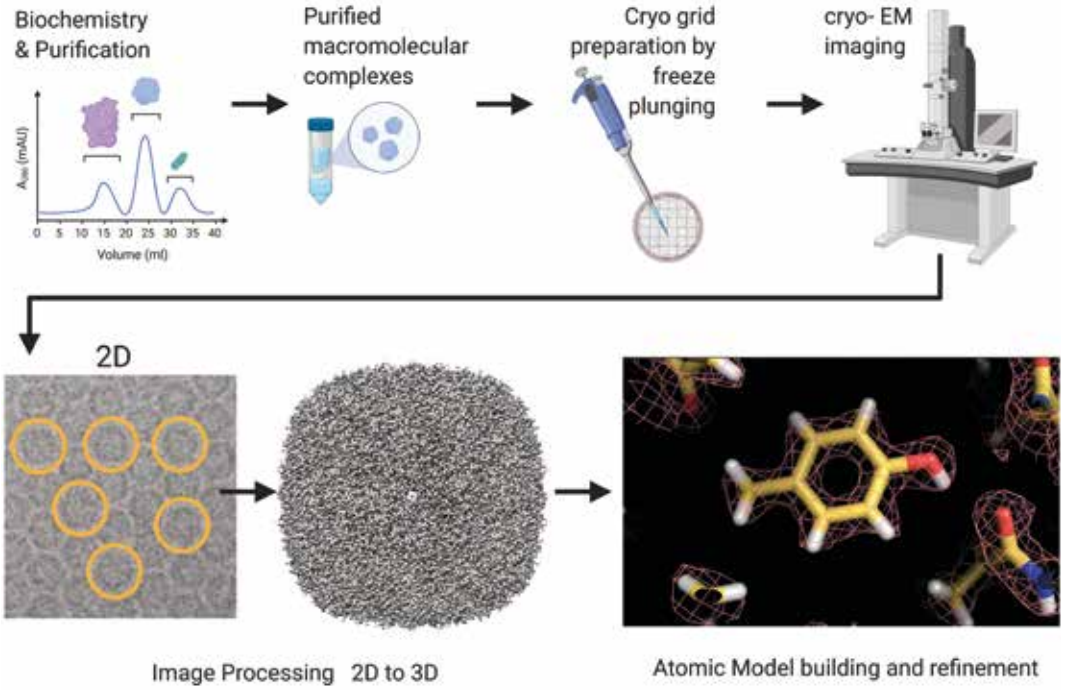

The schematic pathway from biochemistry to 3D structure. For successful 3D structure determination macromolecular complexes are either purified from cells directly or they are reconstituted from individual components. Complexes need to be biochemically pure and structurally intact which is very often one of the most challenging steps of the entire procedure. Purified complexes will then be prepared for cryo-EM in a thin layer of rapidly frozen buffer by plunging an electron microscopic grid into liquid ethane – a method that was pioneered by Jacques Dubochet. The macromolecular complexes are embedded in a thin layer of amorphous ice and as such they are protected from dehydration in the electron microscope. Images are recorded in an automated computer controlled cryo electron microscope in which the sample is kept at liquid nitrogen temperature. Usually several ten to several hundred thousand individual particle images are required to calculate a 3D structure. This requires individual particles to be boxed, aligned and their relative angular orientation to be determined prior to calculate the three-dimensional density map. Atomic models can be build into these density maps at resolutions better than about 3.8 Å resolution when some of the large bulky side chains of proteins become visible. Only at true atomic resolution individual atoms become visible as individual atoms.

tion with a second-generation spherical aberration corrector to improve the optical quality and resolution power of the microscope. While both microscopes were able to reach close to 1 Å resolution structures of the protein apoferritin, each one of them is still not powerful enough to break the 1 Å resolution barrier with reasonable image statistics. However, even this next step in resolution improvements might not be too far away from now when these latest technological developments will be combined within one instrument.

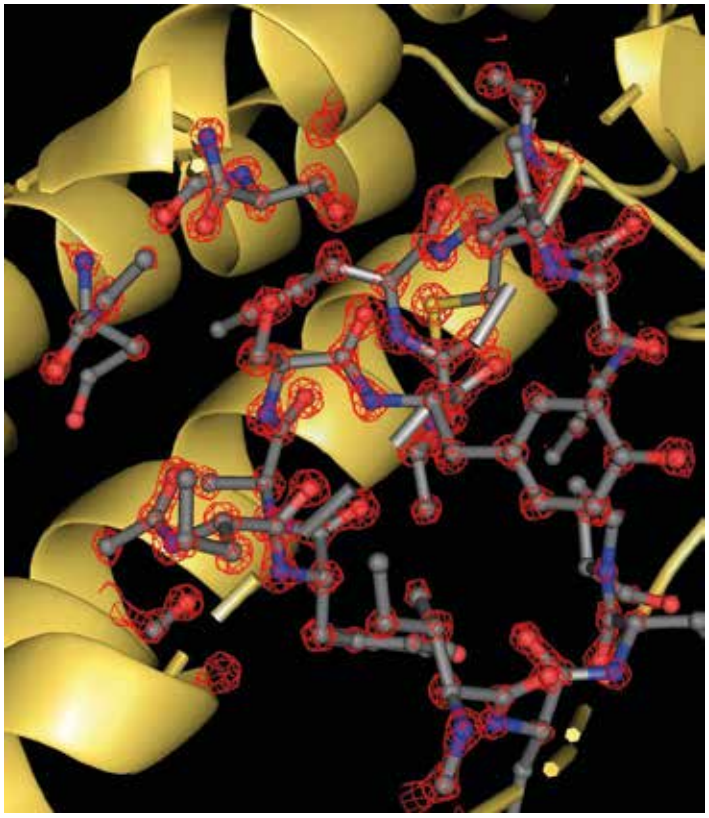

Atomic model of apoferritin built into the atomic resolution density map. From 1 million particle images we determined the 3D structure of apoferritin at 1.25 Å resolution. This resolution is sufficient to visualize atoms as separate entities (red mash) which allows highly accurate model building. The yellow ribbon model is the cartoon representation of one apoferritin chain.

In recent years the number of solved protein structures by cryo-EM followed an exponential growth that is still ongoing. Cryo-EM is becoming increasingly more popular among structural biologists because it does not require to grow 3D crystals of the proteins like in X-ray crystallography. Especially for very large macromolecular complexes and for medically relevant membrane bound protein complexes, the success rate in structure solving by cryo-EM is higher compared to X-ray crystallography. Nevertheless, all three structure solving techniques (X-ray, NMR and Cryo-EM) have certain advantages and disadvantages which makes them highly complementary in their applications. Real understanding of protein function requires many more different techniques to be combined and cryo-EM is a very powerful addition to this set of techniques. Cryo-EM is also still in a development phase and has lots of potential for further improvements to come in the next few years.

Image Processing

Electron microscopic images of protein complexes are considered to be 2D projection images of the same 3D object. Having many projection images from different viewing perspectives allows to reconstruct the three-dimensional density map of the protein making use of reconstruction algorithms. This is similar to X-ray tomography in medical applications with the difference that the relative angular orientations of the individual particle images are unknown and need to be determined by computational means.
Because of the extremely high noise level of cryo electron microscopic images, Bayesian approaches offer currently the most powerful solution to not only determine the correct projection angle but also the accurate alignment parameters for each individual particle image of the protein. By comparing the raw images with a set of re-projections obtained from a 3D model the structure itself and all the required alignment parameters can be improved in a highly iterative procedure. Additionally the microscopic raw images need to be very carefully corrected for the contrast transfer function of the respective electron microscope and other electron optical aberrations (such as coma and astigmatism) that play resolution limiting roles in high-resolution cryo-EM.

Comment by Jacques Dubochet

Thirty-four years ago we published a model of a virus reconstructed at 35 Å resolution by cryo-electron microscopy. Improved each year by a growing number of dedicated groups, a tenfold better resolution became routinely achievable some years ago. This is a breakthrough because, at 3.5 Å, the atomic structure of a complex biomacromolecule starts to emerge from the model; cryo-EM enters chemistry. For this achievement, three of the major contributors shared the 2017 Nobel prize in chemistry. Since then the pace accelerated. I only follow the field at a distance but I am flabbergasted and enthusiastic by the progress, as described in this report.

One point disturbs me, however. The prices of the instruments are exploding. I don't believe that, scientifically, it must be so. I share this view with my friend Richard Henderson, the still very active Nobel co-laureate from Cambridge. He is pushing hard towards a relatively low-voltage instrument (100 kV) that would democratise cryo-EM. Industry would earn less from a single microscope but could sell many more. Perhaps it would be good business. Certainly it would be good for science and, perhaps, for the well-being of mankind.

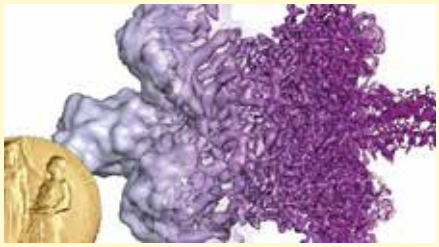

Cryo-Electronmicroscopy has become the tool of choice to elucidate the structure of biomolecules. (J. Dubochet, Nobel Prize 2017)
© Martin Högbom / The Royal Swedish Academy of Sciences

Milestones in Physics (21)

Philip W. Anderson, a pioneer in modern condensed matter physics

Phil Anderson, who with his dictum „more is different“ and concept of „emergence“, more than any other person showed that naive reductionism is insufficient to form a scientific understanding of the world around us, died on 29 March 2020 in New Jersey. As a mentor and colleague, he also touched the lives of many scientists around the world. There have been countless obituaries in the international press, so our aim here in the journal of the Swiss Physical Society, is to supplement rather than replicate these by providing impressions and recollections of some scientists in Switzerland who interacted with Phil, primarily at Bell Laboratories, but also via Maurice Rice, the ETH professor who was the closest Swiss-based associate of Phil.

Thierry Giamarchi (University of Geneva)

To say that Phil Anderson was a giant in physics, who has shaped what modern condensed matter physics is, is to state the obvious. He is one of the very rare theorists to have left a deep mark on the entire spectrum of subjects in the field ranging from disordered classical and quantum systems (spin glasses, pinning of vortices, localization, etc.) to quantum systems (magnetism in metals or insulators, disordered quantum systems, superconductivity, etc.). There is clearly not a theorist working in the field today that has not been deeply influenced by one of Phil's papers.

On my side he had a decisive impact on my career from the start: as a young undergrade student I heard a seminar on Anderson localization (the effect of disorder on quantum systems, one of the theories for which he got the Nobel prize), and found it so beautiful that I decided there and then to do my PhD on this topic (which I did). In addition to the work on Anderson localization, I had during my PhD the occasion to discover with awe several others of his papers such as the one on the Anderson orthogonality catastrophe or the one on the "poor man's scaling" of the Kondo problem, which were pure jewels. I only had later the occasion to meet the man, during a conference in Cargese, and found him surprisingly accessible, and totally driven by the scientific aspects of a discussion without bothering about any aspects of seniority or such considerations.

But it was only during my stay as a postdoc at Bell labs at the beginning of the 1990's that I had serious occasions to discuss with him. He had at the time the idea that the physics of 1D systems (so called Luttinger liquids) was a key to the understanding of high T_c superconductors. This led to many discussions with him, often heated, but always profoundly interesting and leading to deep thinking afterwards. Understanding him was not easy. He had this "impressionist" way of arriving to a result, a mixture of deep knowledge of experiments and some blazing intuition, that was very orthogonal to the very strict "analytical" training that I received during my PhD. This style of physics, also going for the most unconventional explanation to find the crack and new theories – something for which he has been tremendously successful – made it quite difficult to convince him just by calculation alone. He had to be convinced deep down at the physical level. Needless to say, this forced to think deep, and definitely generated a host of new ideas and research directions, even when the original idea was not successful as intended. So, discussing with Phil was always a tremendous source of inspiration, and I had the extreme fortune to be able to do so at various occasions till the last time I saw him in Geneva in 2006.

In addition to the pure scientific aspects, he had some impish manners that were infectious. One evening during a dinner at a conference in Trieste, I asked him whom he was considering as the best theorist he had met (wondering whether he would say Landau, or Feynman, or someone of the sort). His answer was with a twinkle in the eye (and although I think he was not at all religious): God!

For the 1991 Nobel Jubilee there was a very imposing and very solemn photo of the laureates, where one person – with a big smile on his face – purposefully displayed his name upside down. Guess who!

Dirk van der Marel (University of Geneva)

Anderson was in many ways the father of modern solid state physics. His thoughts and ideas have inspired generations of physicists, experimentalists and theoreticians alike. His works are pearls of original thinking and clarity of the scientific discourse. His papers on magnetism and disordered systems, the Anderson–Higgs–Kibble mechanism, disordered superconductors, resonating valence bond theory, and interlayer tunneling in the high T_c cuprates, have provided the scientific basis of my scientific research from the early eighties until now.

I had the tremendous privilege to have met and interacted with Anderson over the years on multiple occasions. Our interactions ranged from pizza lunch at Princeton while his colleagues and he were sorting hundreds of applications, dinner conversations on chamber music, hiking with a group of conference participants in the Swiss alps while picking mushrooms, and, of course discussions on theoretical and experimental condensed matter physics.

Anderson showed a human kindness and interest to the ideas of his colleagues regardless of their age and experience. He didn't hesitate to express his opinion about what is and what isn't relevant in scientific research and favored conceptual insights, analytical methods, and an intuitive approach over sheer number crunching.

His approach to science was strictly anchored in the scientific method, confronting theoretical predictions with experimental data and, after all checks and balances had been made, using experimental facts as a reference point for developing theoretical insights. Although probably other examples exist, from nearby experience I remember the heated debate about the pairing symmetry in the cuprates. In the late 80s and early 90s the dominating view shared by most theoreticians including Anderson was, that the gap in the cuprates was isotropic. As a result of improved sample qual-

ity and novel experimental methods experimental evidence started to accumulate in the early 90s that the cuprates have an isotropic gap with line nodes with a d-wave symmetry. Anderson's position on the issue of the pairing symmetry was largely experiment based. His account in his book "the theory of superconductivity in the high-T_c cuprates" (Princeton, 1997) gives the benefit of the doubt to d-wave pairing, in part motivated by experimental evidence from Josephson interference experiments, in part photoemission showing a large gap along $(\pi,0)$ and deep nodes along (π, π), in part neutron scattering at 2Δ indicating that the gap changes sign. Anderson warns against oversimplification and points out the importance for repeating the experiments on additional members of the cuprate family.

A second episode concerned the interlayer tunneling theory of Chakravarty, Sudbø, Anderson, and Strong. The model started from the observation that the normal state is "strictly two-dimensional and coherent transport in the third dimension is blocked." Microscopically, Anderson explains this as a consequence of the normal state being a Luttinger liquid. In the superconducting state interplanar Josephson tunneling of Cooper pairs occurs as usual for coupled superconducting films, so that in this sense the superconducting state of the cuprates is more normal than the normal state. "Along the c-axis there is a great defect in conductivity: there is no coherent motion of electrons in the c-direction. This means that there is, in the normal state, a missing energy ... which is regained in the superconducting state". Interlayer hopping together with the "confinement" is either the mechanism of or at least a major contributor to the superconducting condensation energy. This state of affairs implied a simple relationship between the interlayer Josephson coupling (which could be determined from the c-axis penetration depth or the c-axis Josephson plasma resonance) and the condensation energy of the superconducting state which can be determined from specific heat experiments. This lead in the period 1996 - 1998 to a series of experiments by Kathryn Moler, John Kirtley, John Loram, and my group. Theoretical guidance in the form of discussions and scientific publications was provided by Anderson and, independently, by Leggett. Measurements of the aforementioned quantities in $Tl_2Ba_2CuO_6$ showed that the Josephson coupling was at least an order of magnitude too low to account for the superconducting pairing. In the field of high T_c superconductivity theoreticians rarely declare forfeit in the face of experimental evidence. Anderson, however, displayed true greatness; he didn't hesitate to defend our experiments to his theoretical colleagues, and he switched the attention of his great mind to different approaches of the high T_c puzzle.

In private discussions it was not always easy to understand everything he said. This was in part due to the fact that he tended to overestimate my understanding of theoretical physics, and in part due to the fact that he tended to speak softer and softer as the information that he conveyed became more important. I remember him with fondness.

Gabriel Aeppli (ETHZ, EPFL, PSI)

Anderson's approach to complex problems by identifying the relevant low energy degrees of freedom via consideration both of data and underlying physical principles has really been the defining paradigm for my entire life as a scientist. Apart from this influence obtained through his papers and talks, I did have the good fortune to interact personally with Phil. My first encounter with Phil was during my job interview – a two day process - at Bell Laboratories. He seemed to be asleep during most of the presentation, but at the end he asked a question, concerning "reentrant" spin glasses, about my thesis which could not have been asked had he been genuinely asleep. Of course, as the co-inventor of the Edwards-Anderson order parameter and replica trick, the concepts which together set the agenda for the study of frozen states in disordered media because they brought mathematical rigour to a messy corner of physics and chemistry, with eventual broad impact on fields from biomedicine to economics and computer science, he was well-positioned to formulate interesting questions on the subject of magnetic glasses.

The last real encounter was many years later on a trail at Aspen, where he was hiking - not struggling - in the opposite direction on the Buckskin Pass (3798 m) trail by himself (almost certainly against the advice of the authorities) at an age north of seventy. In between, there were interactions mainly in the tea room at Bell Laboratories, which he frequented even though he was spending most of his time at Princeton. Given his stature as Nobel laureate and my position as a starting scientist, it was remarkable that he had the patience to listen to me about problems which were by that time to a large extent peripheral (he had already solved them!) to his own contemporary research. My sense though is that this relationship was typical of that with other experimentalists - he had tremendous respect for and little fear of real data, which he probed thoroughly to establish trustworthiness.

Bertram Batlogg (ETHZ)

A keen interest in the latest results from the lab and close interactions with experimentalists were a characteristic of Phil's working style. He would sit down for hours analyzing data and suggesting new measurements. For young hires at Bell Labs in the 1980's this was particularly exciting and rewarding at the same time as Phil would patiently explain his latest theoretical concepts, such as his take on intermediate valence Rare Earth compounds, Heavy Fermions and Kondo lattices. With fellow theorists his patience might be shorter. Decades earlier in the 1950s the close contact with experiments on doped Silicon led him to the seminal theory of electron localization.

The traditional afternoon tea was a Bell Labs institution when dozens of researchers from the Physical Research Area would gather for informal, and quite often heated, chats on physics (or in early April on US tax law). When his turn would come Phil dutifully would put the huge aluminum kettle on the heater, brew the tea and supplied pounds of all sorts of cookies. Apparently he liked mixing with colleagues. Once at a workshop on superconductivity with numerous students participating, Phil presented a poster, in addition to the key note talk. And he did it in a most memorable way. In the dimly lit basement hall he was sitting on a chair next to the poster "camouflaged" with a hat, big glasses and a fake mustache. Thus junior scientists and students would indeed feel comfortable engaging this "just ordinary" presenter for

explanations. His friends and colleagues will never forget these hours and will treasure the memory of Phi's humor and art of disguise.

Manfred Sigrist (ETHZ)

"More is different", a most remarkable and insightful article from 1972 was probably my first encounter with the author Phil Anderson. As an undergraduate student I did not appreciate fully the depth of the ideas yet. Only over time I started to appreciate his school of thought and feel a strong boost in my pride of being a condensed matter physicist.

Becoming a student in Maurice Rice's group then gave me the opportunity to also meet Phil Anderson, as they kept close ties since their common years at Bell Laboratories. In that time the news of the discovery of cuprate high-temperature superconductivity broke, which influenced much of the research in Zurich and I became a direct witness of many of the developments. Amazingly quickly Phil Anderson understood that the physics of a hole-doped Mott-insulator in the CuO_2 plane was the essence for superconductivity in these materials. The spins originating from one hole per Cu-ion coupled through superexchange would be starting point and the key ingredient of what would eventually become one of the most comprehensive paradigms of cuprates.

In a pioneering article in Science (1987) he introduced the notion of the resonating valence bond (RVB) state, which he developed together with Baskaran. The idea was so stunning that it needed a genius to find it. The RVB state constitutes a short-range correlated quantum liquid phase of strongly correlated electrons. Phil Anderson realized that such a state could be described by the Gutzwiller projection of a wave function of uncorrelated electrons, enforcing the presence of a single hole per Cu-ion, and would correspond to BCS-type of ground state, which then upon hole doping yields superconductivity. The so-called "t-J-model" incorporating the superexchange and doped mobile holes became the essential framework for the RVB physics. Despite being a rather simple model it is highly non-trivial to analyze due to correlation. The idea was taken up immediately at ETH and Fuchun Zhang and Maurice Rice provided with the Zhang-Rice singlet a solid microscopic basis for this model.

The Gutzwiller projection represents a real challenge and many groups invented techniques for this purpose, such as variational Monte Carlo calculations (Maurice Rice), slave boson mean field approaches (Gabriel Kotliar and Hide Fukuyama) or gauge field treatments (Patrick Lee, Xiao-gang Wen and Naoto Nagaosa). Interestingly, the superconducting phase predicted by the RVB concept has d-wave pairing symmetry, a fact which actually prompted Phil Anderson to abandon his idea for several years, as it seemed to contradict experiments, and to follow a completely different line to explain cuprate superconductivity. After d-wave pairing had eventually been established, however, Phil returned and promoted what is known nowadays as the "plain vanilla" version of the RVB paradigm, as reviewed in 2004 in the famous "A-to-Z" paper with the authors Anderson, Lee, Rainderia, Rice, Trivedi and Zhang.

The plain vanilla RVB theory not only predicts the correct pairing symmetry, it also gives a good account of the basic phase diagram of cuprates upon doping, such as the superconducting dome and the pseudogap phase. A theory developed in Maurice Rice's team, the YRZ propagator ansatz (Yang-Rice-Zhang), shows that the RVB picture incorporates features, which describe even more details of cuprate physics such as the Fermi arcs of the pseudogap phase. Cuprates are among the best studied material classes in condensed matter physics. Naturally it is not surprising, that many details have been observed which are not contained in the RVB picture. Nevertheless, it remains undoubtedly among the most convincing and beautiful guides to understand cuprates.

As Maurice's student I was a member of the family and it was easy for me to approach Phil. I remember one occasion when I met him in Japan in the late nineties. It was shortly after John Horgan's infamous book "The end of science" was published, for which also Phil had been interviewed. Unlike for most of the other people which are displayed most unfavorably, I had the impression that Horgan showed at least some respect for Phil. So I asked Phil how he got into this book. I learned from him that we scientists are naïve indeed when talking openly to a journalist whose intention it is to lure you into statements which promote his thesis. Surely, Phil was most unhappy about the book, whose views he absolutely did not share, and how his statements were distorted by very selective accounting of what he had said. Indeed he stated that he now also understands why politicians, who are specially trained for this, would give interviews without much content. In the same meeting I also learned that Phil and I share a common experience: both of us celebrated our 30th birthday as gaijins (visiting scientists) in Japan.

A section from the picture on the title page: In the first row Phil Anderson (left), Richard Greene and Øystein Fischer (right), the organisers of the Gordon Conference on Superconductivity from 17-22 September 1995 in Les Diablerets. In the last row the second from right: Maurice Rice.

Physik Anekdoten und persönliche Erinnerungen (22)

Um auch den Erinnerungen von Zeitzeugen an bedeutsame Ereignisse in der Physik ein angemessenes Forum zu geben, wird ab dieser Ausgabe die Reihe "Physik Anekdoten" zu "Physik Anekdoten und persönliche Erinnerungen" umbenannt.

Die Gründung des Paul Scherrer Instituts

Andreas Pritzker

Das Paul Scherrer Institut PSI wurde am 1. Januar 1988 gegründet, und es gehört zweifellos zu den wichtigsten Forschungsinstituten weltweit. Es bietet eine einzigartige Kombination von Grossforschungsanlagen für experimentelle Untersuchungen in den Gebieten Teilchenphysik, Physik der kondensierten Materie, Biologie, Chemie sowie für medizinische Therapien. Einen Überblick über die wissenschaftlichen Tätigkeiten in den ersten dreissig Jahren findet man im Bericht *30 Years of PSI* [1]. Hier konzentrieren wir uns auf die Umstände, die zur Gründung des PSI führten.
Zentrale Person der Gründerjahre des PSI war *Jean-Pierre Blaser* (1923-2019), der Nachfolger des legendären ETH Physikprofessors *Paul Scherrer* (1890-1969). In Würdigung der wissenschaftlichen und wissenschaftspolitischen Leistungen Blasers wurde am 29. Februar 2020 in Zürich ein Symposium veranstaltet, dessen Vorträge als Podcasts zur Verfügung stehen [2].

Das PSI entstand durch die Fusion von zwei sogenannten Annexanstalten der ETH, nämlich des Schweizerischen Instituts für Nuklearforschung SIN (Villigen) und des Eidgenössischen Instituts für Reaktorforschung EIR (Würenlingen).

Das SIN besass ein grosses Entwicklungspotenzial, stiess aber an Grenzen

Das SIN wurde 1968 von Jean-Pierre Blaser gegründet. Es entwickelte einen Protonenbeschleuniger von hoher Leistung, der Forschung in Teilchenphysik und weiteren Gebieten ermöglichte. Es funktionierte als Benutzerlabor und stellte seine Anlagen Forschern aus der Schweiz und aus anderen Ländern zur Verfügung.
Dank des leistungsfähigen Beschleunigers besass das SIN ein grosses Entwicklungspotenzial. Es zielte daher auf die verstärkte Nutzung seiner Forschungsanlagen in medizinischen Wissenschaften und – mit einer Neutronenquelle – in der Materialforschung ab. Anfang der 1980er Jahre gab es am SIN eine Warteschlange für entsprechende Ausbauprojekte. Diese kosteten jeweils mehrere Millionen Franken, Geld, das der Schweizerische Schulrat (heute ETH-Rat) als Oberbehörde des ETH-Bereichs beim Bundesrat und den Eidgenössischen Räten in Form von Baubotschaften beantragen musste. Dabei stand das SIN in Konkurrenz zu den Ausbauplänen der ETHs und der Schwesterinstitute im ETH-Bereich. Die beiden ETHs hatten aufgrund wachsender Studentenzahlen Priorität, sodass die Investitionen für das SIN über Jahre hinausgeschoben wurden. Dies brachte die Gefahr einer Stagnation, welche das dynamische Institut schlecht verkraften konnte. Zudem war das Institut zu klein, um all die Ausbauprojekte zu meistern. Hierzu brauchte es eigenes Fachpersonal, und die Personaldecke war angesichts der vielen Vorhaben zu dünn.

Das EIR war nach der Krise stabil, aber seine Zukunft war nicht gesichert

Das Reaktorforschungsinstitut war von der schweizerischen Industrie 1955 als Reaktor AG gegründet worden. Nachdem sich herausstellte, dass die Schweiz keine eigene Reaktorlinie entwickeln wollte, gelangte das Institut 1961 in den Besitz des Bundes. Das EIR geriet früh in eine Krise. Diese führt zu einer Motion des aargauischen Nationalrats Wartmann, welche den Bundesrat veranlasste, zu reagieren. Danach stellte sich das EIR in den 1970er Jahren unter seinem neuen Direktor *Heini Gränicher,* Physikprofessor an der ETH, neu auf.
Schwergewicht des Auftrags des EIR blieb die Nutzung der Kernenergie in der Schweiz. Daneben wandte das Institut sein kerntechnisches Knowhow in anderen Gebieten an. Es wurde zu einer Referenzstelle für den Strahlenschutz und übernahm die Verantwortung für die Entsorgung schwach- und mittelradioaktiver Abfälle aus Forschung, Medizin und Industrie. Daneben betrieb es im geringeren Umfang – je nach vorhandenem Knowhow – Forschung und Entwicklung in Umweltfragen und Solarenergie.
Zwar hatte das Schweizervolk den Ausstieg aus der Kernenergie wiederholt abgelehnt, doch blieb diese umstritten – und damit die Zukunft des EIR als Kernenergieforschungsinstitut.

Die gemeinsamen Aktivitäten von SIN und EIR nahmen zu …

Die Reaktoren des EIR dienten einerseits als Neutronenquelle für die Materialforschung, andererseits der Produktion von Radionukliden für die Medizin. Der Protonenbeschleuniger des SIN war geeignet, eine Neutronenquelle zu generieren und ebenfalls Radionuklide zu produzieren. Somit rückten die Institute thematisch zusammen.
Für Materialuntersuchungen im Hinblick auf künftige Kernfusionsreaktoren, die das EIR betrieb, erwies sich zudem der Protonenstrahl des SIN als anwendbar.
Schliesslich nutzte das SIN bereits Infrastruktur des EIR. Auf dieser Basis ermöglichten die beiden Institute anfangs der 1980er Jahre gemeinsam die Realisierung der Fernwärmeversorgung REFUNA (Regionale Fernwärme Unteres Aaretal) aufgrund von Abfallwärme, die aus dem Kernkraftwerk Beznau ausgekoppelt wurde. An diesem Projekt waren Kaderpersonen von EIR und SIN beteiligt, und in ihrem Kreis wurde erstmals die Idee geäussert, die Institute zu fusionieren.

1 *SPG Mitteilungen* Nr. 58, 2019, S. 44 ff, https://www.sps.ch/fileadmin/articles-pdf/2019/Mitteilungen_PSI30.pdf

2 http://www.video.ethz.ch/events/2020/blaser

… aber auch die Konflikte

Die beiden Institute besassen unterschiedliche Interessengruppen: das SIN war vernetzt mit Hochschulen, das EIR mit Behörden, Industrie und Spitälern. Dementsprechend war die Unternehmenskultur im ersten Fall durch die Nähe zu den Universitäten, im zweiten durch die Nähe zu Ämtern und Industrie geprägt. Die grundsätzlichen Kulturen behinderten oft das gegenseitige Verständnis für einander.
Abgesehen davon kam es zum Streit, als das EIR ein konventionelles Heizreaktorkonzept präsentierte und das SIN mit einem innovativen Projekt nachdoppelte. Allerdings verlief die Angelegenheit im Sand, da sich angesichts schlechter Marktaussichten für Heizreaktoren keine Industriefirma engagieren wollte.
Ein weiterer Konflikt betraf die Nutzung der Ressourcen des EIR bei Konstruktion und Werkstätten für die Neutronenquelle des SIN, wobei das EIR schliesslich einlenkte.

Die SIN-Direktion mischte sich zunehmend in die Wissenschaftspolitik ausserhalb ihres Aufgabengebiets ein

Jean-Pierre Blaser vertrat die Ansicht, wissenschaftspolitische Impulse sollten bottom up, von den Wissenschaftlern her, kommen. Er beobachtete die Entwicklungen in der Wissenschaftspolitik und fühlte sich bei verschiedenen Anlässen genötigt, aktiv einzugreifen. Dies tat er immer mit dem Einverständnis von Schulratspräsident *Maurice Cosandey*.

Als Blaser erkannte, dass die Politik sich daran machte, starken Einfluss auf die Energieforschung zu nehmen, forderte er, die Energieforschung des Schulratsbereichs nach wissenschaftlichen Kriterien zu konzipieren. Der Schulrat setzte auf seine Initiative hin eine entsprechende Kommission aus ETH-Fachprofessoren ein. Diese erarbeitete ein Konzept, das später teilweise eine der Grundlagen für die Energieforschung am PSI wurde.
Nach der Übernahme der US-Firma RCA durch General Electric beschloss GE, das RCA-Forschungslabor in Zürich aufzuheben. Die Halbleiterindustrie war an der Weiterexistenz des Labors interessiert, weil es ihr Zugang zur Grundlagenforschung in technisch interessanten Gebieten gewährte und weil es einen funktionierenden Technologietransfer ausweisen konnte. Sie sah sich allerdings nicht in der Lage, das Labor zu übernehmen. Die SIN-Direktion bemühte sich daher um eine Übernahme des Labors durch den Schulratsbereich. Der Schulrat kaufte das Labor für 1 $ und gliederte es 1987 provisorisch dem SIN und 1988 definitiv dem PSI an.
Und als die ETH beschloss, den Tandem-Beschleuniger auf dem Hönggerberg aus Kostengründen zu schliessen, da dessen Einsatz in der Kernphysik obsolet geworden war, setzte sich Blaser zusammen mit dem Direktor der EAWAG, *Werner Stumm*, für den Erhalt der Anlage ein, da diese inzwischen für hochgenaue Altersbestimmungen verwendet wurde. Da sich das SIN finanziell engagierte, konnte die Anlage gerettet werden.

Luftaufnahme von 1988. Links das Gelände des SIN (heute PSI Ost), rechts das des EIR (heute PSI West). © PSI

Der Schulrat beauftragte das Büro Hayek Engineering mit einer Optimierungsstudie

Der Schulrat stand Mitte der 1980er Jahre vor notwendigen grossen Investitionen für die beiden Schulen in Zürich und Lausanne. Es gab politischen Druck, die Ressourcen zu optimieren. Der Schulrat gab daher beim bekannten Organisationsberater Hayek eine Optimierungsstudie in Auftrag. Diese sollte Doppelspurigkeiten und mögliche Synergien mit dem Potenzial, Ressourcen einzusparen, ermitteln.
Den grössten Handlungsbedarf ortete Hayek bei der Zukunft von EIR und SIN. Der Schulratspräsident stellte ein Gremium von vier erfahrenen Wissenschaftsmanagern zusammen, die Vorschläge für die Zukunft von EIR und SIN erarbeiten sollten: *Jean Teillac*, französischer Hochkommissar für Atomenergie; *Pierre Aigrain*, Staatssekretär für Forschung in der französischen Regierung; *Wolf Haefele*, Vorstandsvorsitzender der Kernforschungsanlage Jülich; *Geoffrey Manning*, Direktor des Rutherford-Appleton Labors bei Oxford.
Die vier hochrangigen Physiker kamen zum Schluss, dass die optimale Lösung der Zusammenschluss der beiden Institute sei. Es zeichnete sich ein Mehrzweck-Forschungsinstitut ab mit den bisherigen Richtungen Teilchenphysik und Kernenergie in reduziertem Umfang und den neuen Bereichen Biowissenschaften, Materialwissenschaften und nichtnuklearer Energie.

Der Schulrat gründete das Projekt "Zusammenlegung EIR-SIN"

Der Schulrat richtete im September 1986 ein Projekt für die Zusammenlegung von EIR und SIN ein. Dieses bestand aus einem Lenkungsausschuss, der von *Michael Kohn* präsidiert wurde und dem die Bundesamtsdirektoren *Eduard Kiener* und *Urs Hochstrasser*, die ETH-Präsidenten *Heinrich Ursprung* und *Bernard Vittoz* sowie Professorin *Verena Meyer* vom Wissenschaftsrat angehörten.
Zudem ernannte er Blaser als Projektleiter. Der Projektleitung gehörten an *Wilfred Hirt* von der SIN-Direktion sowie Heini Gränicher und *Edmund Loepfe* von der EIR-Direktion, und mit beratender Stimme der Schreibende als wissenschaftlicher Berater des Schulrats für die Annexanstalten.

Der Auftrag lautete, Vorschläge für den wissenschaftlichen Auftrag, die Organisation und den Betrieb der neuen Annexanstalt zu erarbeiten. Die Projektorganisation hatte dafür rund ein Jahr zur Verfügung, denn das neue Institut sollte bereits anfangs 1988 seinen Betrieb aufnehmen.
Es war offensichtlich, dass die Zusammenlegung dem Schulratspräsidenten Cosandey und dem zuständigen Bundesrat *Flavio Cotti* ein Anliegen war. Mit Blaser wurde ein Projektleiter bestimmt, der von der Fusion überzeugt war und dessen wissenschaftspolitische und wissenschaftliche Erfahrung Erfolg versprach. Im Weiteren hatte die Projektleitung das Recht, sämtliche Massnahmen bei EIR und SIN (neue Projekte, Anstellungen), welche die Fusion behindern könnten, zu verbieten. Bei Meinungsverschiedenheiten hatte der Projektleiter den Stichentscheid. Mit Gränicher sass der Hauptgegner der Fusion in der Projektleitung, aber er war ein pflichtbewusster Mensch, der akzeptierte, was die vorgesetzte Behörde entschied.

Das Projekt wurde ohne Verzug und mit grossem Einsatz durchgezogen

Projektleiter Blaser konzentrierte sich, zusammen mit seinem Stellvertreter Hirt, auf die Gespräche mit den wissenschaftlichen Institutionen – Nationalfonds, Wissenschaftsrat, Universitäten – sowie mit wichtigen Vertretern der Wirtschaft, vor allem der Industrie. Es galt, ihnen den Vorteil der Fusion zu vermitteln und ihre Vorstellungen zum neuen Institut anzuhören.
Blaser setzte zudem ein Team von Führungspersonen aus SIN und EIR ein, welches nicht nur Vorschläge für das Forschungsprogramm erarbeitete, sondern verschiedene multifunktionale Institute in Europa und in USA besuchte, um deren Auftrag und Organisation abzuklären. Danach entwarfen erfahrene Stabsmitarbeiter von SIN und EIR Vorschläge zur Finanzplanung und Finanzierung der Aktivitäten des neuen Instituts.
Aus allen diesen Abklärungen folgte schliesslich ein Vorschlag für den Auftrag und die Organisation des neuen Instituts, formal in eine Bundesratsverordnung gefasst.
Es handelte sich um ein Geschäft von grosser Ausstrahlung, welches nicht nur in wissenschaftlichen Kreisen, sondern auch bei Kantonen, politischen Parteien und Verbänden auf grosses Interesse stiess. Der Bundesrat ordnete daher eine umfassende Vernehmlassung an. Ihre Ergebnisse zeigten den grundsätzlichen Konflikt zwischen Innovation und Besitzstandwahrung auf. Eine deutliche Mehrheit der befragten Institutionen stimmte der Zusammenlegung zu. Schliesslich konnte der Bundesrat das ***Paul Scherrer Institut*** – der Name wurde erst kurz vor der entscheidenden Bundesratssitzung vorgeschlagen – auf den 1. Januar 1988 gründen. Damit war die grösste Fusion im Bereich des Bundes seit der Gründung der SBB beschlossen worden.

Wer sollte erster Direktor des PSI werden?

Dass der Bundesrat Jean-Pierre Blaser zum Direktor bestimmte, war logisch. Er besass einen hervorragenden Ruf in der Wissenschaft, hatte sich als Direktor bereits bewährt und hatte das Fusionsprojekt erfolgreich durchgezogen. Und er war als starke Persönlichkeit geeignet, das PSI in den unausweichlichen Fusionswirren zusammenzuhalten.
Jean-Pierre Blaser führt das Institut bis zu seiner Pensionierung im Frühling 1990. Er war sich bewusst, dass seine Gestaltungsarbeit unvollendet war. Aber er hatte die Grundlage gelegt und die Richtung für die künftige Entwicklung vorgegeben. Und es war ihm gelungen, das PSI in den ersten Jahren trotz externer und interner Widerstände zusammenzuhalten.
Bei seinem Rücktritt war das PSI nicht stabil. Seinem Nachfolger *Anton Menth* gelang es nicht, das PSI auf Kurs zu bringen. Das Institut musste um seinen Ruf, womöglich um seine Existenz bangen. Menth trat folgerichtig schon bald zurück.
Zum Glück übernahm 1992 *Meinrad Eberle* die Direktion. Ihm gelang es, dem PSI bei Politik, Wirtschaft und Wissenschaft Anerkennung zu verschaffen und das Institut zum Blühen zu bringen.

How dangerous is the non-ionizing radiation used in mobile communication?

Hansruedi Völkle, Physics Department, University of Fribourg, hansruedi.voelkle@unifr.ch

The health risks from electromagnetic radiation, in particular those used in mobile communication and the introduction of the 5G technology, raise fears and stimulate controversial discussions. For a better understanding of the effects of electromagnetic radiation used in telecommunications, as well as of possible impacts on human health, some basic knowledge of the physics and biological effects of non-ionizing radiation are presented. International recommendations as well as existing Swiss legislation are also discussed, as Swiss legislation in this area is more severe than in our neighbouring countries. If the Swiss standards are met, then one can, according to current scientific understanding, exclude any health risks with a reasonable and moderate use of mobile communication technologies.

General remarks

The exposure of a person staying close to a source of electromagnetic radiation (i.e. an emitter of non-ionizing radiation, and in particular a cellular phone antenna), depends on a variety of factors. These factors include the intensity of the radiation; the frequency, shape and direction of the antenna's emission pattern (which, for a mobile phone antenna, generally takes the form of a shell); the distance from the antenna; and the attenuation by walls, roofs or windows of buildings. It should be noted that higher frequencies lead beams to become more directional and attenuated, i.e. absorbed, scattered and reflected by interposed objects. The stronger attenuation at higher frequencies on the one side, but the ongoing technical improvements of the sensor sensitivity on the other side, may lead to a moderate increase of the antenna density. The depth at which non-ionizing radiation penetrates the human body also depends on the frequency: for 1 GHz this is a few centimetres, whereas for 10 GHz this is reduced to the millimetre range.

In densely populated urban areas such as cities, exposure includes the total radiation of all mobile phones surrounding an individual, in addition to other radiation-emitting sources also in use in the area. However, the primary exposure to radiation comes from the individual's own mobile phone.

Radiation of cellular phones

Mobile phones are limited in their emission power so that the Specific Absorption Rate (SAR) should not exceed 2 W per kg of organ mass in an exposed person. The SAR value of most commercially-available phones are below 1 W/kg (close to the body). To obtain the Blue Angel label it should not produce more than 1 W/kg (close to the body) or less than 0.5 W/kg (close to the ear). For 0.5 W/kg, the warming of the brain is below 0.1°C. Health consequences will appear only if the body or an organ is heated above 1°C for an extended period of time. On the other hand, the heat felt in one's ear after a long telephone conversation is not caused by the mobile's electromagnetic radiation, but rather the phone's screen and battery as well as the missing cooling by the ambient air.

What frequencies are used for wireless communication and data exchange?

Mobile telecommunication has evolved tremendously in recent years. Not only have the intensities and number of applications increased, but data rates are also soaring from 2G (GSM), 3G (UMTS), 4G (LTE) to now 5G. The frequency band between 700 MHz and 3500 MHz (3500 MHz is used only for 5G) is not only in use for mobile telephony, but also for Bluetooth (2402 to 2480 MHz), WLAN (the bands of 2400-2484 MHz and 5150-5725 MHz; for WLAN-6: 2400 to 5000-6000 MHz) and cordless telephone (DECT), the later in the field from 1880 to 1900 MHz. Other applications like digital radio (DAB), TV and satellite telephony use frequencies ranging from one hundred to a few hundred MHz. Further applications are broadcast programs by satellites at 10 to 20 GHz, whereas the carrier frequencies for radio-relay systems fall between 1 and 86 GHz (Fig. 1). The frequency bands allocated by Swiss authorities to the different provid-

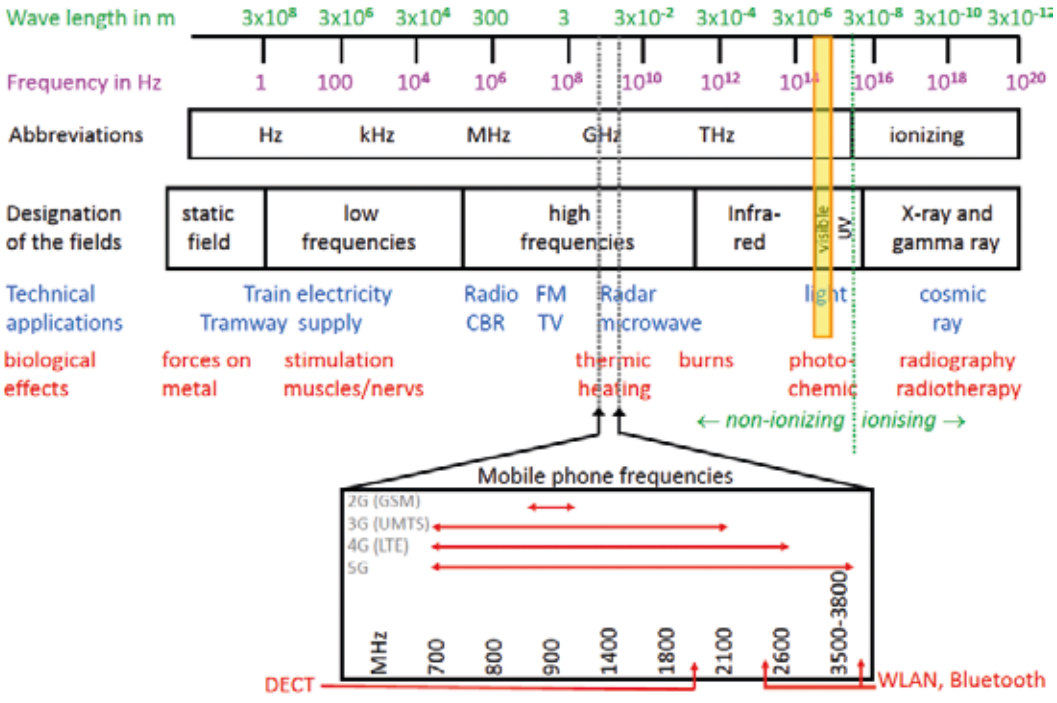

Figure 1: Frequency domain of the electromagnetic spectrum indicated in Hertz (Hz) with the corresponding wavelengths in meters (m). The graph shows the most important technical applications and the biological effects in the different frequency regions. The area used by mobile communication is shown enlarged at the bottom of the graph.

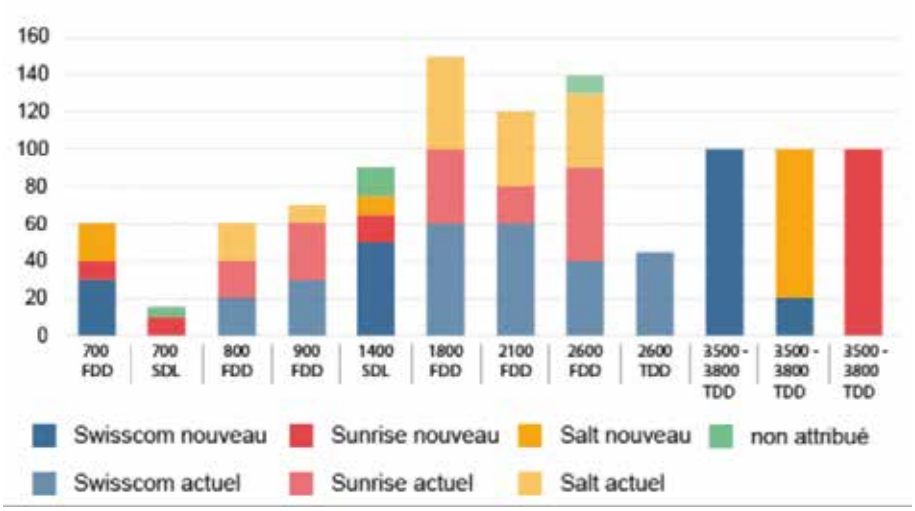

Figure 2: In February 2019 the BAKOM/OFCOM (The Federal Office of Communication) allocated the different frequency domains for mobile communication to the three Swiss operators Salt, Sunrise and Swisscom. Abbreviations: FDD: Frequency Division Duplex = Two radio channels are used for a link; TDD: Time Division Duplex = only one radio channel is used for a link; SDL: Supplemental Downlink = Three radio channels are used for a link.

ers are illustrated in Fig. 2. In 2019, the World Radio Conference identified new bands to be used by mobile telephony which would cover future demand for still-growing data rates. These bands are at 24.25-27.5 GHz, 37-43.5 GHz, 45.5-47 GHz, 47.2-48.2 and 66-71 GHz; after national regulations are put in place, they will be used by mobile phone systems in the near future..

Biological effects of non-ionizing radiation

In the frequency range of mobile phones, thermal effects are considered as the most important ones, but also the possibility of so-called non-thermal effects should be discussed, as some individuals pretend to suffer from them. Such effects are said to affect nerves, brain and metabolism of cells; the consequences could be decreased sleep quality and impaired concentration; damages to genes and other biochemical effects; and even cancer. To date, such effects have not been validated by science at doses below the limits recommended by the ICNIRP [1], whose recommendations are adopted in most national legislations. The health disorders described here, which are attributed to mobile phone radiation by those affected, are very difficult to record with scientific rigor. Evaluating these health disorders qualitatively by proving a cause-effect relationship is challenging, as such studies are based exclusively on the descriptions of psychosomatic symptoms provided by the individuals in question. These studies are therefore mostly non-reproducible.

Moreover, the driving mechanisms are unclear from a biological point of view. Even if such effects can be demonstrated in laboratories at higher doses, they must not necessarily have impact on human health as in a real situation the exposure is for sure below the ICNIRP recommendations. Yet while health risks from exposure to mobile phone radiation have not been validated scientifically, they can also not be excluded with certainty. Reliable statements require long-term studies under realistic conditions.

A selection of biological effects is described in greater detail below.

Attenuation of non-ionizing radiation by matter: The effects of non-ionizing radiation on chemical compounds and biological organisms depend on both the energy of the radiation and its frequency. To produce a physiological effect, the radiation's energy must be absorbed. The attenuation function of non-ionizing radiation or electromagnetic waves by the human body is – apart from the density – similar to the earth's atmosphere. Both are transparent in a wide frequency band, except in the microwave and infrared regions. Responsible for the attenuation is the absorption by the greenhouse gases, water vapor, carbon dioxide, ozone, methane and nitrous oxides. Water vapor in the atmosphere is the most important of these gases, and water constitutes with some 60 and 75% also a dominant component of the human body.

Exposure or dose: The intensity of radiation interaction with biological tissues is given by the dose, i.e. the in a tissue or organ-absorbed radiation energy [J/kg], integrated over the time of exposure. The unit Sv (Sievert) is used for ionizing radiation, whereas the Specific Absorbed energy (SA) is used for non-ionizing radiation. The human body behaves like an antenna: the highest sensitivity is around 50 MHz for adults and around 100 MHz for children. For a

Looking beyond 5G [1]

Even as wireless 5G moves into mainstream, technologists are already looking ahead to the next generation 6G, expected to come on stream in the 2030s. Accessing the terahertz band (sub-millimeter waves) will yield to:

- Extreme high data rate > 100 Gbps exploiting new spectrum bands at 100 x capacity
- Extreme blanket global Gbps coverage, expanded to 10 km in the sky and extended coverage at sea
- Massive connected devices (10 M/km^2) with sensing capabilities and high precision positioning (cm-order)
- Extreme low latency (end to end) of < 1 ms
- Extreme high guaranted quality of service with 99.99999% reliability
- Extreme low energy and cost: Affordable mmW/THz networks and devices.

1 Source: 2020 NTT DOCOMO, 5G Evolution and 6G (cited from 'Optics and Photonics News', July/August 2020)

1 ICNIRP: The International Commission on Non-Ionizing Radiation Protection is a professional body specialized in non-ionizing radiation protection. The organization's activities include determining exposure limits for electromagnetic fields used by devices such as cellular phones. ICNIRP is an independent nonprofit scientific organization chartered in Germany. It was founded in 1992 by the International Radiation Protection Association (IRPA) to which it maintains close relations. The mission of ICNIRP is to screen and evaluate scientific knowledge and recent findings toward providing protection guidance on non-ionizing radiation, i.e. radio, microwave, UV and infrared. (*https://www.icnirp.org/*)

person standing upright, a vertical electrical field induces a current flowing from head to feet and vice versa.

Specific Absorption Rate (SAR) is used as parameter to quantify the absorbed energy in human tissue exposed to non-ionizing radiation between 100 kHz and 10 GHz. SAR [W/kg] is the amount of absorbed energy per unit of time and mass of a tissue exposed to radiation.

$$SAR = \int_{Sample} \frac{\sigma(r)|E(r)|^2}{\rho(r)} dr$$

E is the electric field produced in a tissue or organ, with σ representing the electrical conductivity and ρ the mass density. As not all organs have the same sensitivity, the reference mass (1 g or 10 g) must be indicated. To study the heating effect of electromagnetic waves on human bodies, a standard human was defined with a height of 175 cm, a weight of 70 kg, and a total body surface of 1.85 m^2. When exposed to a radio wave radiation of 14 W, the corresponding SAR value is 0.2 W/kg [2].

The ***specific absorption of energy*** (SA), is defined by: SA [J/kg] = SAR [W/kg] x Exposure time [s]. The relative heat capacity per unit mass is C_ρ [J/kg·K] = ΔQ [J/kg]/ΔT [K]. ΔQ is the amount of heat needed to produce a rise in temperature of ΔT [K or °C] = SA [J/kg]/C_ρ. For liquid water at 15°C and atmospheric pressure of P = 101.325 kPa the relative heat capacity is C_ρ{Water} = 4185.5 J/kg·K. Exposing a human body to SAR = 4 W/kg for 15 minutes can cause an increase of 1°C as long as no cooling system such as blood circulation is active. The following are some values for C_ρ [J/kg·K] with density ρ [g/cm^3] in parentheses: skeletal muscle: 3470 (1,06), fat 2260 (0,94), cortical bone 1260 (1,79), spongy bone 2970 (1,25) and blood 3890 (1,06). For experiments, a model of a human body or plastic doll (phantom) is used, filled with material of the same dielectric and absorption data as the body organs. The produced heat by radiation is measured on the phantom by an infrared camera [2].

Surface charges: Low-frequency electric fields can induce surface charges on the body and, consequently, cause surface currents. Important parameters for the exposure effects are the position of the body and its size, the conductivity of skin tissues and the direction of electric vector.

Induced currents, burning, shocking [3]: An electric current induces an electrical and a magnetic field. According to the law of induction in physics, changes in the magnetic flux density cause electric vortex fields. The low-frequency magnetic fields pose more health problems than the low-frequency electrical fields, as magnetic fields are not shielded by the skin. If an alternating magnetic field flows through an electrically conductive object (for example the human body, which contains electrically non-neutral particles such as electrons, ions and polarized molecules), then this field induces eddy currents that move primarily where the interior of the body is particularly conductive (such as blood vessels and well-perfused tissue). The type of induction also depends on the geometrical configuration of the human body and its organs.

Electrical injury is a physiological reaction caused by an electric current passing through the body after contact with electricity. Contact with energized wiring or devices is the most common cause. It depends on the current density, tissue resistance and duration of contact. The effects range from tingling sensations and injuries caused by jerking away or falling, to pain and induced involuntary muscle contractions, to tissue damage and even – at very high currant densities – ventricular fibrillation or cardiac arrest. Inductions in the human body could be more intensive in the lower part of body, as the ankle cross section is lower than the other parts of legs; high current density there may therefore cause burning. In addition, implanted circuits like pacemakers or ear-amplifiers can be damaged by strong electromagnetic fields. In cases of exposure to high voltages, such as those found on a power transmission tower, direct contact may not be necessary to experience an effect because the voltage may 'jump' the air gap to the electrical device.

2 Moghavvemi M. et al: *Exposing to EMF*, from the book: *Behaviour of Electromagnetic Waves in Different Media and Structures* (June 2011), DOI 10.5772/931, ISBN : 978-953-307-302-6

3 *Magnetic Resonance Imaging* for medical diagnostics needs high-power magnetic field in order to penetrate body with sufficient intensity. Exposing to such fields are limited by IEC Standards. So, a maximum of 2 W/kg for whole body at 6-minute exposing is recommended.

Interaction of electromagnetic waves with the human body

Frequencies	*Wavelength*	*Biological effects*
From static electric or magnetic fields to low frequencies		Forces on metals, metallic implants, conductors with currents
0 – 10 MHz	below 30 m	Stimulation of muscles and nerves; maximum sensitivity of the human body is between 20 und 50 Hz
100 kHz – 10 GHz Microwaves: 300 MHz – 300 GHz	3000 m – 3 cm 1 m - 1 mm	Thermal effects (mainly oscillation of water molecules); Maximum sensitivity of the human body (acting as an *antenna*): For adults 50 MHz, for children: 100 MHz
10 GHz – 1 PHz	3 cm – 300 nm	Burns to the skin and body organs
0,4 – 0,8 PHz	750 nm – 380 nm	Visible light = photochemical reactions
0,79 – 0,95 PHz 0,95 – 1,1 PHz 1,1 – 3,0 PHz	380 nm – 315 nm 315 nm – 280 nm 280 nm – 100 nm	UV-A UV-B UV-C
above 3 PHz	below 100 nm	Ionizing radiation: corresponding energy around 10 eV

Table 1

Non-thermal effects: Various possible biological, physiological and/or biochemical effects are included under this heading, such as lowering melatonin levels – which control our immune system's response to cancer and other diseases – or having an impact on genes (DNA), the nervous system and hormonal functions. Growth hormones of glands can also be influenced, which affects children differently than adults. Whether or not non-thermal effects are harmful to human health essentially depends on the type and dose of exposure. Even if previous experiments on non-thermal effects do not always show clear results, a hazard can be excluded on the basis of current scientific knowledge as long as the radiation exposure is below the ICNIRP limits.

Electro-sensitivity

Some people (according to the cited studies, about five percent of the population) consider themselves electro-sensitive. Their complaints include sleep problems, headaches, nervousness, general fatigue, trouble concentrating, tinnitus, nausea and joint pain, among others. It is obvious that these symptoms have an impact on their quality of life, but it is not possible to say with certainty that these problems are caused by electromagnetic radiation. From the current medical perspective, a specific diagnosis of electro-sensitivity is lacking. But it is psychologically understandable that the mere presence of an antenna could trigger aversions and fears that would lead to psychosomatic phenomena. According to the WHO, there is currently no scientific verification that such complaints are linked to electromagnetic radiation exposure. A cause-effect relationship between the symptoms described by electro-sensitive people and electromagnetic radiation can therefore be excluded with a fairly high probability.

Epidemiological studies

As a matter of fact, it is not possible to prove that a substance or technical application is safe. Limit values for intensity or dose can be set only if the effect on biological matter caused by radiation exposure can be measured quantitatively and reliably. Even then, it must be questioned whether this affects health and if yes, whether other risk factors need to be taken into account. Recent epidemiological studies by Martin Röösli [4] *et al.* come to the following deductions: "In conclusion, epidemiological studies do not suggest increased brain or salivary gland tumor risk with M(obile)P(hone) use, although some uncertainty remains regarding long latency periods (> 15 years), rare brain tumor subtypes, and M(obile)P(hone) usage during childhood."

The international recommendations and the Swiss legislation

The Swiss legal bases are:

- The Federal Act on the protection from non-ionizing radiation and noise (***Bundesgesetz über den Schutz vor Gefährdungen durch nichtionisierende Strahlung und Schall***, NISSG of 16 June 2017),
- The Federal Ordinance on protection against non-ionizing radiation (***Verordnung über den Schutz vor nichtionisierender Strahlung***, NISV of 23 December 1999, version from 1 June 2019). This Ordinance fixes exposure limits (***Immissionsgrenzwerte***) for non-ionizing radiation as shown in Table 2, and the so-called precautionary installation limits (***Anlagegrenzwerte***) as shown in Figure 3. The latter apply to locations such as offices, housings, schools, hospitals and homes, etc. and are 4 V/m for frequencies below 900 MHz, 6 V/m above 1800 MHz and 5 V/m in between.

As telecommunications legislation (which includes legislation on ionizing radiation and radioactivity) is ruled on a federal level in Switzerland, cantons or municipalities are not entitled to apply other rules or standards. The cantons are, however, commissioned as executing agencies to control the fulfilment by testing and monitoring (***Kantonale Fach- und Meldestelle***). Despite industry pressure, the Federal Parliament refused a parliamentary motion in 2018 that aimed to modify such legislation by changing the limits for non-ionizing radiation.

The owner of an installation producing non-ionizing radiation must carry out regular measurements, either alone or with institutions commissioned by authorities. These measurements must be performed at locations that are either easily accessible or where high intensity values can be expected. The owner must inform the competent authority of the three points where radiation is most intense, as well as where people might be most strongly affected. In addition, the owner must perform intensity simulations for the area surrounding the antenna. If the simulated values exceed 80 percent of the limit value (*Anlagegrenzwert*), then field strength measurements must be carried out.

The measurements of Prof. Röösli (see box on p. 38) and other similar studies have clearly shown that the exposure of individuals depends not only on the radiation from mobile phone antennas, but on many other sources of radia-

4 Martin Röösli, Susanna Lagorio, Minouk J. Schoemaker, Joachim Schüz and Maria Feychting: *Brain and Salivary Gland Tumors and Mobile Phone Use: Evaluating the Evidence from Various Epidemiological Study Designs* in Annu. Rev. Public Health (2019) Vol. 40: 221-238.

Frequencies	Electric field intensity E_{Gf} [V/m]	Magnetic field intensity H_{Gf} [A/m]	Magnetic flux density B_{Gf} [μT]	Duration of application [min]
for continuous operation				
400 – 2000 MHz	28 – 61	0.073 – 0,16	0.092 – 0,20	6
2 – 10 GHz	61	0,16	0,20	6
for pulsed operation				
400 – 2000 MHz	880 – 1960	2.4 – 5,4	3.0 – 6,7	Duration of the pulses
2 – 300 GHz	1950	5,1	6,4	

Table 2: Frequency bands and intensity limits (Immissionsgrenzwerte) for electric-magnetic fields as established in the Swiss NIS-Ordinance (Verordnung über den Schutz vor nichtionisierender Strahlung) and based on the recommendations of the ICNIRP.

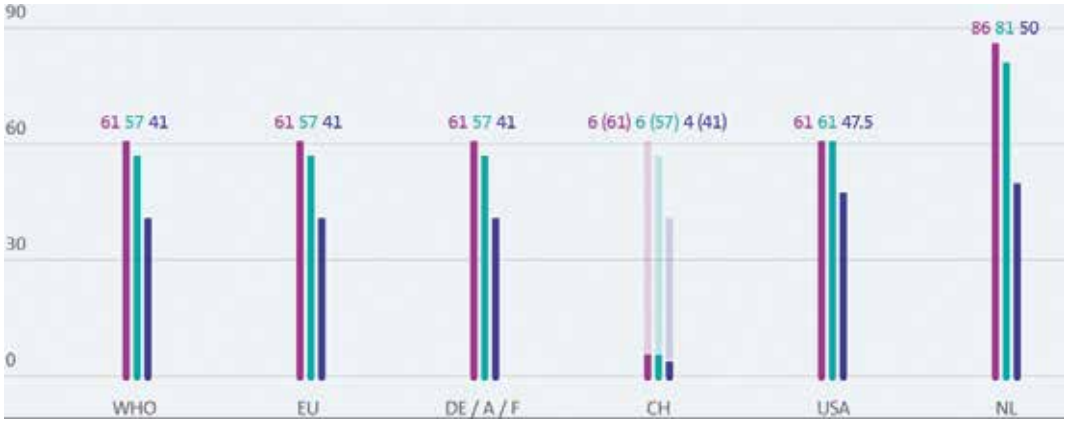

Figure 3: Recommended intensity limits in V/m and subsequent national legislation for the protection from electromagnetic radiation in the domain of mobile communication. Most countries base their national legislation on the recommendations of the ICNIRP (International Commission on Non-Ionizing Radiation Protection). The Swiss NIS-Ordinance (Verordnung über den Schutz vor nichtionisierender Strahlung) fixes, however, two sets of limits: In light colors the so-called Exposure Limits (Immissionsgrenzwerte) and in dark colors the Installation Limits (Anlagegrenzwerte). This unique legislation procedure is based on the precautionary principle, as it is fixed in the Swiss Environmental act (Umweltschutz-Gesetz). Legend: magenta 2100 MHz or above; green 1800 MHz; blue 900 MHz.

tion in their immediate environment. These can include mobile phones belonging to other users, cordless telephones (DECT), WLAN and Bluetooth, which may contribute more to radiation than the exposure from the nearest mobile phone antenna. Individuals are therefore able to control and reduce radiation impact by adhering to the following precautions:

- Do not place the DECT or WLAN base station in a location where you remain for long periods of time, for example near your bed, your home office workplace or the armchair in front of your television.
- Use a mobile telephone with a low SAR value.
- If possible, use wired headphones and microphones.
- Do not use your mobile phone in premises or places with poor reception. In such situations, your phone will increase its emission power to ensure good communication with the nearest antenna.
- When driving a car, use the car's hands-free communication system to minimize radiation intensity – or even better, don't use a mobile phone at all while driving for safety reasons.

Expert judgments

According to the German Federal Office of Radiation Protection (***Bundesamt für Strahlenschutz***), no effects in humans caused by exposures below the ICNIRP limits have been proven so far. The Office based its conclusions on the *Deutsches Mobilfunk Forschungsprogramm* reports. These findings are valid for thermal and non-thermal effects, general health and cognitive functions, risks of cancer and damage to an embryo or a child. According to the Office, these considerations also apply to other applications of non-ionizing radiation, such as 5G. While we do not yet know enough about the long-term effects of radiation beyond 15 years, research in this area should continue. See also the recommendations of the Swiss FOPH [5] in this context.

It is worth remembering the words of Paracelsus: "All things are poison, and nothing is without poison; only the dose makes a thing not poisonous." As with any potentially toxic substance, it is the intensity or the dose that matters. It is the intensity of the electromagnetic radiation that determines whether or not a thermal effect is perceived. It is also the intensity that determines whether radiation is more broadly harmful to human health, either by disturbing or reducing the quality of life, or interfering with the functioning of cells or organs.

How the limits are set

As a general rule, it is not possible to show that an object, substance or technology is not dangerous. Danger can therefore only be assessed through experiments or epidemiological studies that point to what intensity of or exposure to radiation might expose people to side effects. These effects must be reproducible and documented by scientific methods, which will help establish the relationship between exposure to radiation and the likelihood of getting sick or developing cancer. One then determines the corresponding exposure to a certain risk level that is deemed acceptable by the population, taking into account the risks of everyday life. A safety margin is added to this value which is large enough to take into account individual sensitivities. The recommended limits are then obtained, such as those from the ICNIRP [6]. In this procedure, particularly sensitive populations have been taken into account, such as children, the elderly, and possible synergies with other pollutants or harmful substances. In Switzerland – and only in Switzerland – the legislator has added to this an additional layer of security by setting installation limits (*Anlagegrenzwerte*) at ten times lower than the intensity limits (*Immissionsgrenzwerte*) recommended by the ICNIRP. These installation limits are applicable for places with sensitive use such as offices, housing, schools, hospitals and homes. The additional precautionary margin in the Swiss regulation is based on the Federal Act on the Protection of the Environment (***Bundesgesetz für den Umweltschutz***), which calls for lowering emissions to the extent possible as long as such reductions are technical feasible and economically supportable.

Conclusions and recommendations

- What matters is the exposure to electromagnetic fields. Exposure depends on the intensity of radiation at an individual's location and how long that person remains there. The frequency and modulation of the signal, however, play a secondary role, at least for the radiofrequencies used in today's mobile phone networks.
- Switzerland applies the exposure limits (*Immissionsgrenzwerte*) recommended by the ICNIRP while also fixing installation limits (*Anlagegrenzwerte*) applicable for

5 https://www.bag.admin.ch/dam/bag/de/dokumente/str/nis/faktenblaetter-emf/faktenblatt-smartphone.pdf

6 See also the 2020 ICNIRP recommendations: https://www.icnirp.org/en/activities/news/news-article/rf-guidelines-2020-published.html

places with sensitive use, in accordance with the precautionary principle of the environmental act. These are ten times lower than the ICNIRP exposure limits. It is not expected that the Swiss Parliament and the Federal Council will change the values.

- As long as the recommendations of the ICNIRP are respected, there is, according to current scientific knowledge, no danger to human health with a reasonable and moderate use of mobile communication.
- The Federal Office for the Environment (BAFU/OFEV) will install a monitoring system of non-ionizing radiation and perform calculations of the local exposure density. The data will be publicly available.
- Exposure to electromagnetic radiation is only partially due to mobile phone antennas. Radiation can also include other mobile phones being used in surrounding areas, WLAN, DECT (cordless telephones), Bluetooth and other applications of non-ionizing radiation.
- Everyone's behaviour has a greater impact on personal exposure to electromagnetic radiation than the exposure situation at the place of residence.
- The frequencies which are planned (or implemented) for 5G are already partly used by other applications. 5G is therefore not going to create a fundamentally different exposure situation than the current one. However, it appears that 5G will eventually require a higher antenna density.
- As indicated in the Info Box on p. 34, the 5G network technology is only an intermediate step to the significantly more powerful 6G variant. Since no modern industrial nation can afford not to participate in the development of this technology, it is increasingly important to consider the concerns of many people. This will require further scientific study to better understand the influence of high-frequency radiation on soft matter and on human health. It will also necessitate novel technologies to achieve higher sensitivity of the communication hardware, as well as the development of novel data coding methods to minimize radiation intensities without increasing the transmission error rate.

Exemple of exposure measurements in a Swiss City

Individual exposure to high frequency electromagnetic radiation from mobile communication have been investigated by a project of Prof. Martin Röösli and his team of the Swiss Tropical and Public Health Institute in Basel (Fig. 4). For this study, 115 people living in 12 municipalities in the Canton of Zurich were chosen randomly. The localities have been selected in order to cover all of the different exposure situations that may arise in this area. The study participants were adolescents 12 to 15 years of age, their parents, and young adults 18 to 30 years of age. For a period of 48 to 72 hours they were provided with a portable instrument to record every 4 seconds the intensity of the electromagnetic radiation to which they were exposed and in the 14 different frequency bands used in telecommunications, i.e. between FM radio (87.5 MHz) and that of mobile telephony (2690 MHz). Study participants were also required to complete an activity log and the coordinates (GPS) of the respective locations were also recorded.

The average personal exposure in the study population was 0.18 V/m, slightly higher in young adults (0.22 V/m) than in adolescents and their parents (0.16 V/m). The highest measured average value was 0.42 V/m. The main contributions to the average exposure came from mobile telephone base stations (38 %) and users' individual mobile telephones (35 %), while broadcasting contributions (18 %), WLAN (5 %) and cordless phones (4 %) were less important. The highest exposure was recorded in public transport (train: 0.55 V/m, bus: 0.39 V/m, tramway: 0.33 V/m). In cars, the exposure was 0.29 V/m, outside 0.30 V/m and at the workplace 0.22 V/m. The lowest values were those at school with 0.15 V/m and in houses with 0.11 V/m. The differences between rural and urban residents were relatively small. However, the intensity increases with the rate of urbanization. Individual behavior has a significant influence on exposure, since having a smartphone and how long Internet is used are the dominant factors. On the other hand, the use of a personal WLAN or a cordless telephone at home is of less importance. The study did not find a significant correlation between the exposure of adolescents and that of their parents living in the same household. The authors conclude that everyone's behavior has a greater impact on personal exposure to electromagnetic radiation than the exposure situation at the place of residence.

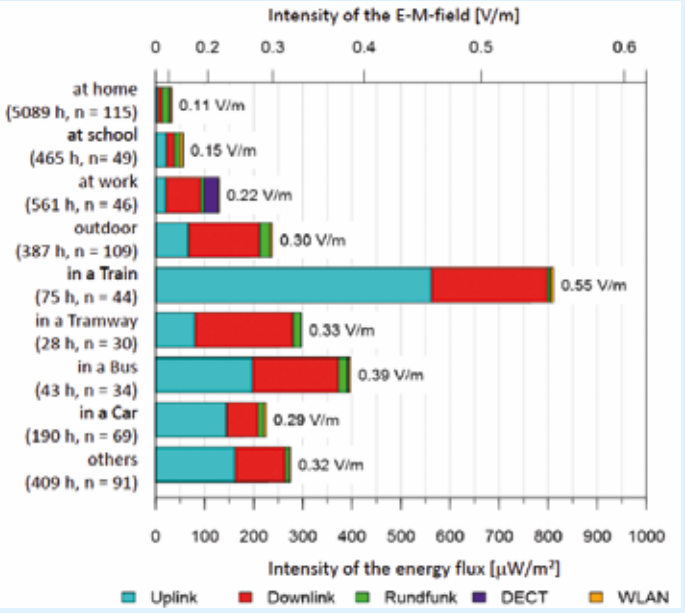

Figure 4: Exposures recorded for inhabitants of the Canton of Zurich by the group of Prof. Martin Röösli: The graph shows the intensities of the electromagnetic radiation from different sources, as well as the hours of exposure and the number of participants. (Uplink = from the user's mobile phones to the antenna; Downlink = from the antenna to the user)

Finals of the 26th Swiss Physics Olympiads: promoting young physics talents in challenging times

Adrian Rutschmann

Last September the Physics Olympiad started with 649 high school students from all over Switzerland and Liechtenstein. After two rounds of competition and training camps in Lausanne and Vordemwald the 24 best students were selected for the final round of the Physics Olympiad. At the final round the participants normally solve different theoretical and experimental problems for two days. In the end the best students qualify for the International Physics Olympiad (IPhO) or the European Physics Olympiad (EuPhO). But this year the final round took place under special circumstances. Due to the Corona virus, we could not hold it as planned in Aarau on 14 and 15 March.

Instead, the final round was postponed to 6 June and rearranged to an online format. We wrote a new experimental task, because for the online competition the experiment needed to be realizable with simple means at home. In addition, we set up a system to prevent the students from cheating. This means a supervisor watched the student via webcam for the whole time. All these adjustments were only possible thanks to the great effort of the volunteers who organize the Physics Olympiad.

In the end, the online competition consisted of three theoretical problems and one experimental task. In one theoretical problem the students were following the trail of the Swiss Nobel Prize laureates Michel Mayor and Didier Queloz. In this task they learned how one can discover exoplanets with the Doppler effect. In the experimental part the students had to determine the static friction within a syringe and the mass ratio of the casing and the piston of the syringe. To complicate things a bit, they could only use a chewing gum and a piece of plastic to perform the measurements. Along with the knowledge of the physical phenomena also the creativity of the participants was tested.

An advantage of the new digital format was, that we had plenty of time to correct the exams, because the closing ceremony took place three weeks after the final round instead of one day after the exams. So, night shifts could be easily avoided. The closing ceremony was rearranged into a digital format, where all the participants joined a Zoom meeting and their families could watch per livestream. We were lucky to welcome a special guest at the ceremony. Claude Nicollier joined us in the Zoom meeting and shared his enthusiasm for Physics with the participants.

Dominik Moos (top) and Leo Thom, the winners of this year's "SPG Nachwuchförderpreis".

At the closing ceremony the medalists were announced. Five gold, silver and bronze medals were awarded to the fifteen students, who achieved the most points in the exam. Unfortunately, this year the winners cannot travel to any foreign country and meet other young Physics enthusiasts from all over the world at IPhO or EuPhO. The IPhO was cancelled this year and the EuPhO was held in an online format from the 20 to 26 July, which for sure was not the same experience. Nevertheless, we hope that the participants, Dominik Moos, Leo Thom, Max Wipfli, Tobias

With kind permission from the authors of the problems we print here an example from this year's final round. You have only 60 minutes to find a solution, but it's not so trivial as it may look...

Problem 1: Syringe (18 points)
We would like to do some simple experiments with a syringe. You can find all the material for the experiment in the envelope that we sent to you. You will need the following material:

- 1 syringe
- 1 plastic block
- 4 sheets of graph paper
- 1 chewing gum

Note: You must ONLY use the 4 items listed above to make measurements for this experiment, so no pencil, no set-square or ruler, nothing else. Also none of the other items in the envelope. For the documentation of the tasks on paper you may of course use writing utensils, set-square, etc.

To solve the problems you get the following information:

- Inside radius of syringe : r = 7.4 mm
- If you need other quantities, make a reasonable assumption and indicate it as such.

Part A. Friction (9 points)
i. (9 pts) Measure the static friction force of the piston in the syringe. Document your solution as follows:

1. Describe and do a sketch of your setup and your approach for the measurements.
2. Calculate the static friction force (the calculation method must be documented).
3. Do an error calculation and use it to justify your approach.

Part B. Mass (9 points)
i. (9 pts) Measure the mass ratio of the piston and the cylinder of the syringe. Document your solution as follows:

1. Describe and do a sketch of your setup and your approach for the measurements.
2. Display your data points graphically and calculate the mass ratio (the method of your solution must be documented).

Riesen and Loïc Nicollerat enjoyed the EuPhO here in Switzerland. In addition, the two best students were awarded with the SPS “Nachwuchsförderpreis” / ”Prix de la Relève”. The first prize went to Dominik Moos from Zug and the second prize was won by Leo Thom from Bottighofen.

For sure this year’s edition of the Physics Olympiad will not be forgotten easily. On one hand the whole atmosphere at the final round was of course totally different and one of the most important things was missing: the exchange between young talents in Physics. On the other hand, we learned many new things during the reorganization into a digital event, which probably can be used for future events. Nevertheless, this will hopefully be the first and last online Physics Olympiad.

Kurzmitteilungen - Short Communications

Jost Bürgi Symposium 2021

Das wegen der Pandemie leider nicht durchgeführte Programm des 4. Internationalen Jost-Bürgi Symposiums 2020 soll am **Freitag, 30. April und Samstag, 1. Mai 2021** in modifizierter Weise nachgeholt werden. Der Veranstaltungsort bleibt derselbe, nämlich das historisch bezaubernde Städtchen Lichtensteig im st. gallischen Toggenburg, dem Geburtsort Bürgis (1552-1632). Informationen zum abgesagten 2020-Programm finden Sie unter
https://www.jostbuergi.com/experten-workshop/ und unter *https://www.jostbuergi.com/symposium/*

Der Freitag soll somit wieder einen ganztägigen Workshop bringen, der zwar primär für Bürgi Experten ausgerichtet ist, aber durch die breitere Themenwahl jeden an der Geschichte der Wissenschaften Interessierten ansprechen dürfte. Einer der thematischen Schwerpunkte wird der 400. Jahrestag der Veröffentlichung von Bürgis "Progresstabulen" sein: Das Prinzip der Logarithmen – Addieren von Exponenten statt Multiplizieren von Potenzen – war schon in der Antike bekannt. Für praktische Rechnungen anwendbar wurde dieses allerdings erst, nachdem hinreichend kleinschrittige Tabellen zur Verfügung standen, in denen Exponenten und Potenzen einander gegenübergestellt wurden. Zum eigenen Gebrauch hatte Bürgi solche schon vor 1590 angefertigt. Auch durch die Zeitumstände bedingt, wurden seine "Progresstabulen" allerdings erst 1620 gedruckt, so dass ihm in dieser Hinsicht Napier und Briggs zuvorkamen.

Zwischen den Referaten wird genügend Zeit für Diskussionen eingeplant, um logarithmische Ansätze auch in unserer heutigen, rechenschieberfreien Zeit zu entdecken, wie zum Beispiel bei kryptographischen Methoden.

Das würde dann nahtlos den Bogen zum Programm des Samstagvormittags schlagen, wo in mehreren Vorträgen die breite Öffentlichkeit und hier besonders Jugendliche mit scheinbar provozierenden Themen von aktueller Bedeutung zum Nachdenken angeregt werden sollen. Der Leitgedanke dieses Zukunftsforums "**Neudenken, Querdenken, Umdenken**" beschreibt gut dieses Anliegen und bietet so mehr als reine Wissensvermittlung. Die historische Person Bürgi dient dabei exemplarisch als Vorbild für ein energisches Durchsetzen kühner Ideen entgegen etablierter Meinungen und inmitten erstarrter gesellschaftlicher Strukturen.

Für die SPG als Mitveranstalter sind die alljährlichen Bürgi Symposien beste Gelegenheit, einer interessierten Öffentlichkeit zu zeigen, dass grosse Ideen, Entdeckungen und Erfindungen auch heute nur dann entstehen und langfristig sich auswirken können, wenn solides Grundlagenwissen mit Applikationsvorstellungen vereint wird. Bürgis Instrumente wie seine präzisen Sekundenuhren und seine intelligenten Rechenmethoden wie die der "Progresstabulen" illustrieren das beispielhaft.

Bernhard Braunecker

Pre-announcement: Joint Annual Meeting of SPS and ÖPG 2021

The next Annual Meeting will take place at the ***University of Innsbruck***, in the week of ***28 June - 2 July 2021***. The well established tradition of organising the conference every second year jointly with the Austrian Physical Society (ÖPG) will be continued, possibly again with contributions from further partners.

Save the date !

It is **your** conference, so we welcome contributions from all topical fields. The detailed announcement will be published in the next *SPG Mitteilungen*, available in early 2021, as well as on our website.

Journées de Réflexion der SATW zu Industry Relations

Anlässlich der Journées de Réflexion diskutieren Vorstand, Mitglieder des wissenschaftlichen Beirats, Leiterinnen und Leiter von Themenplattformen sowie weitere Mitglieder und Mitarbeitende der SATW jeweils strategische und thematische Fragen. 2020 fand der Anlass am 19. und 20. August in Brunnen statt und der Fokus lag auf den Beziehungen zur Industrie.

Das Motto der Veranstaltung war 2020 «SATW – Industry Relations». Zu Beginn zeigte Hans Hess, Präsident von Swissmem, im Rahmen seiner Keynote auf, welche Erwartungen und Anforderungen aus Sicht der Industrie und Behörden an die SATW gestellt werden. Dabei betonte er, dass Schweizer Unternehmen bei der Innovation besser werden müssen. Dies hiesse vor allem und dort könne die SATW unterstützen, dass der Technologietransfer besser und schneller ablaufen müsse. Mit Vorträgen aus den Bereichen Mechanische Industrie, Pharma und Chemie sowie IT und IT-Sicherheit wurden im Anschluss diese Bedürfnisse konkretisiert. So wies Ulrich Claessen, CTO bei maxon motors und damit Vertreter der mechanischen Industrie, darauf hin, dass der Kontakt zu den CTOs schon gut, aber der Kontakt zu den CEOs besser oder zu den Inhabern der Firma am besten sei. Djordje Filipovic verwies auf die Parallelen seines Arbeitgebers Novartis und der SATW bei den Schwerpunkten und äusserte sich positiv zum Industrie-Beirat. Dies sei eine gute Idee gewesen. Roger Halbheer führte die Anwesenden in die Welt der IT und vor allem der IT-Sicherheit ein, in der Zeithorizonte von sechs Monaten bereits lange seien. Aus seiner Sicht ist es wertvoll, dass die SATW eben keine Lobby-Organisation ist. Alle vier Referenten des Vormittags sind entweder Mitglieder oder Experten der SATW.

Am Nachmittag stellten sich die Teilnehmenden in zwei Gruppen der Herausforderung, konkrete Massnahmen zur Intensivierung der Zusammenarbeit mit der Industrie zu kreieren. Dabei kamen wertvolle Ideen zusammen, die nun weiter konkretisiert werden sollen.

Beatrice Huber, SATW

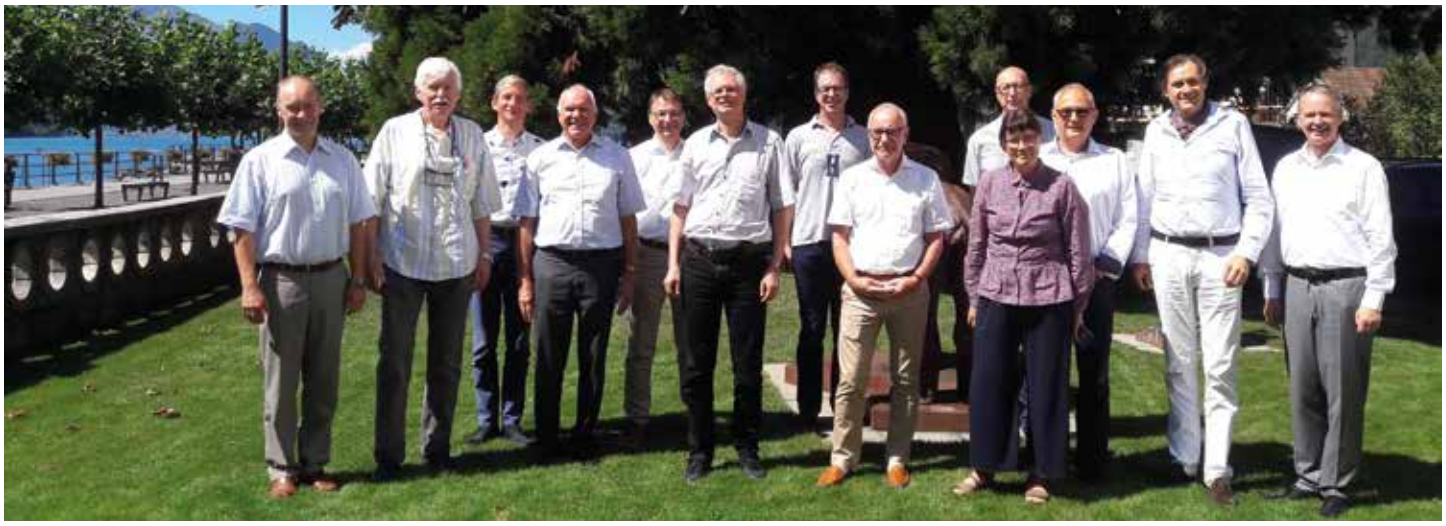

Gruppenbild in der Mittagspause bei strahlendem Sonnenschein (v.l.n.r.): Rolf Hügli, Generalsekretär SATW, Ulrich W. Suter, Präsident WBR SATW, René Hüsler, Mitglied WBR SATW, Hans Hess, Präsident Swissmem und Einzelmitglied SATW, Christofer Hierold, Vorstand SATW und Präsident Wahlkommission, Peter Seitz, Vize-Präsident SATW, Roger Halbheer, Mitglied SATW Advisory Board Cybersecurity, Willy Gehrer, Präsident SATW, André Golliez, Einzelmitglied SATW, Rita Hofmann, Vorstand SATW, Djordje Filipovic, Mitglied WBR SATW, Benoît Dubuis, Mitglied Vorstand SATW, Ulrich Claessen, Mitglied WBR SATW

IDL 2020

The IDL 2020 organizers wish to thank you all for your participation and engagement with the 2020 International Day of Light around 16 May. Various online and virtual activities have taken place over the past few days and a variety of events will still take place throughout the year. To date, events are registered in 70 countries worldwide and we are sincerely grateful for your continued support and enthusiasm for IDL, particularly amid these uncertain times.

We welcome you to enjoy and share the new 2020 International Day of Light Video, created by the Optical Society (OSA), SPIE and the IEEE Photonics Society with support from the IDL Steering Committee. This video message addresses how light science and technology can provide efficient solutions to current global challenges:

International Day of Light
16 May

https://youtu.be/uf-9ALTf6Tk

Ausschreibung der SPG Preise für 2021
Annonce des prix de la SSP pour 2021

Auch im Jahr 2021 sollen wieder SPG Preise, die mit je CHF 5000.- dotiert sind, vergeben werden.

En 2021, la SSP attribuera à nouveau des prix de CHF 5000.- chacun, à savoir:

- SPG Preis gestiftet von *Hitachi ABB Power Grids Schweiz* für eine hervorragende Forschungsarbeit auf **allen Gebieten der Physik**
- Le prix SSP offert par *Hitachi ABB Power Grids Schweiz* pour un travail de recherche d'une qualité exceptionnelle dans **tout domaine de la physique**
- SPG Preis gestiftet von der Firma *IBM Research GmbH* für eine hervorragende Forschungsarbeit auf dem **Gebiet der Kondensierten Materie**
- Le prix SSP offert par l'entreprise *IBM Research GmbH* pour un travail de recherche d'une qualité exceptionnelle en **physique de la matière condensée**
- SPG Preis gestiftet von der Firma *Oerlikon Surface Solutions AG* für eine hervorragende Forschungsarbeit auf dem **Gebiet der Angewandten Physik**
- Le prix SSP offert par l'entreprise *Oerlikon Surface Solutions AG* pour un travail de recherche d'une qualité exceptionnelle dans le **domaine de la physique appliquée**
- SPG Preis gestiftet vom *Eidgenössischen Institut für Metrologie METAS* für eine hervorragende Forschungsarbeit **mit Bezug zur Metrologie**
- Le prix SSP offert par *l'institut national de métrologie de la Suisse METAS* pour un travail de recherche d'une qualité exceptionnelle **faisant référence au domaine de la métrologie**
- SPG Preis gestiftet von der Firma *COMSOL Multiphysics GmbH* für eine hervorragende Forschungsarbeit auf dem **Gebiet der computergestützten Physik**
- Le prix SSP offert par l'entreprise *COMSOL Multiphysics GmbH* pour un travail de recherche d'une qualité exceptionnelle dans le **domaine de la physique numérique**

Die SPG möchte mit diesen Preisen **junge** Physikerinnen und Physiker in der Frühphase ihrer Karriere, auf alle Fälle vor Erreichen einer akademischen Festanstellung oder bevor sie mehr als drei Jahre in einer Start-up Firma oder in der Industrie tätig sind, für hervorragende wissenschaftliche Arbeiten auszeichnen.
Die eingereichten Arbeiten müssen entweder in der Schweiz oder von SchweizerInnen und Schweizern im Ausland ausgeführt worden sein. Die Beurteilung der Arbeiten erfolgt auf Grund ihrer Bedeutung, Qualität und Originalität.

Der Antrag muss folgende Unterlagen enthalten:

Beschreibung der wissenschaftlichen Arbeit, die prämiert werden soll, inklusive eines wissenschaftlichen Gutachtens. Ein Lebenslauf des Kandidaten, sowie zusätzliche Informationen, die die wissenschaftliche Leistung unterstreichen: Dazu gehören eine Aufstellung der Publikationen in renommierten Zeitschriften und von Einladungen zu Vorträgen, sowie Informationen über eventuell erhaltene Fördermittel, über angemeldete und erteilte Patente, über akademische Preise und Auszeichnungen, etc. Die Relevanz und der Impakt dieser Arbeit in ihrem wissenschaftlichen Gebiet sollen deutlich herausgestrichen werden.

La SSP distingue avec ces prix des travaux scientifiques exceptionnels de **jeunes** physiciens dans la première étape de leur carrière et qui n'ont pas encore atteint une position permanente universitaire ou qui ne travaillent pas depuis plus de trois ans dans l'industrie. Les travaux soumis doivent avoir été effectuées en Suisse ou par des citoyens Suisses à l'étranger. L'évaluation s'effectue selon des critères d'importance, de qualité et d'originalité du travail soumis à la compétition.

Une nomination complète contient:

Une description du travail scientifique soumis, y compris une lettre de référence. Un curriculum vitae du candidat, ainsi que des informations supplémentaires qui mettent l'accent sur les réalisations scientifiques: notamment une liste de publications dans des revues prestigieuses, des invitations de présenter à des conférences importantes, ainsi que des informations sur des requêtes reçues, des brevets en attentes ou délivrés, des prix ou d'autres distinctions académiques, etc. L'importance et l'impact de ce travail dans son propre domaine scientifique doivent être clairement présentés.

Diese Unterlagen werden elektronisch im "pdf"-Format direkt an das Preiskomitee eingereicht (große Dateien bitte komprimieren (zip)):

Ces documents seront envoyés électroniquement en format "pdf" directement au comité de prix (svp. comprimez des fichiers très grands (zip):

awards@sps.ch

Einsendeschluss: 31. Januar 2021

Délai: 31 janvier 2021

Die Preise werden an der gemeinsamen Jahrestagung 2021 in Innsbruck überreicht. Das Preisreglement befindet sich auf *www.sps.ch*.

Les prix seront attribués à la réunion annuelle commune qui se tiendra en 2021 à Innsbruck. Le règlement des prix se trouve sur *www.sps.ch*.

swiss physical society

Société Française de Physique

Call for nominations for the Charpak-Ritz Prize 2022

The *French Physical Society* and the *Swiss Physical Society* have created a joint prize in 2016, the **Charpak-Ritz Prize** to highlight the tight relationship between the two Societies and to keep the memory alive of ***Georges Charpak*** and ***Walther Ritz*** who both have profoundly contributed to physics in their respective times.

The prize distinguishes exceptional contributions in physics or in its development to honour, in odd years, a physicist (or a small team of physicists) who has produced significant contribution in France, and, in even years, a physicist (or a small team of physicists) who has produced significant contributions in Switzerland.

We are inviting nominations for the **Charpak-Ritz Prize 2022** to honour significant contributions achieved in Switzerland. The nomination file shall comprise the usual items (CV, laudation, list of publications as well as the most important publications, reference letters, …). Self-nominations will not be considered. The dossier shall be sent to the *Swiss Physical Society* in electronic format as pdf files with the mention "Nomination for the Charpak-Ritz prize 2022".

A short-list of the three best evaluated candidates will be sent to the *French Physical Society*, who will take the final decision.

awards@sps.ch

Deadline: 31 May 2021

The award will be given at the annual meeting of the *French Physical Society* in 2022.

Ihre Qubits. Gemessen.

Erleben Sie die nächste Generation der Quantenanalysatoren, die neue Massstäbe für das Auslesen supraleitender Qubits setzt.

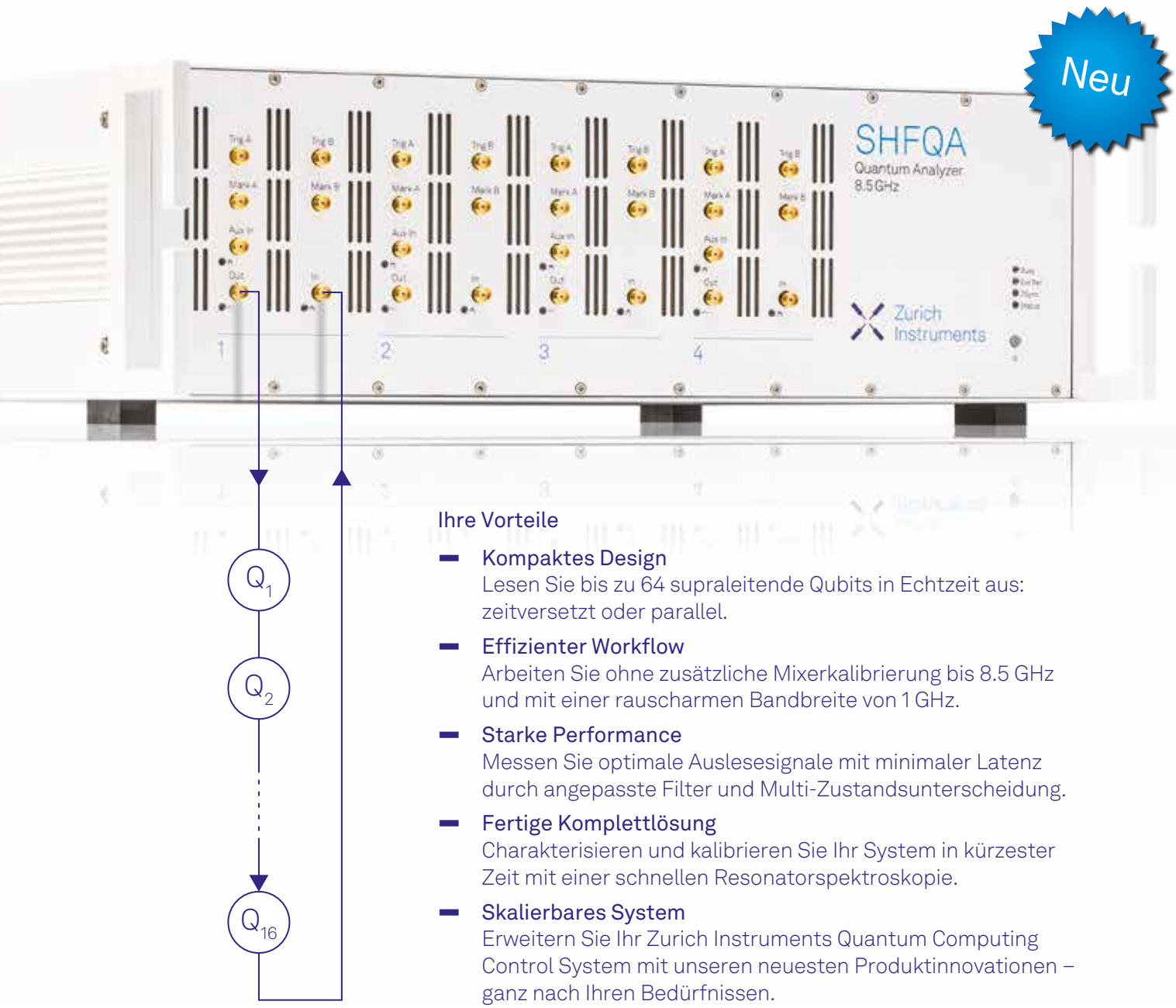

Ihre Vorteile

- **Kompaktes Design**
  Lesen Sie bis zu 64 supraleitende Qubits in Echtzeit aus: zeitversetzt oder parallel.
- **Effizienter Workflow**
  Arbeiten Sie ohne zusätzliche Mixerkalibrierung bis 8.5 GHz und mit einer rauscharmen Bandbreite von 1 GHz.
- **Starke Performance**
  Messen Sie optimale Auslesesignale mit minimaler Latenz durch angepasste Filter und Multi-Zustandsunterscheidung.
- **Fertige Komplettlösung**
  Charakterisieren und kalibrieren Sie Ihr System in kürzester Zeit mit einer schnellen Resonatorspektroskopie.
- **Skalierbares System**
  Erweitern Sie Ihr Zurich Instruments Quantum Computing Control System mit unseren neuesten Produktinnovationen – ganz nach Ihren Bedürfnissen.

Zurich Instruments

Kontaktieren Sie uns
www.zhinst.com